CMS Experiment at the LHC, CERN
Data recorded: 2016-Jul-07 12:00:20.388864 GMT
Run / Event / LS: 276495 / 223808853 / 188

Evidence for Higgs boson decay to a pair of muons from the CMS experiment

oton-proton collisions at
= 13 TeV

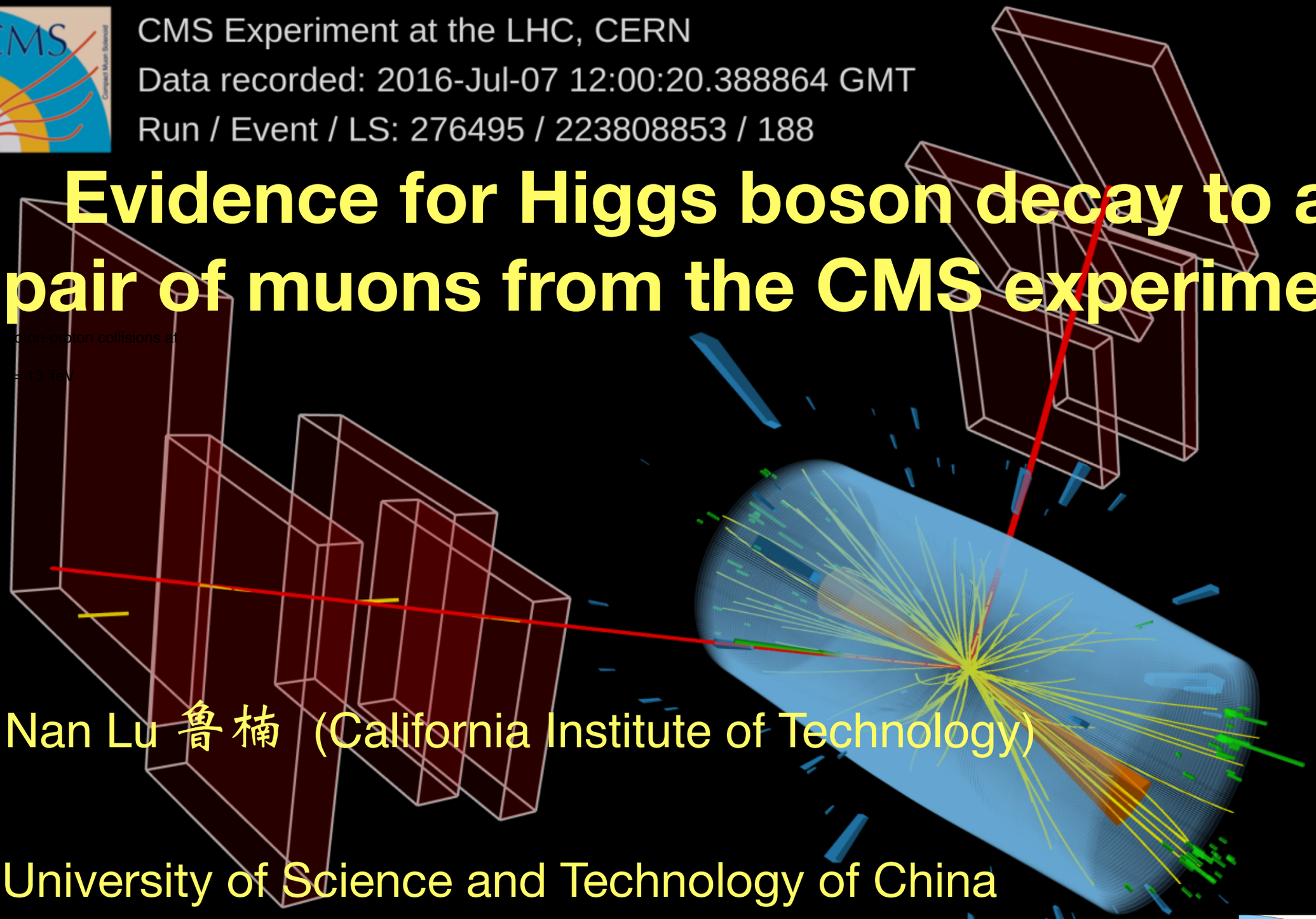

Nan Lu 鲁楠 (California Institute of Technology)

University of Science and Technology of China
Particle Physics Seminar
October 30, 2020

Caltech

The Standard Model Higgs Boson

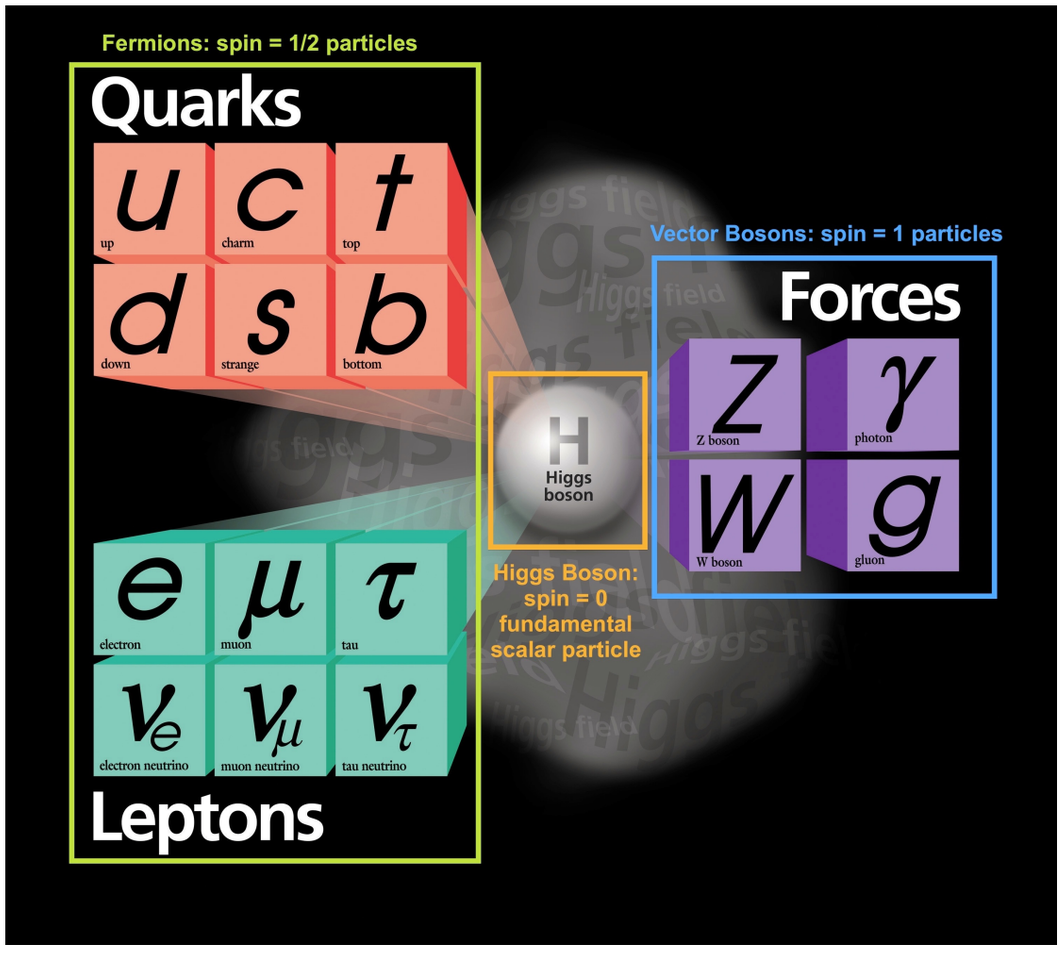

- Quarks, charged leptons, W/Z bosons acquire mass through the Brout-Englert-Higgs (BEH) mechanism in the Standard Model

- Higgs boson physics is one of the most important goals of LHC physics program and the next generation collider experiments

Status of Higgs boson coupling measurements

- Higgs boson couplings to W and Z boson (Run 1), 3rd generation fermions t, b, τ (Run 1+2) have been established
- H→μμ: currently, most experimental sensitive channel to probe Higgs boson coupling to 2nd-generation fermion at LHC
- **topic of the talk today: latest result from CMS experiment on H→μμ search using full Run 2 data (CMS-HIG-19-006, submitted to JHEP)**

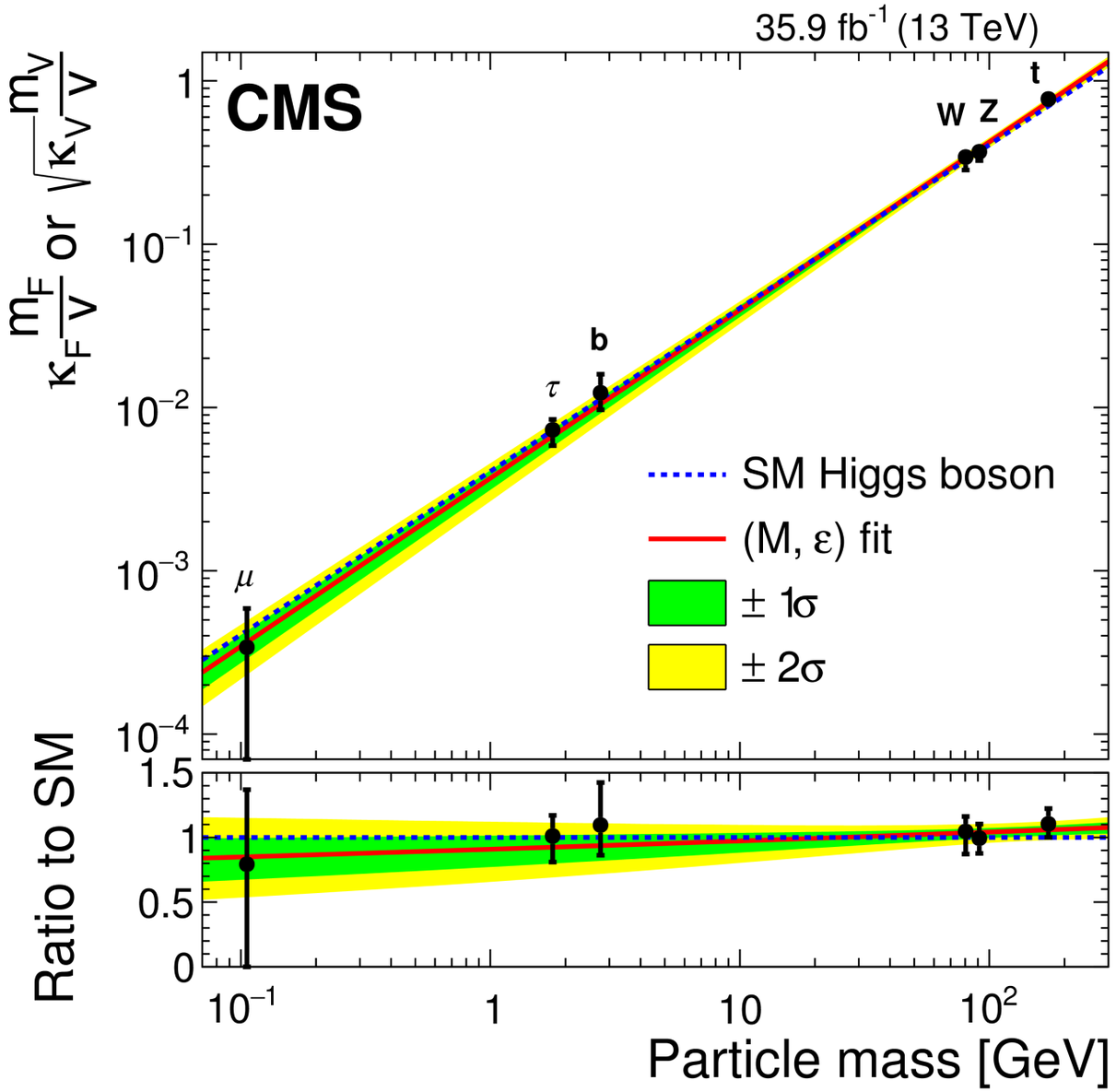

EPJC 79 (2019) 421

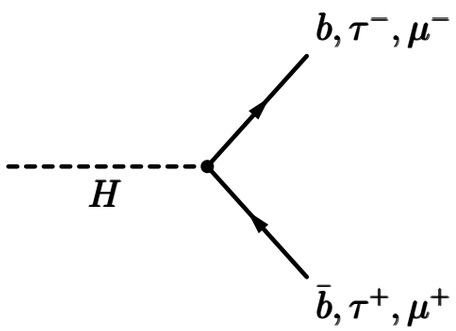

Where to look: Higgs boson mass

- The Higgs boson mass m_H is a free parameter in the SM. Once m_H is known, all Higgs boson couplings to Standard Model particles are fixed
- Most precise m_H measurement currently: **~0.11%** precision by CMS experiment

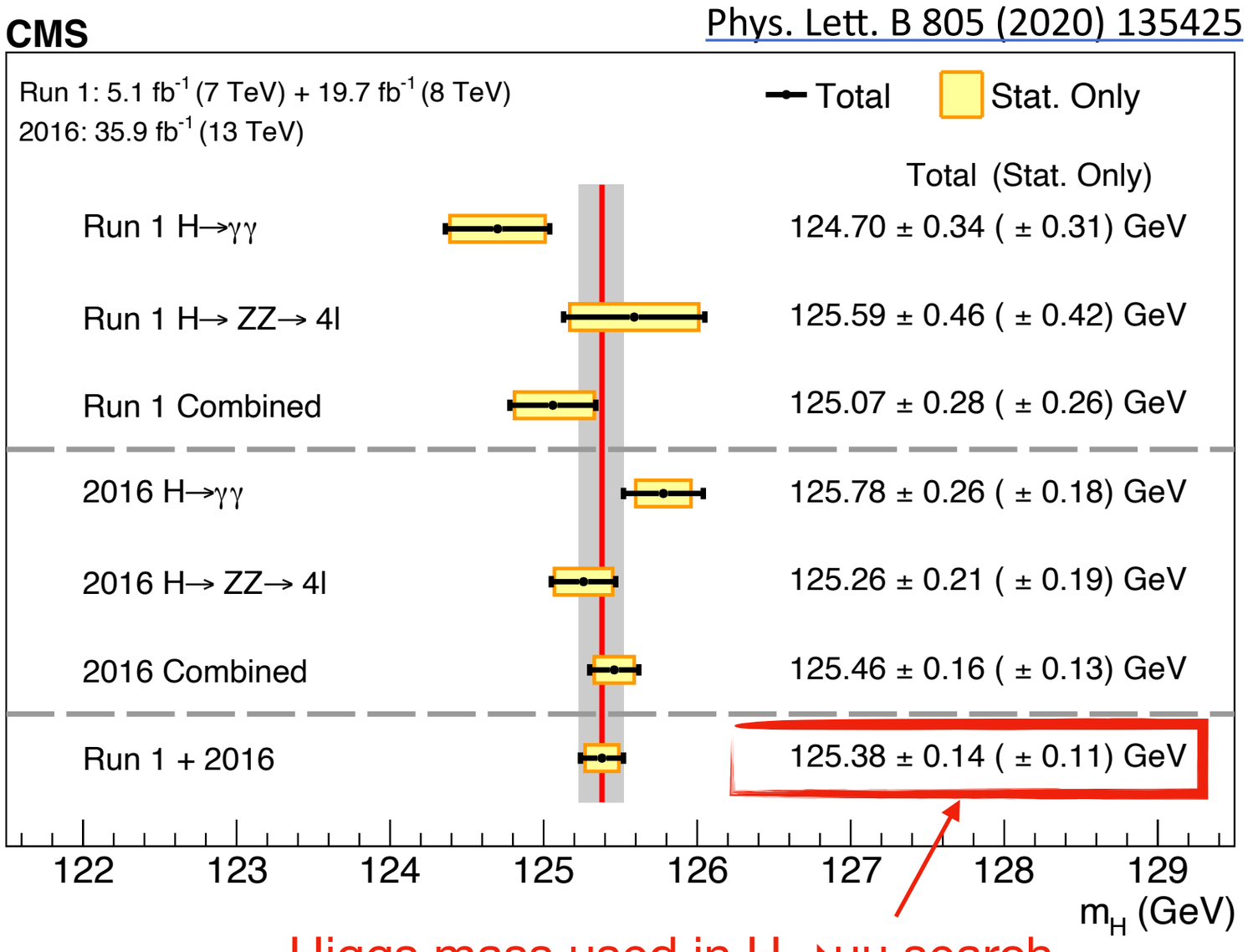

Higgs mass used in H→μμ search

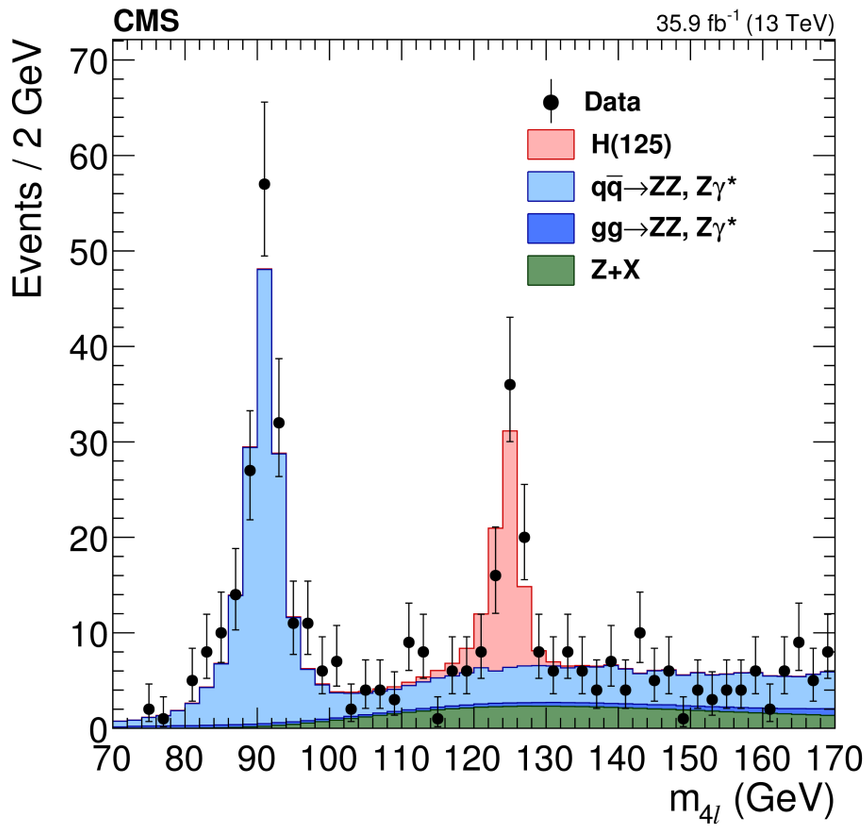

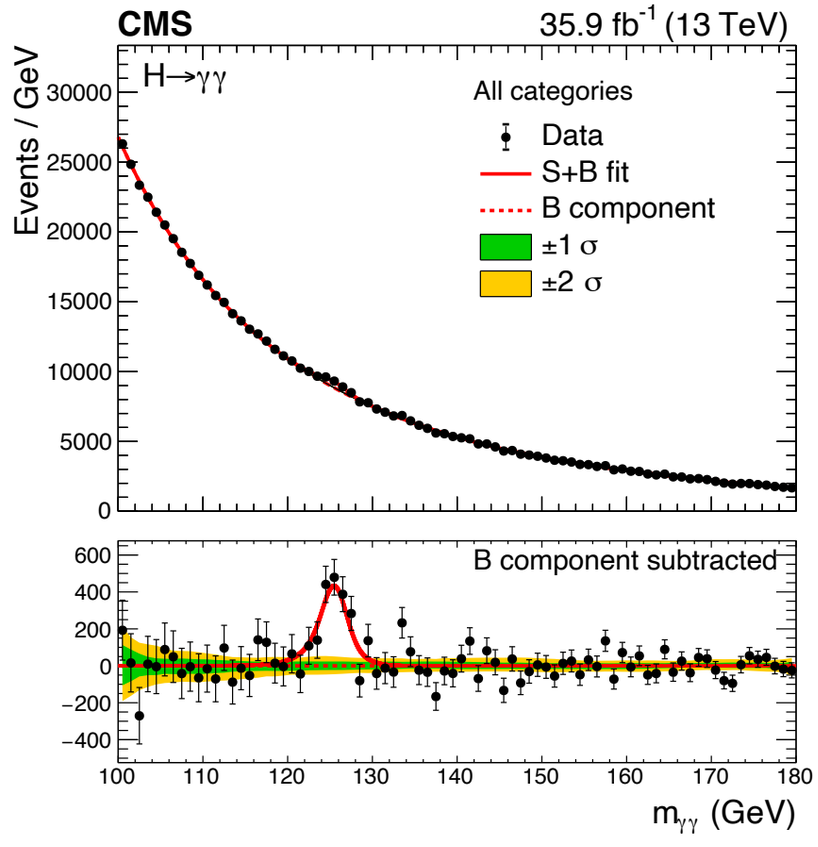

Energy Frontier: Large Hadron Collider

- pp and Heavy Ion collisions (Pb-Pb, p-Pb, Xe-Xe, …)
- pp collision
  - about 5% of data delivered so far
  - 13-14 TeV in Run 3, 14 TeV HL-LHC 3000 fb^{-1}

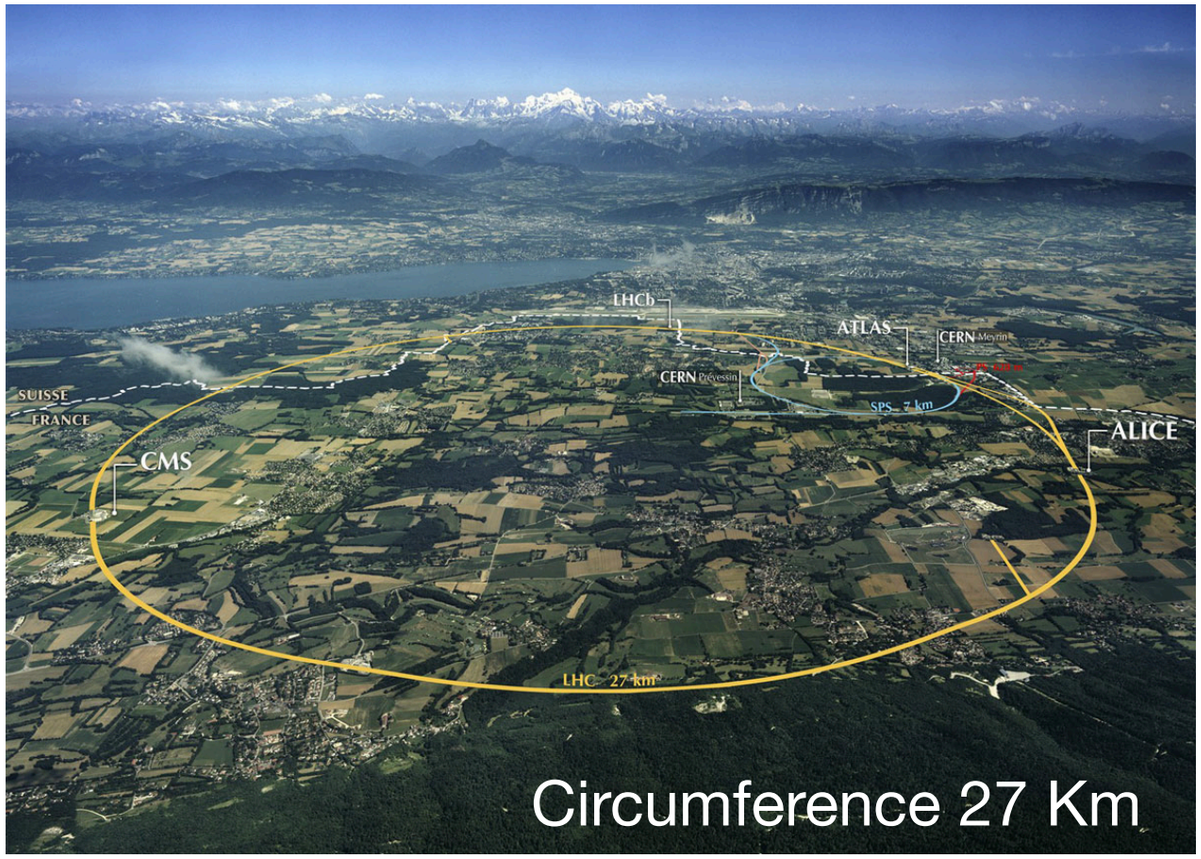

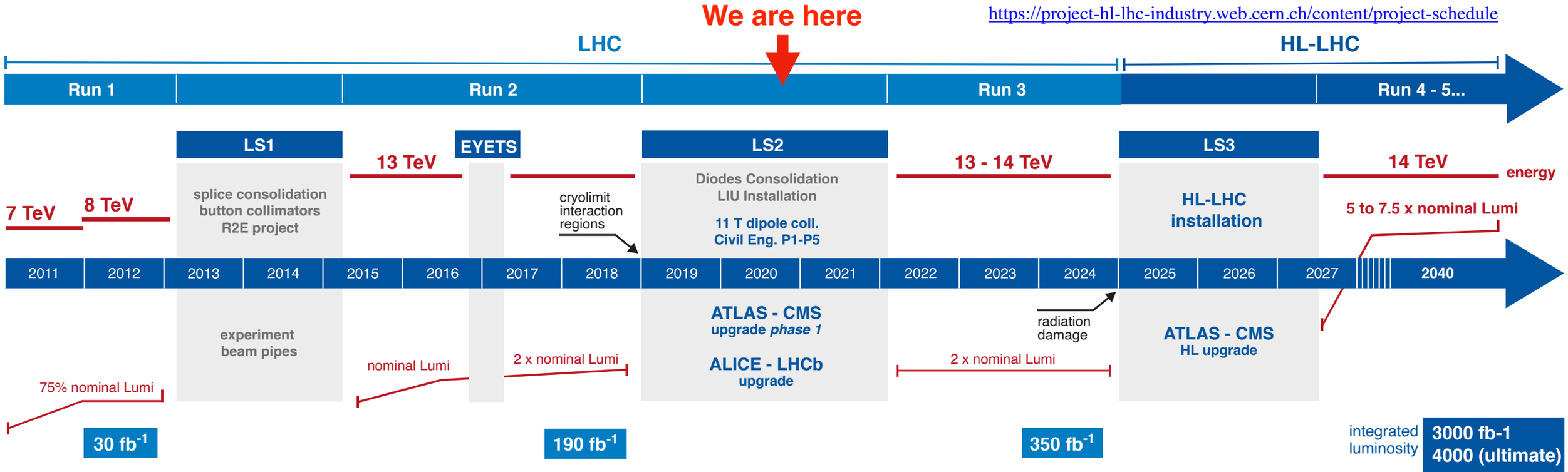

Run 2 data-taking

- Excellent operation of the LHC and performance of the CMS detector in Run 2
- A large dataset recorded in Run 2 with high efficiency and being analyzed:
- 137 fb^{-1} of 13 TeV pp collision data collected by CMS in total after certification for physics (93.7% of CMS recorded data)

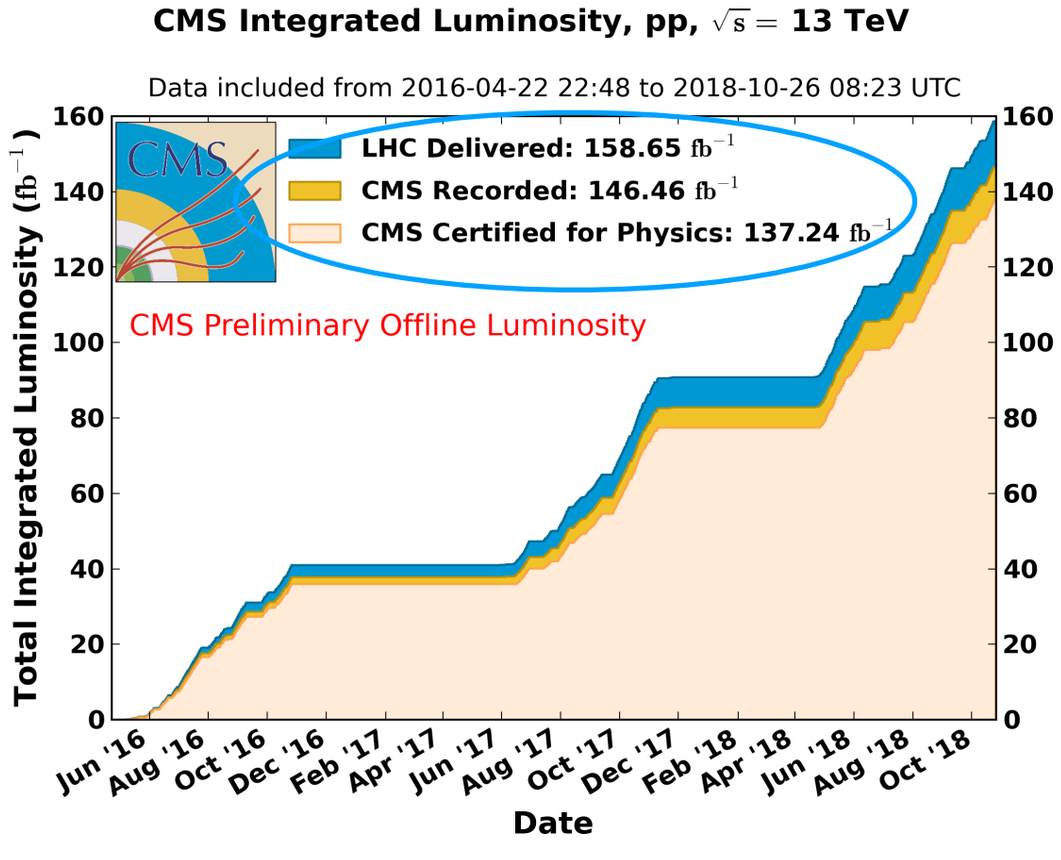

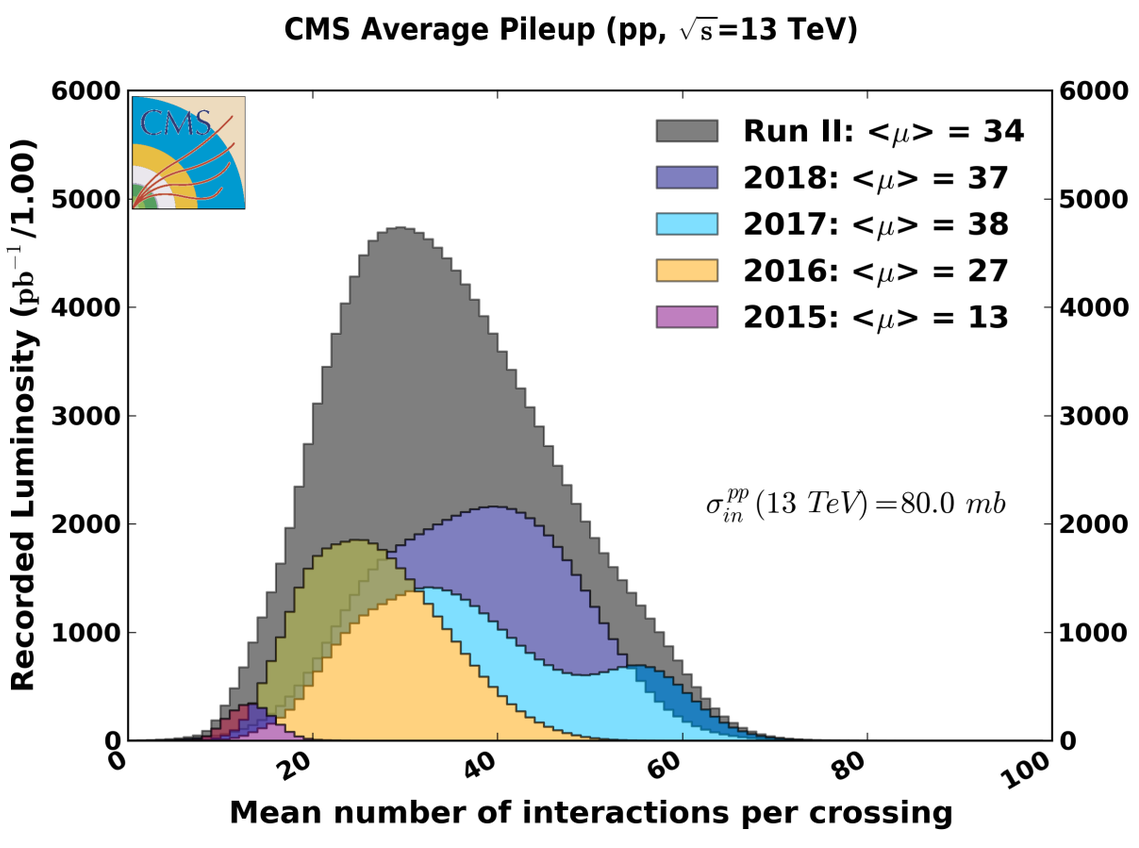

How many H→μμ events produced in Run 2 ?

48 pb

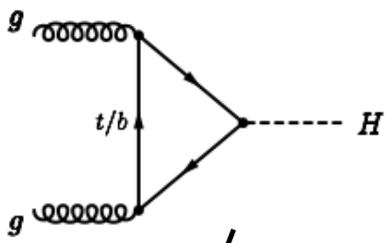

3.8 pb

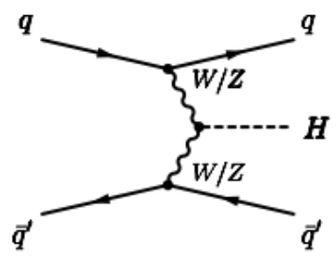

137 fb^{-1} at 13 TeV

production modes	ggF	VBF	WH	ZH	ttH	total ggF+VBF+ WH+ZH+ttH
H→μμ events produced in Run 2 at 13 TeV (137 fb^{-1})	1431	112	40	26	15	1624

2.2 pb

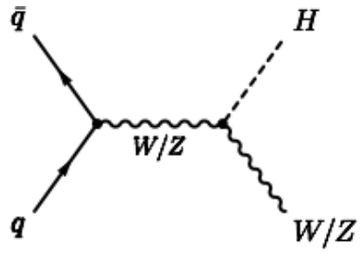

0.5 pb

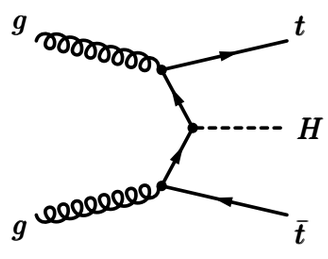

Small Branching Ratio BR(H→μμ): 0.02%

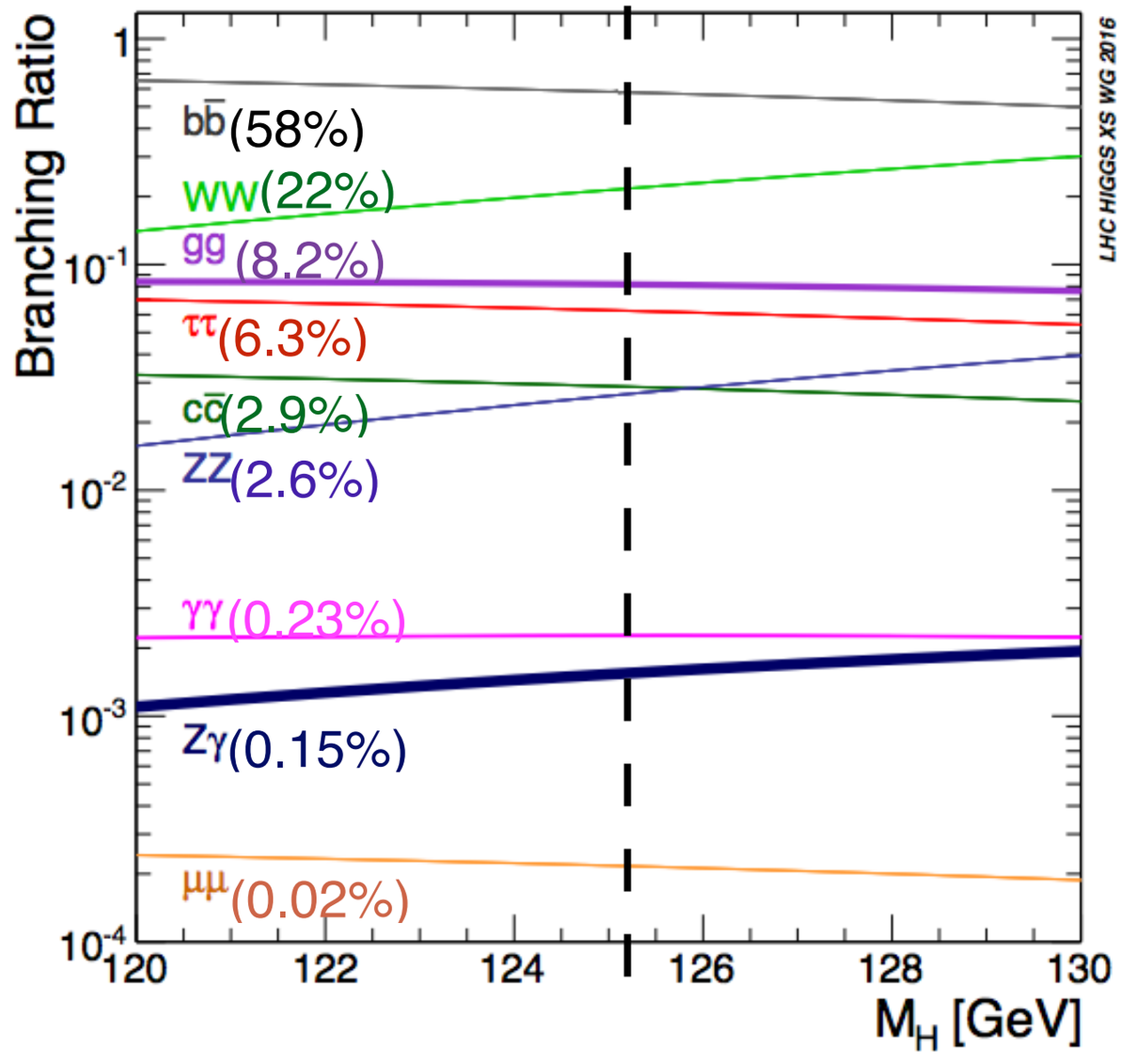

About 1624 events produced at LHC

How many events are reconstructed by CMS and selected by offline analysis?

CMS detector

$\sigma/p_T \approx 1.5 \cdot 10^{-4}\, p_T + 0.005$

CMS DETECTOR

Total weight	: 14,000 tonnes
Overall diameter	: 15.0 m
Overall length	: 28.7 m
Magnetic field	: 3.8 T

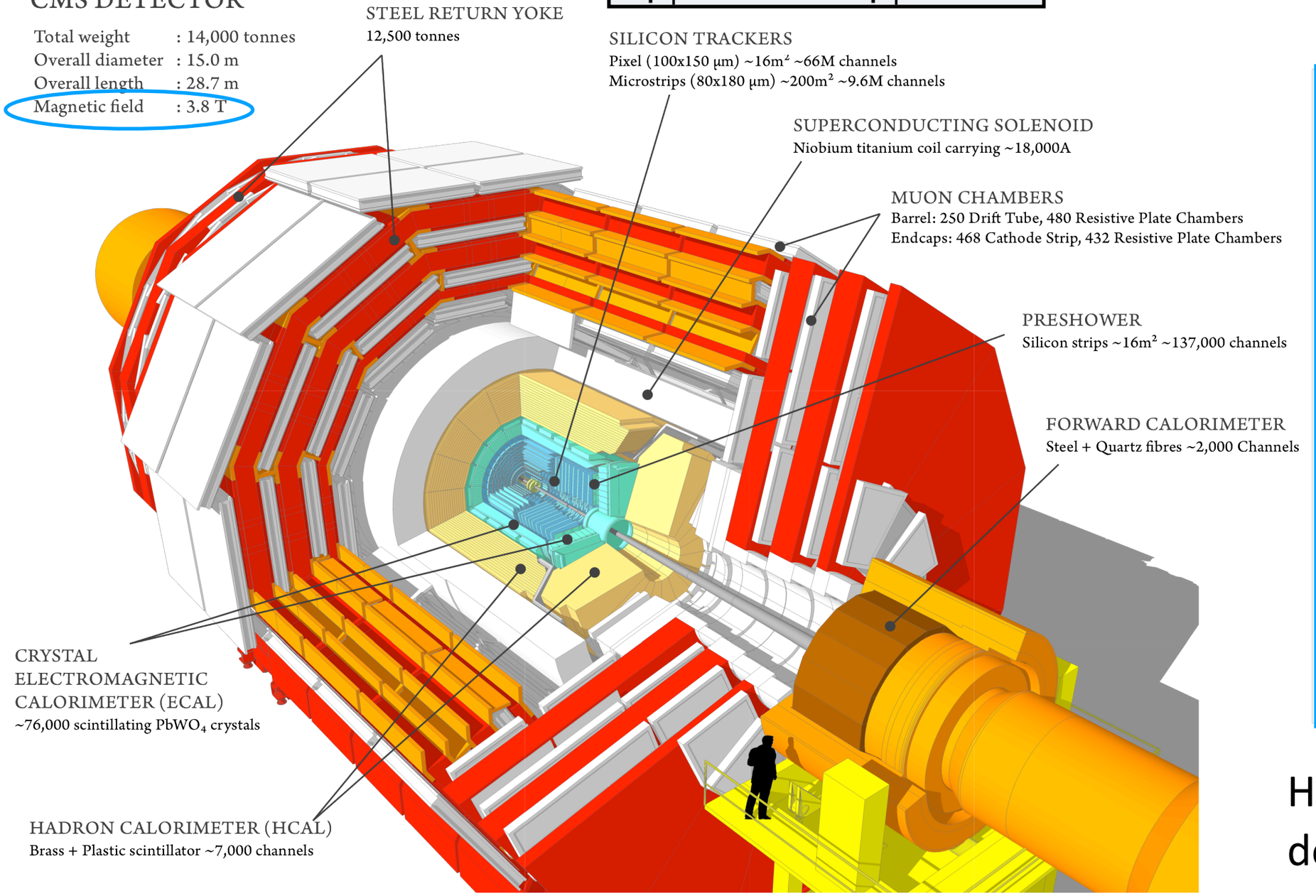

HCAL Readout by hybrid photo-diodes now replaced by silicon photomultipliers (Phase-1 upgrade)

muon p_T resolution

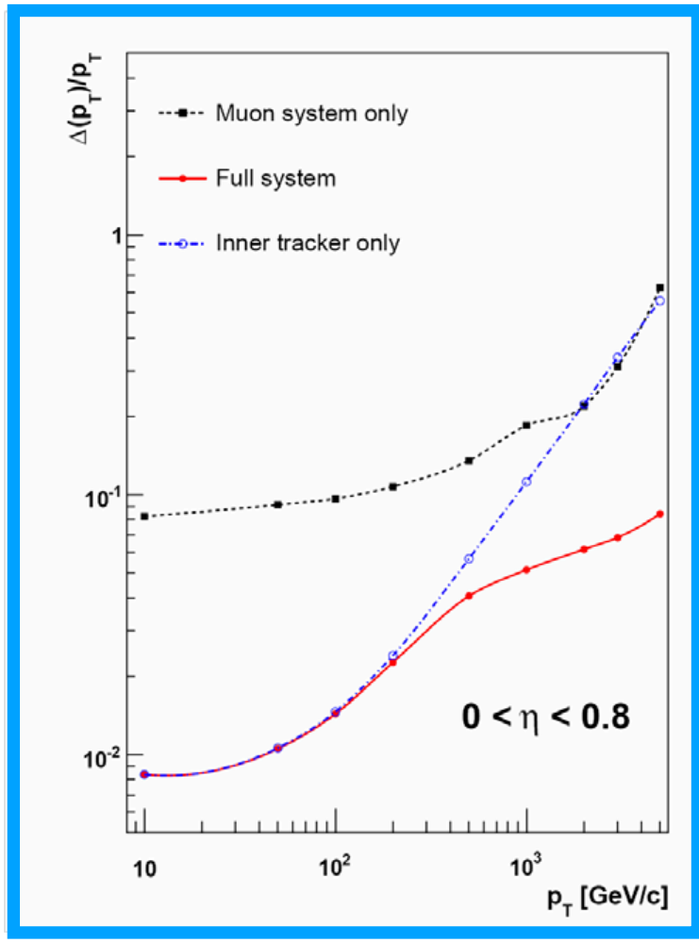

H→μμ: muon p_T resolution dominated by measurements by tracker

Muon reconstruction performance in Run 2

Excellent muon performance in Run 2:

- $|\eta|<2.4$ within geometrical acceptance of muon detectors
- high efficiency for reconstruction and identification >96%, isolation > 95%
- good dimuon resolution: 1~2% for Z→μμ events

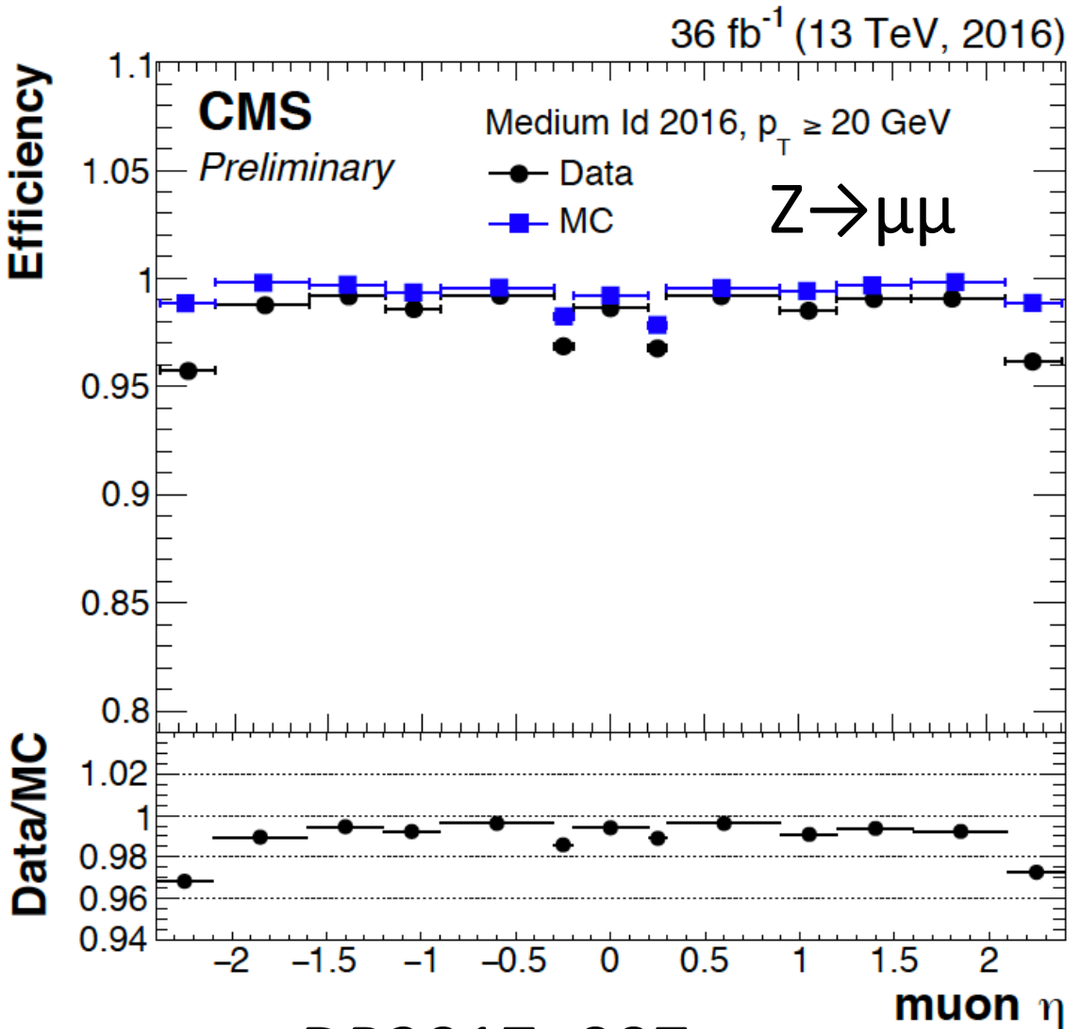

DP2017_007

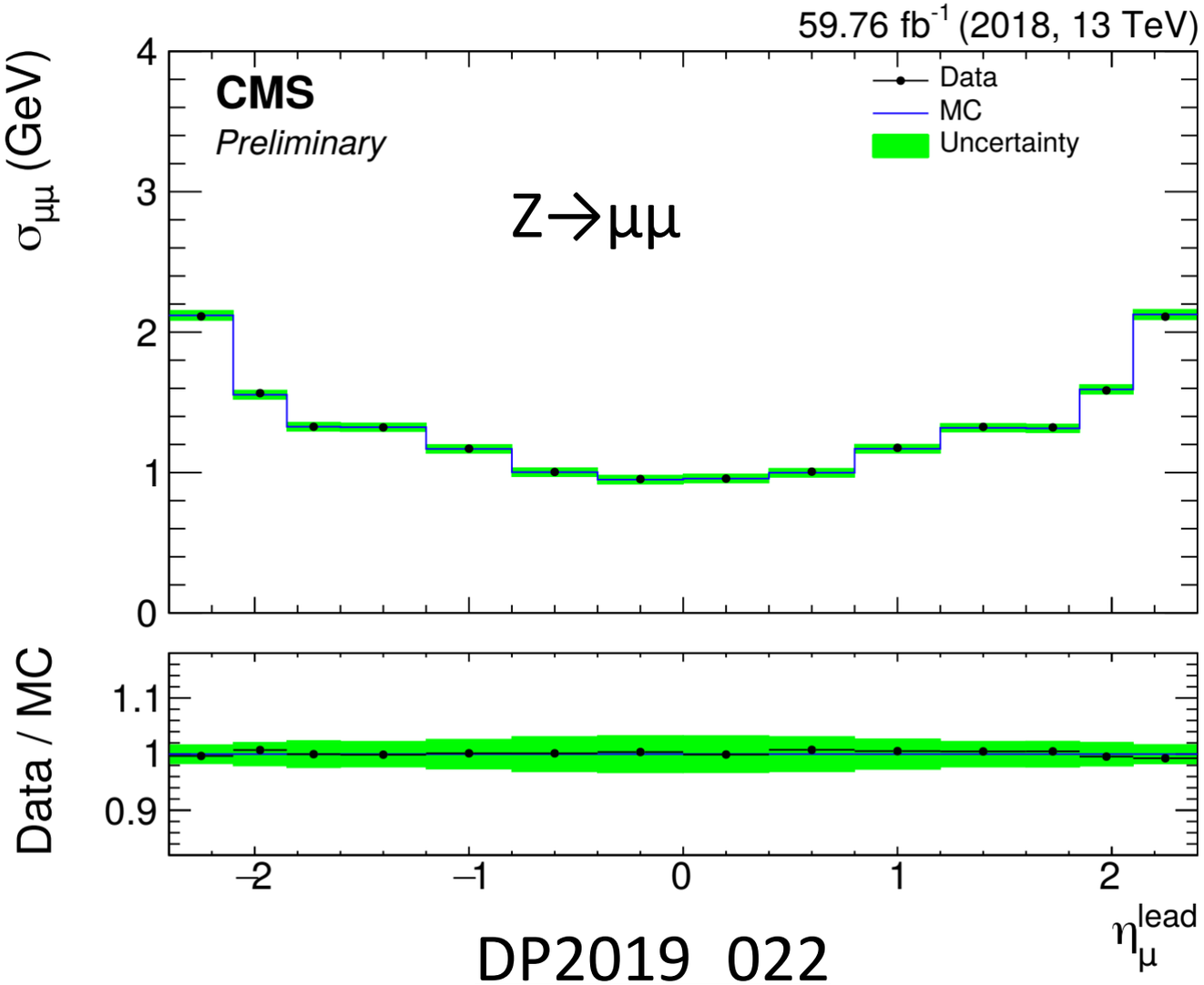

DP2019_022

Recap: CMS H→μμ search with 2016 data

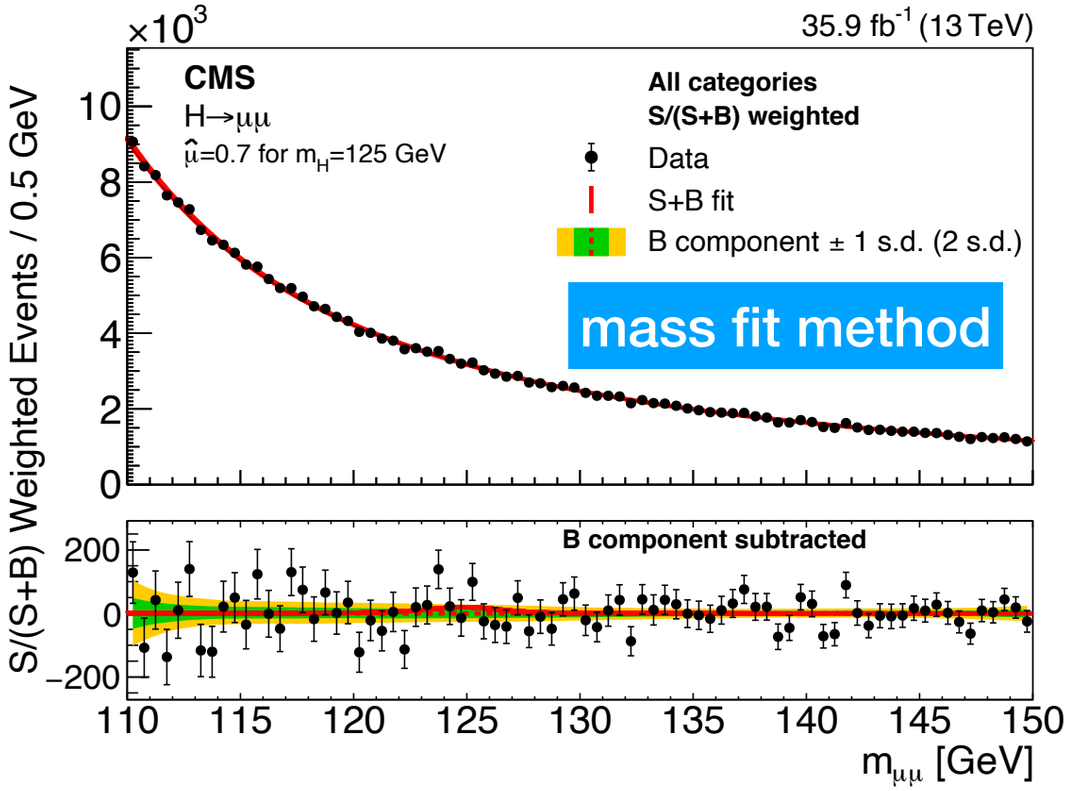

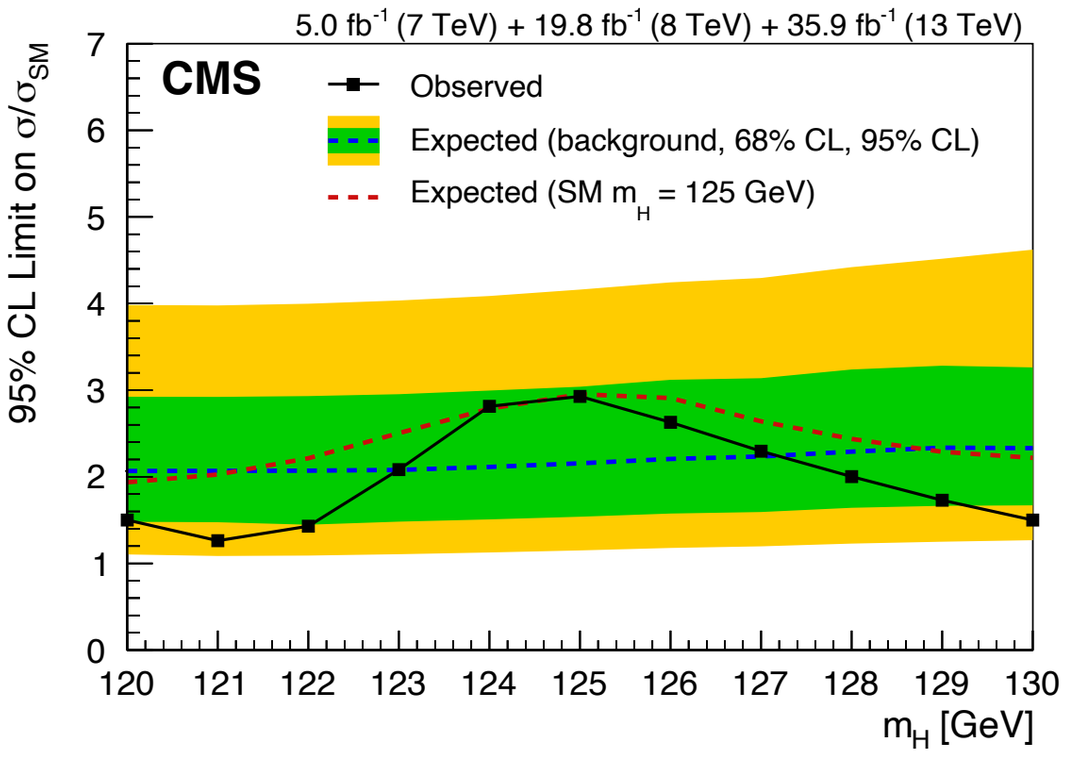

Observed (expected) significance 0.9σ (1.0σ)

Boosted Decision Tree (BDT) trained targeting ggH and VBF signals

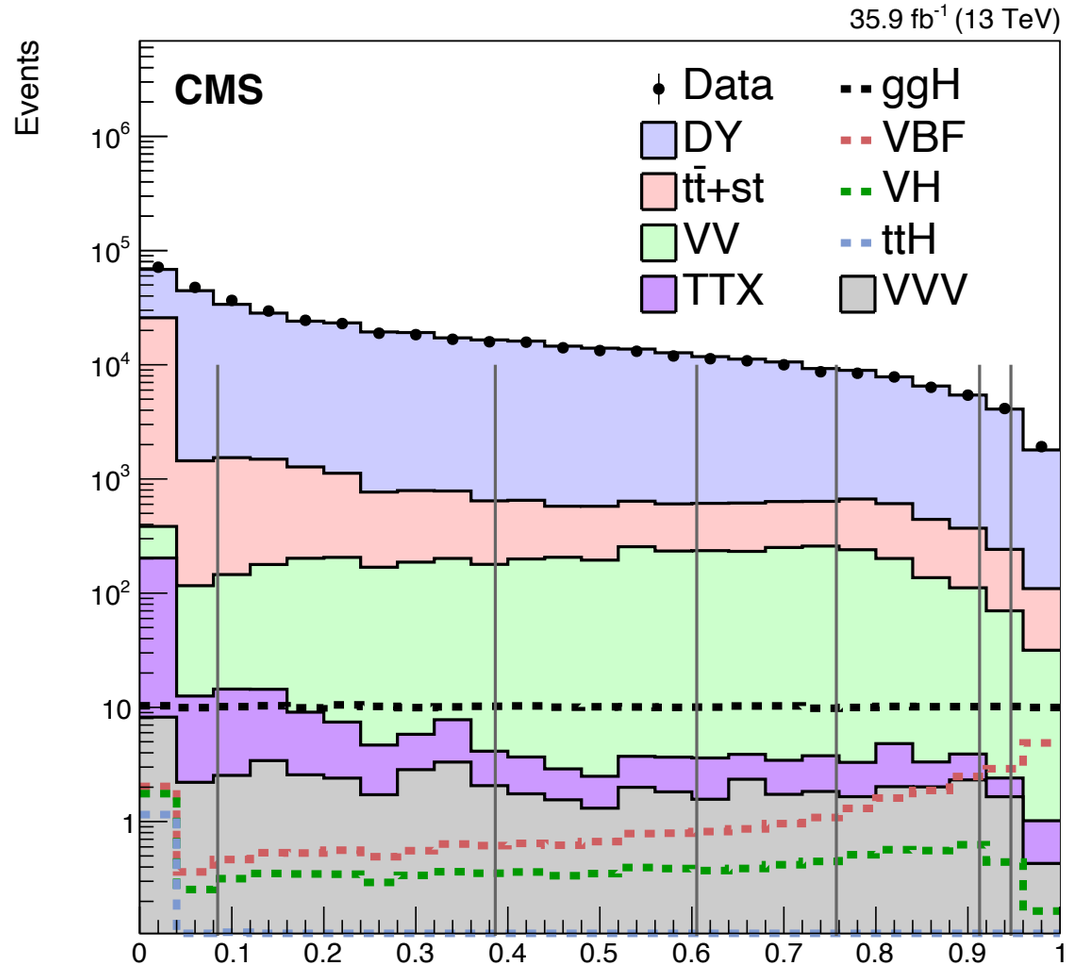

Categorization based on BDT output score and the maximum |η| of the two muons

Phys. Rev. Lett. 122 (2019) 021801

H→μμ characteristics

H→μμ narrow signal on top of smoothly falling background in $m_{\mu\mu}$:

- Narrow signal peak: **$\sigma(m_{\mu\mu})$~ 1.4 GeV**

  signal significance roughly $\propto 1/\sqrt{\sigma(m_{\mu\mu})}$

  new improvements to $\sigma(m_{\mu\mu})$:

  - final state radiation (FSR) photon recovery: 2% improvement on $\sigma(m_{\mu\mu})$, 3% increase in signal yield
  - correction to muon pT by including interaction point position information: 3-10% increase on $\sigma(m_{\mu\mu})$

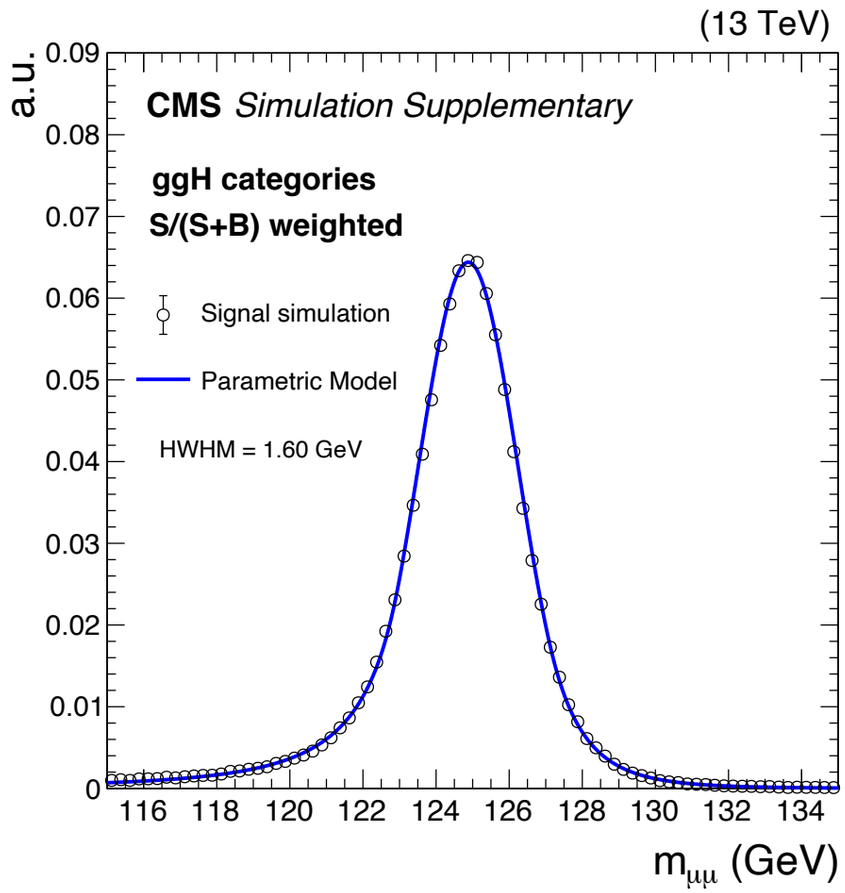

- Large background: **S/B~1/500, how to reduce background is a challenge**
  - main background: Drell-Yan(DY) Z→μμ
  - Others: top (important for ttH channel), electroweak production Z→μμ + jets (for VBF), ttZ(for ttH), diboson (for VH-leptonic)

H→μμ event selection and categorization

- Event selection: expect 954 signal events selected in 110 < $m_{\mu\mu}$ < 150 GeV, efficiency 59% :
  - pass single muon high level trigger
  - require two isolated opposite charged muons: leading muon pT > 26 (2016, 2018)/29 (2017), sub-leading muon pT > 20 GeV

After event selection
110 < $m_{\mu\mu}$ < 150 GeV

$N_{\text{b-tag medium}} > 0$
or $N_{\text{b-tag loose}} > 1$

ttH channel

additional lepton e or μ

VH-leptonic channel

pT_{j1}>35 GeV, pT_{j2} >25 GeV
m_{jj}>400 GeV, $|\Delta\eta_{jj}|$>2.5

VBF channel

the rest of events

ggH channel

new channels dedicated to ttH and VH

new strategy

significantly improved strategy

Analysis strategy:

- ggH, ttH, VH: mass fit method
  - data-driven background estimate
  - binned fit of dimuon invariant mass to data
- VBF: MC template fit method
  - background estimated with MC
  - binned fit of final discriminant to data

ggH, ttH, VH channels: mass fit method

ggH channel: overview

ggH channel includes all events not selected by VBF, ttH and VH channels

- largest signal yield
  - about 890 signals
- smallest S/B
  - best S/B category: S/B~1/50
- main background: DY process
- BDT used to separate signal from background
  - BDT uncorrelated with $m_{\mu\mu}$ to allow using the mass fit method
- Five ggH categories defined:
  - aim to optimize overall best ggH channel significance

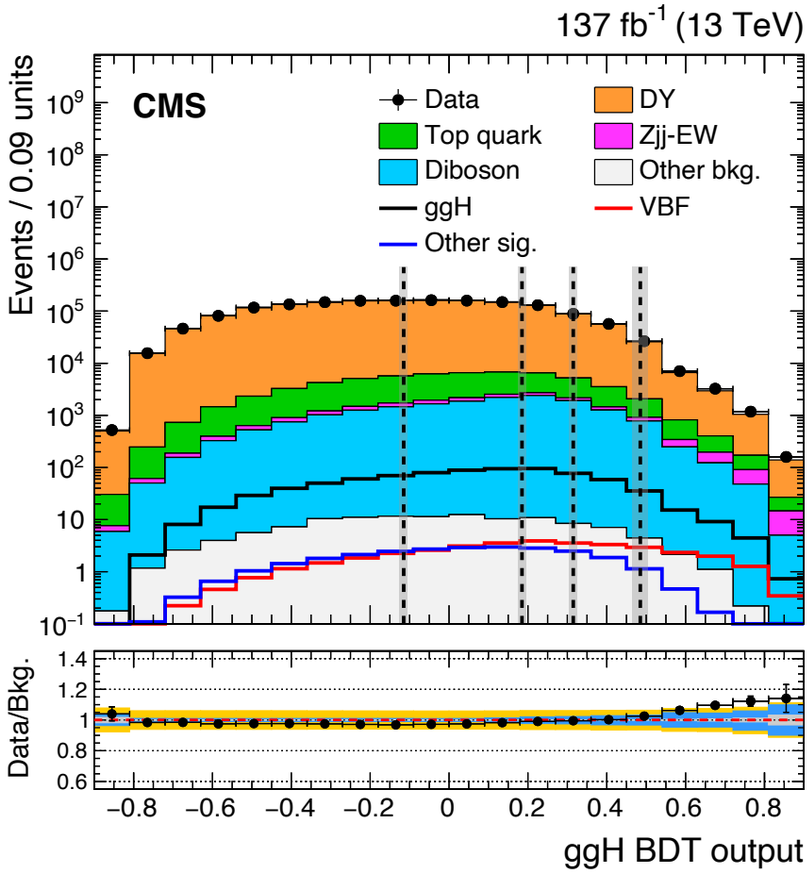

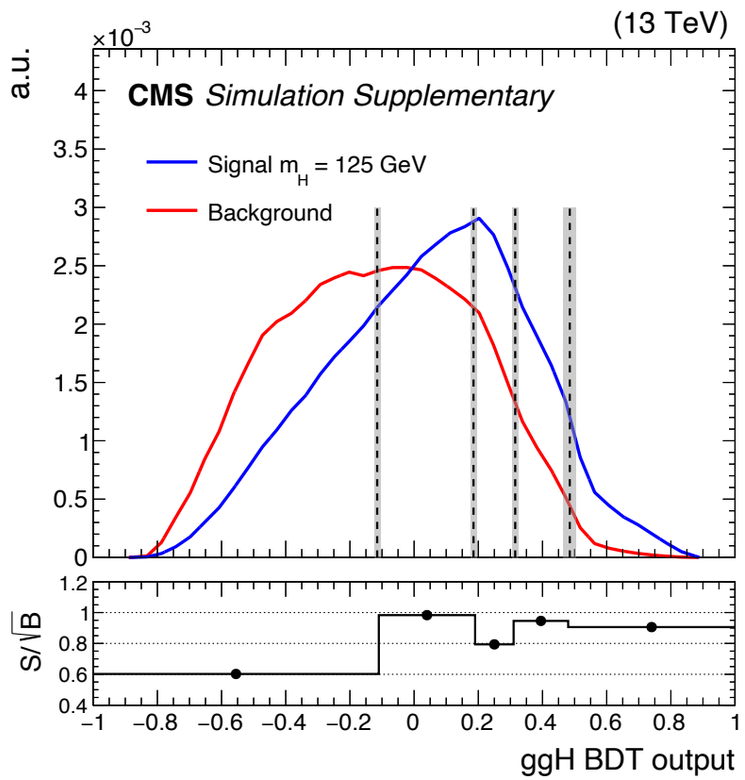

ggH channel: BDT

- BDT encoding as much relevant information as possible
  - training variables: muon and jet kinematic information, N_{jets}
  - signal MC weighted ~ $m_{\mu\mu}/\sigma_{\mu\mu}$: increase the importance of high-resolution signal events
    - technique used in ttH and VH categories too
  - simplify the categorization optimization

- BDT Training variables

(di)muon:
- $pT_{\mu\mu}$
- rapidity$_{\mu\mu}$
- $\cos(\theta_{CS})$, ϕ_{CS} computed in dimuon Collins-Soper rest frame
- $pT_{\mu1}/m_{\mu\mu}$, $pT_{\mu2}/m_{\mu\mu}$
- $\eta(\mu1)$
- $\eta(\mu2)$

muon and jet:
- pT_{j1}, pT_{j2}
- η_{j1}
- N_{jets}
- $\Delta\eta_{jj}$, m_{jj}, $\Delta\phi_{jj}$
- Zeppenfeld variable

$$z^* = \frac{y_{\mu\mu} - (y_{j_1} + y_{j_2})/2}{|y_{j_1} - y_{j_2}|}$$

- min-$\Delta\phi(\mu\mu,(j1,j2))$
- min-$\Delta\eta(\mu\mu,(j1,j2))$

Signal modeling: double-sided Crystal Ball function

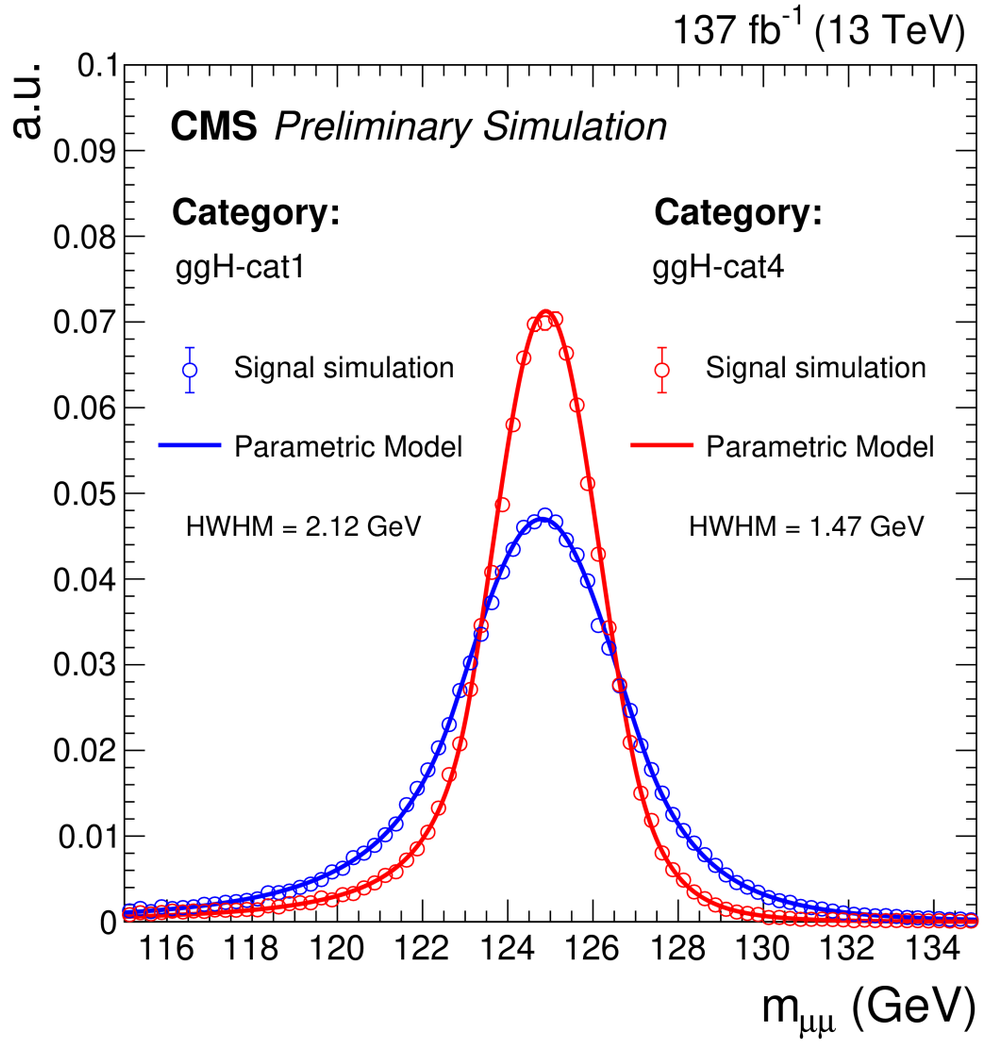

ggH channel: background modeling

- background modeled with analytical functions: core-pdf method

$$B_{cat}(m_{\mu\mu}, \vec{\alpha}, \vec{\beta}) = N_B \times F_{core}(m_{\mu\mu}, \vec{\alpha}) \times T_{SMF}(m_{\mu\mu}, \vec{\beta})$$

Background shape: same core function in all categories

- discrete profiling method[1] choose one from three functional forms during the fit to the data
  - main background DY process physics motivated functions
    - (1) modified Breit–Wigner $\mathrm{mBW}(m_{\mu\mu}; m_Z, \Gamma_Z, a_1, a_2, a_3) = \frac{e^{a_2 m_{\mu\mu} + a_3 m_{\mu\mu}^2}}{(m_{\mu\mu} - m_Z)^{a_1} + (\Gamma_Z/2)^{a_1}}$
    - (2) shape derived from the FEWZ v3.1 generator (NNLO in QCD and NLO in EW) × a third-order Bernstein polynomial
  - agnostic functions
    - (3) a sum of two exponential functions

[1]: 2015_J._Inst._10_P04015

ggH channel: background modeling

- background model with analytical functions: core-pdf method

$$B_{cat}(m_{\mu\mu}, \vec{\alpha}, \vec{\beta}) = N_B \times F_{core}(m_{\mu\mu}, \vec{\alpha}) \times T_{SMF}(m_{\mu\mu}, \vec{\beta})$$

background yield:
uncorrelated across categories

- per-category shape modulation: account for shape variations in categories
  - 2nd or 3rd order Chebyshev polynomial
  - parameters uncorrelated across ggH categories

- Bias from background modeling has < 1% effect on measured signal rate, thus neglected
  - bias on signal extraction < 20% of post-fit uncertainty on the signal yield

Core-pdf method for background modeling brings 10% improvement in sensitivity compared to 2016 data analysis

ggH channel: results

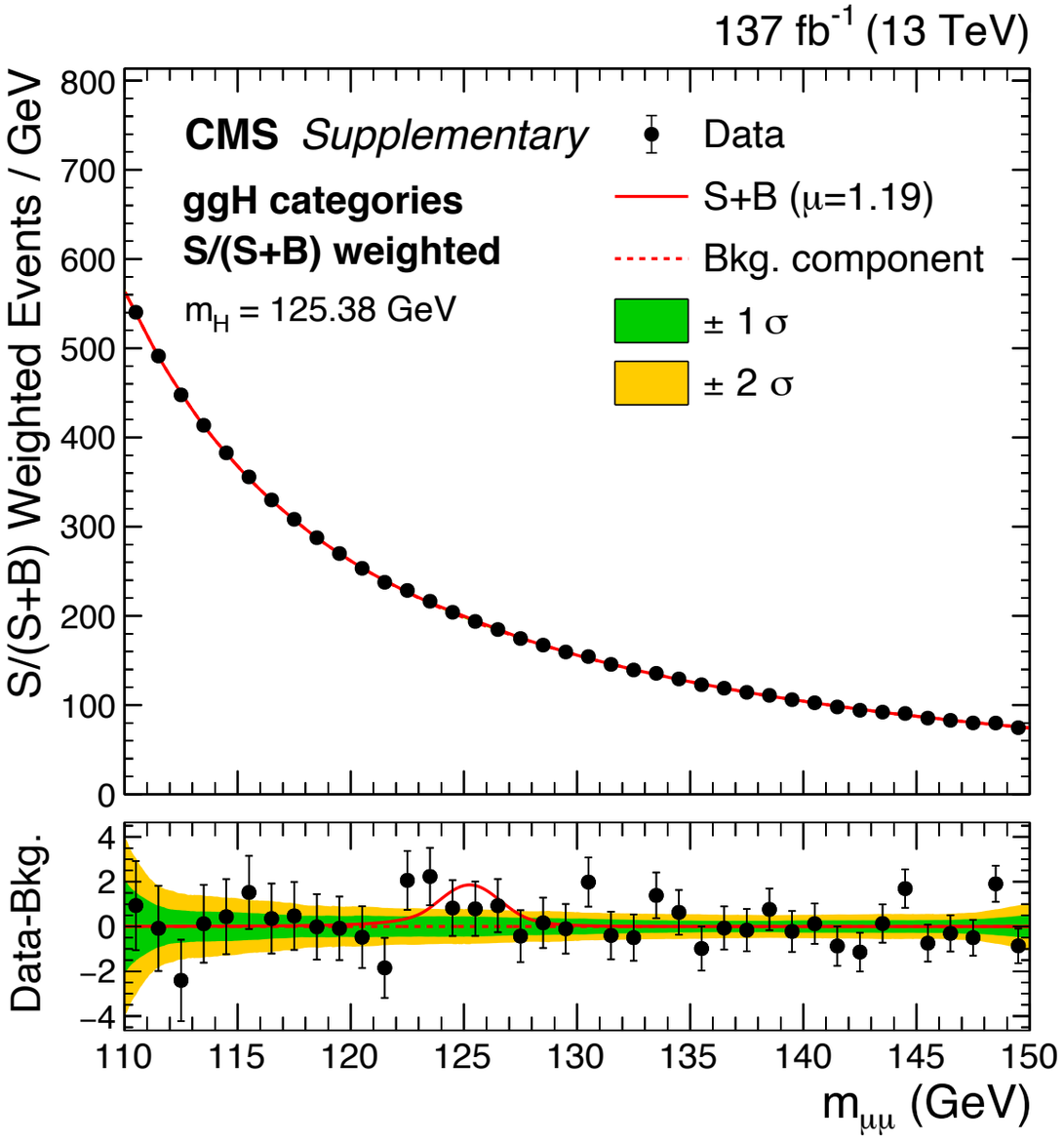

Observed (expected)

significance: 0.99σ (1.56σ)

@m_H = 125.38 GeV

Category	Sig.	ggH (%)	VBF (%)	VH + $t\bar{t}$H (%)	HWHM (GeV)	Bkg. in HWHM	$S/(S+B)$ (%) in HWHM	$S/\sqrt{B}$ in HWHM	Data in HWHM
ggH-cat1	267.6	93.7	2.9	3.4	2.12	86359	0.20	0.60	86632
ggH-cat2	311.5	93.5	3.4	3.1	1.75	46347	0.46	0.98	46393
ggH-cat3	131.4	93.2	4.0	2.8	1.60	12655	0.70	0.80	12738
ggH-cat4	125.6	91.5	5.5	3.0	1.47	8259	1.03	0.96	8377
ggH-cat5	53.8	83.5	14.3	2.2	1.50	1678	2.16	0.91	1711

ggH candidate event

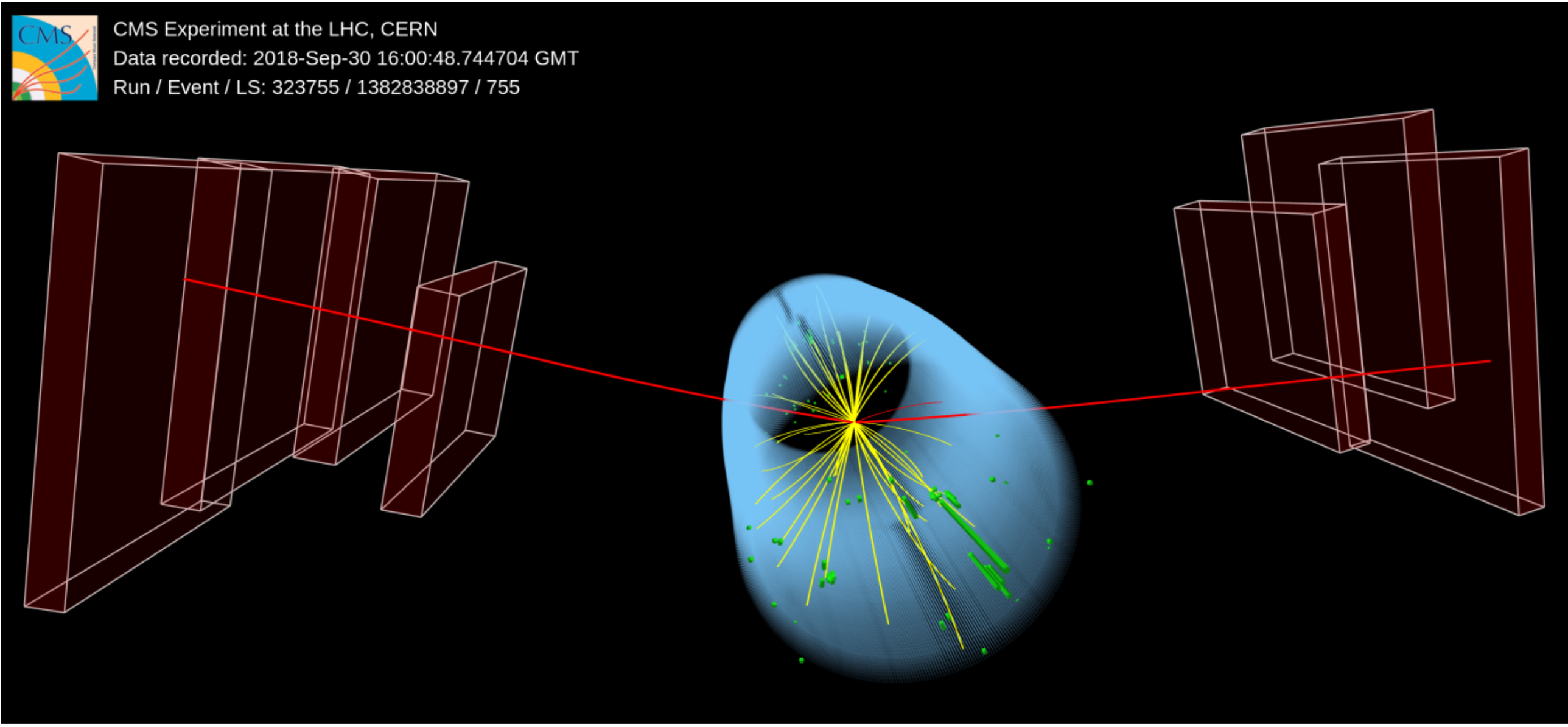

ggH event candidate
$m_{\mu\mu}$ = 125.46 GeV, $\sigma(m_{\mu\mu})$ = 1.33 GeV

ttH channel: overview

- ttH leptonic: extra leptons (e or μ)
  - additional MVA identification for leptons *PRL 122, 132003 (2019)* to reduce background with non-prompt leptons from $t\bar{t}$ and DY
- ttH hadronic: N_{jets} >= 3, no extra lepton
  - hadronic top tagging *PRL 122, 011803 (2019)* used to increase signal purity

ttH signal

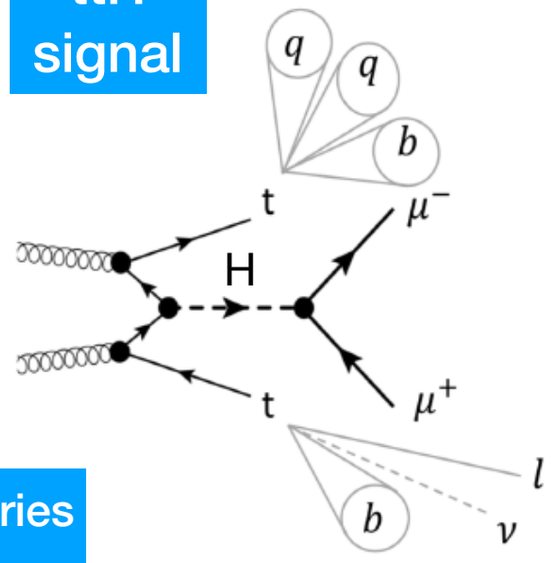

three ttH hadronic categories
main background: $t\bar{t}$

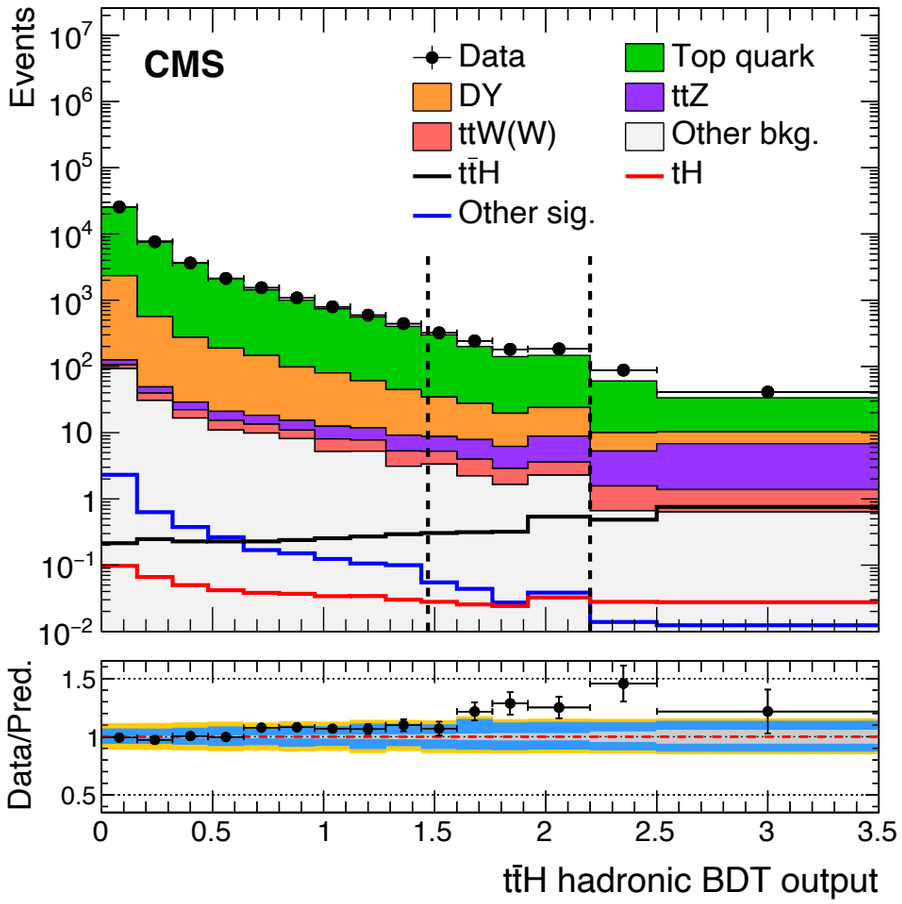

two ttH leptonic categories
main bkg: ttZ

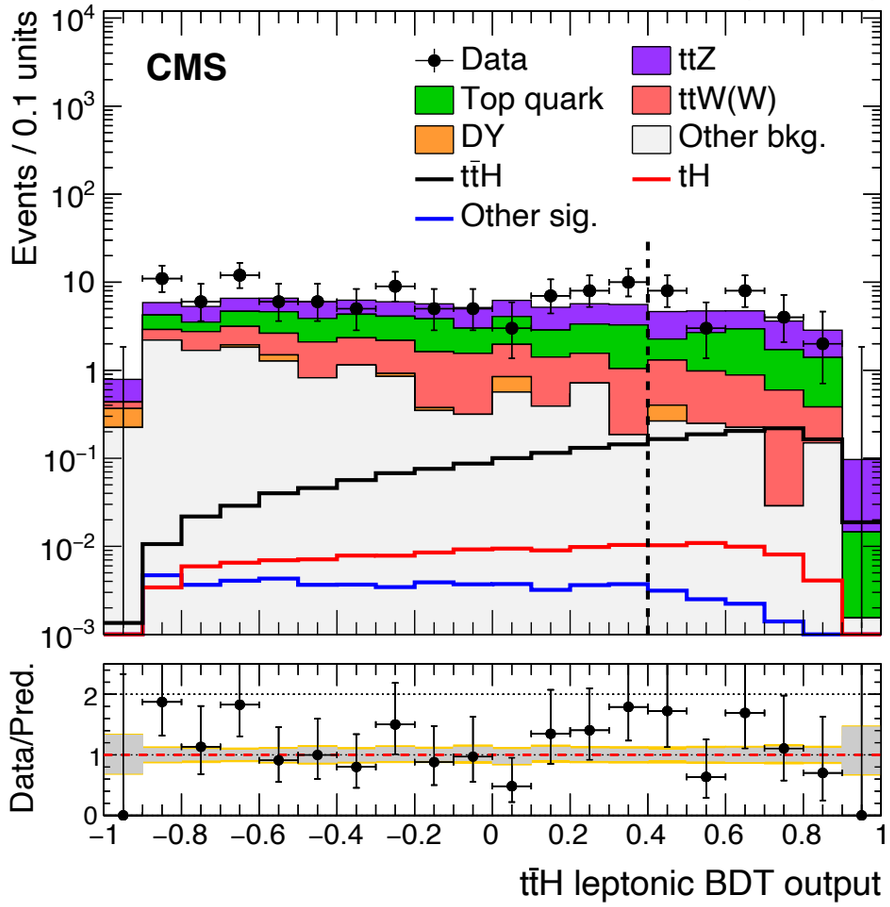

ttH channel: results

Fit strategy and signal modeling similar to ggH categories

- background functional form using agnostic functions:
  - second-order Bernstein polynomial for ttH-hadronic
  - exponential functions for ttH-leptonic

- observed (expected) significance: 1.20σ (0.54σ), m_H = 125.38 GeV

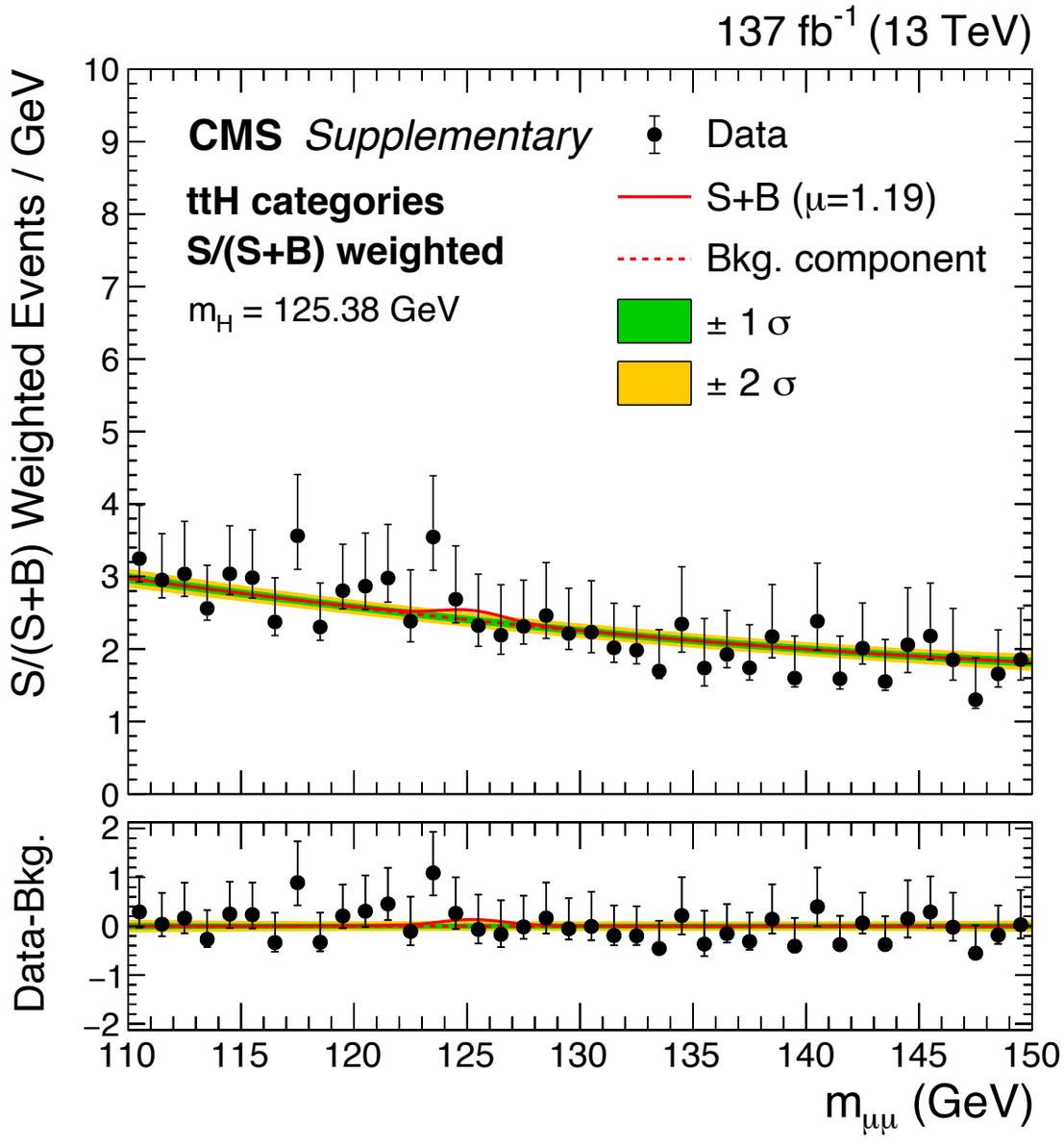

Category	Sig.	ttH (%)	ggH (%)	VH (%)	tH (%)	VBF+bbH (%)	HWHM (GeV)	Bkg. in HWHM	S/(S+B) (%) in HWHM	S/√B in HWHM	Data in HWHM
ttHhad-cat1	6.87	32.3	40.3	17.2	6.2	4.0	1.85	4298	1.07	0.07	4251
ttHhad-cat2	1.62	84.3	3.8	5.6	6.2	—	1.81	82.0	1.32	0.12	89
ttHhad-cat3	1.33	94.0	0.3	1.3	4.2	0.2	1.80	12.3	6.87	0.26	12
ttHlep-cat1	1.06	85.8	—	4.7	9.5	—	1.92	9.00	7.09	0.22	13
ttHlep-cat2	0.99	94.7	—	1.0	4.3	—	1.75	2.08	24.5	0.47	4

ttH candidate event

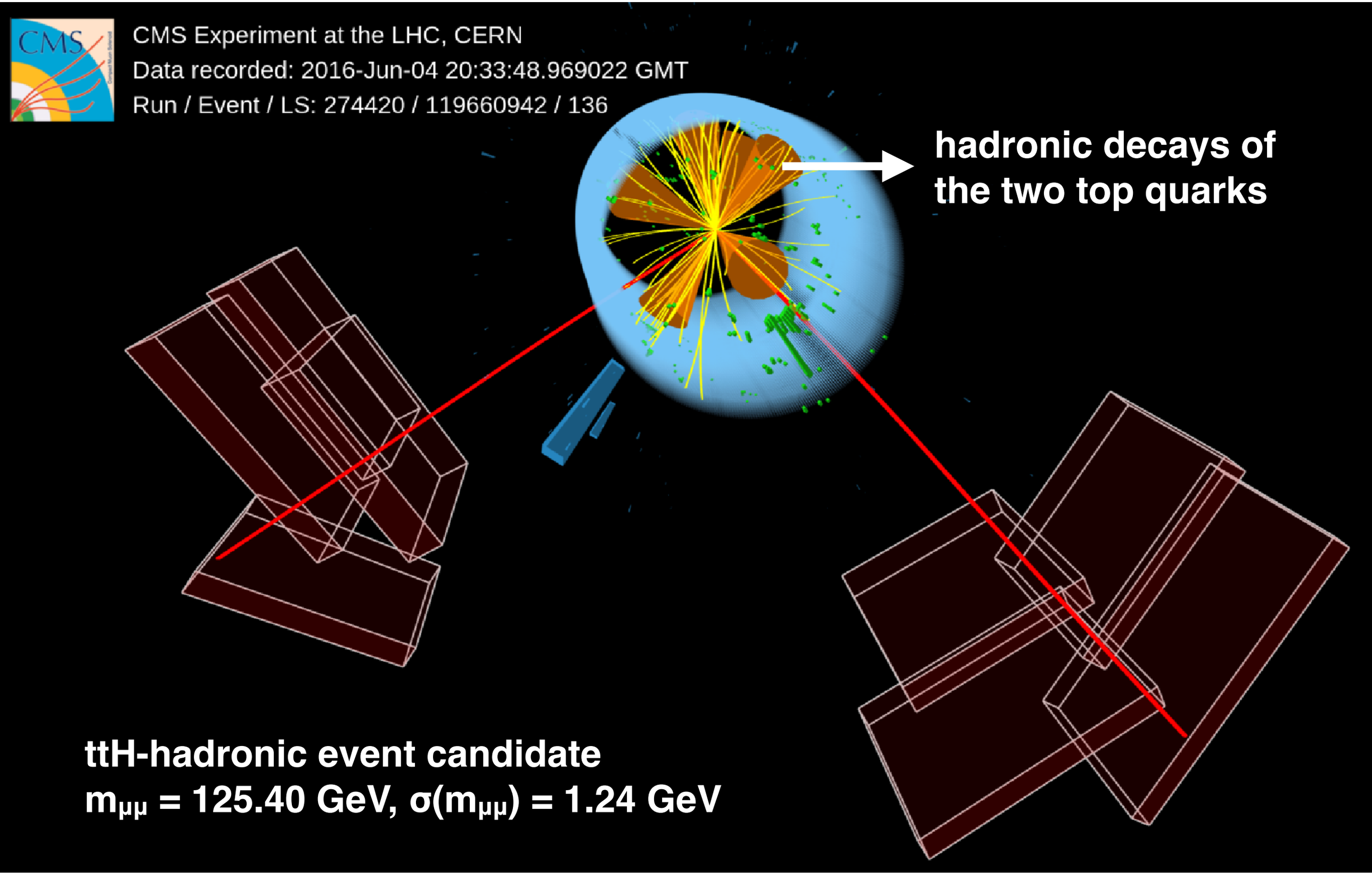

VH channel: overview

- One extra lepton in WH category, additional same-flavor opposite-charge lepton pair for ZH category
- Additional MVA identification for leptons (as in ttH categories) to increase signal purity and reject non-prompt leptons coming from $t\bar{t}$ and DY
- Optimized lepton pairing forming the Higgs boson candidate

3 WH categories

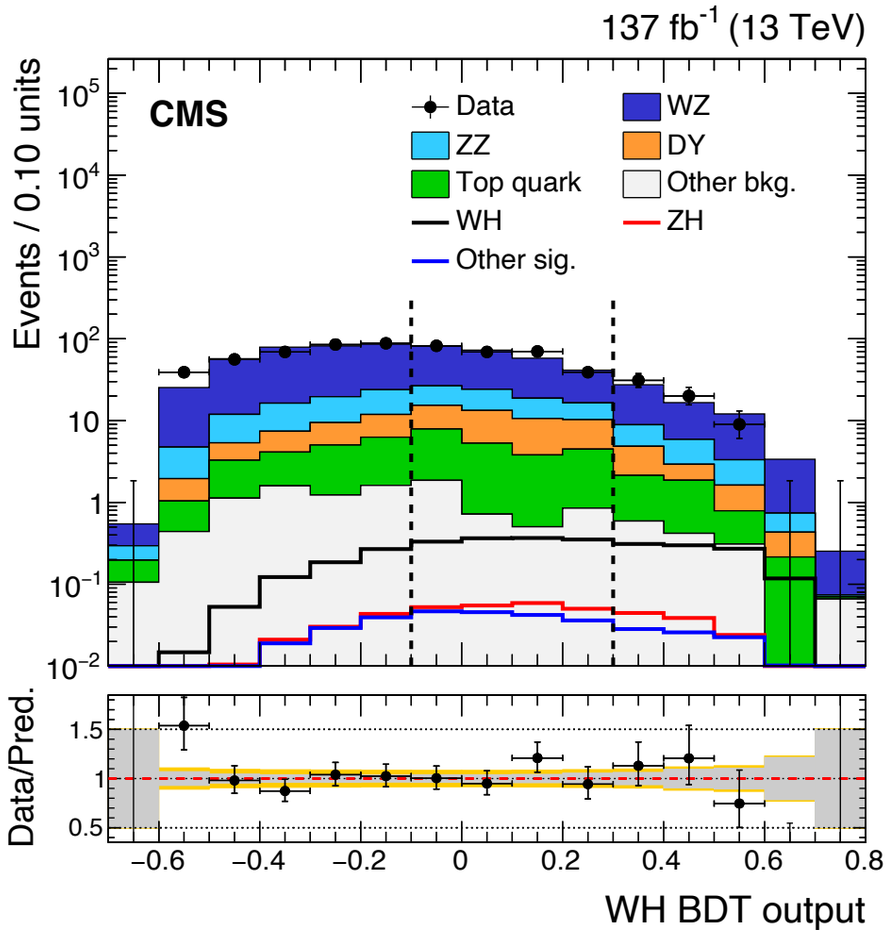

2 ZH categories

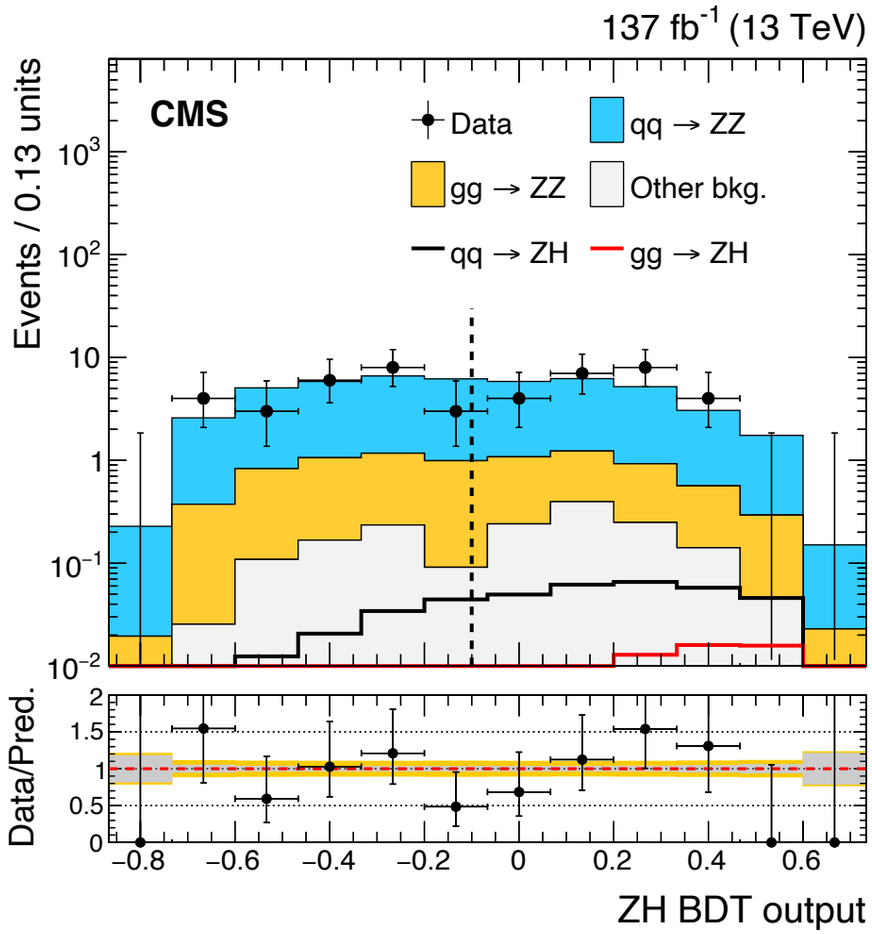

VH channel: results

Fit strategy and signal modeling similar to ggH categories

- Background functional form:
  - modified Breit-Wigner => due to background dominated by WZ and ZZ

- Observed (expected) significance: 2.02σ (0.42σ), m_H = 125.38 GeV

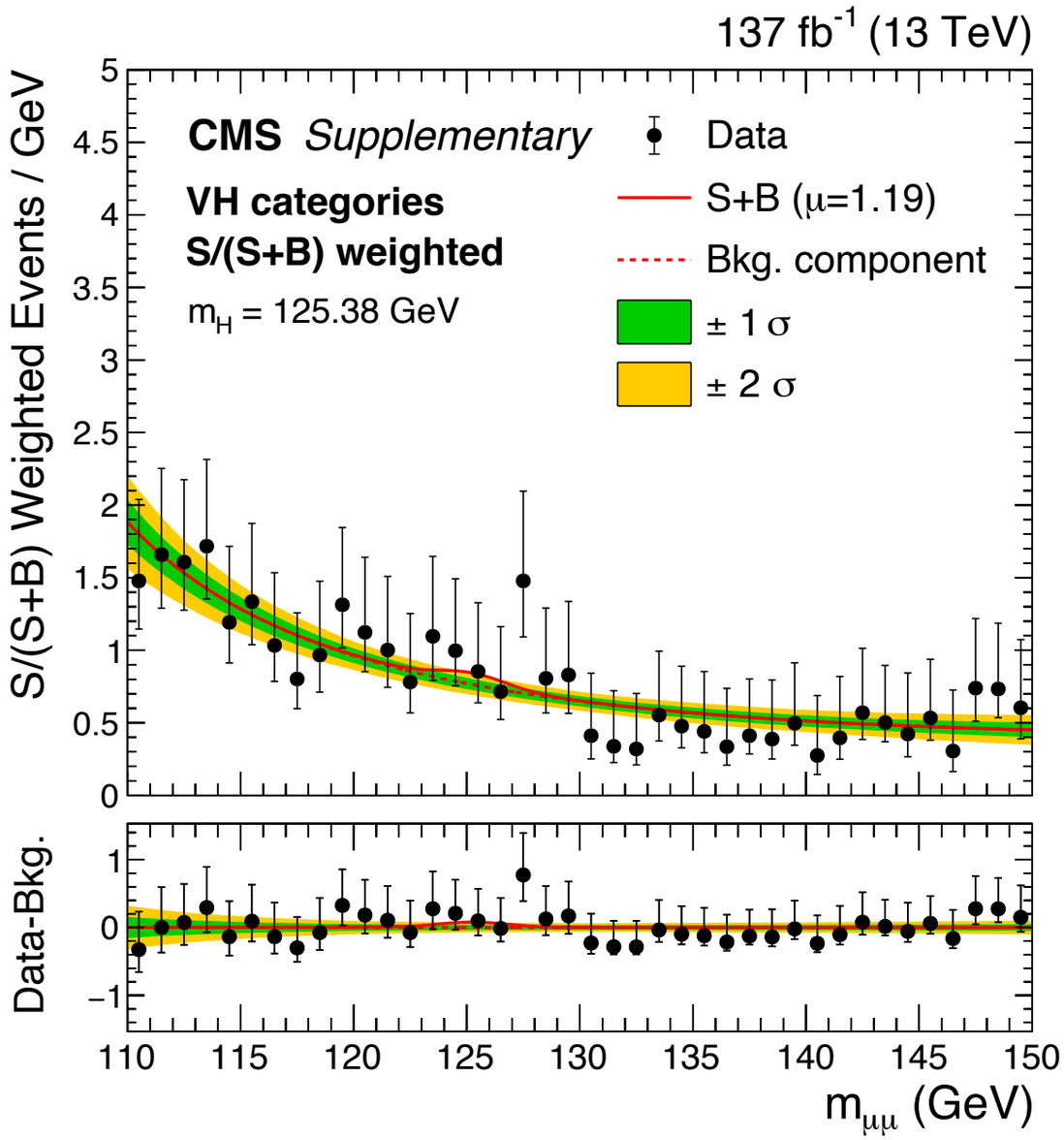

Category	Sig.	WH (%)	qqZH (%)	ggZH (%)	$t\bar{t}H + tH$ (%)	HWHM (GeV)	Bkg. in HWHM	$S/(S+B)$ (%) in HWHM	$S/\sqrt{B}$ in HWHM	Data in HWHM
WH-cat1	0.82	76.2	9.6	1.6	12.6	2.00	32.0	1.54	0.09	34
WH-cat2	1.72	80.1	9.1	1.5	9.3	1.80	23.1	4.50	0.23	27
WH-cat3	1.14	85.7	6.7	1.8	4.8	1.90	5.48	12.6	0.35	4
ZH-cat1	0.11	—	82.8	17.2	—	2.07	2.05	3.29	0.05	4
ZH-cat2	0.31	—	79.6	20.4	—	1.80	2.19	8.98	0.14	4

WH candidate event

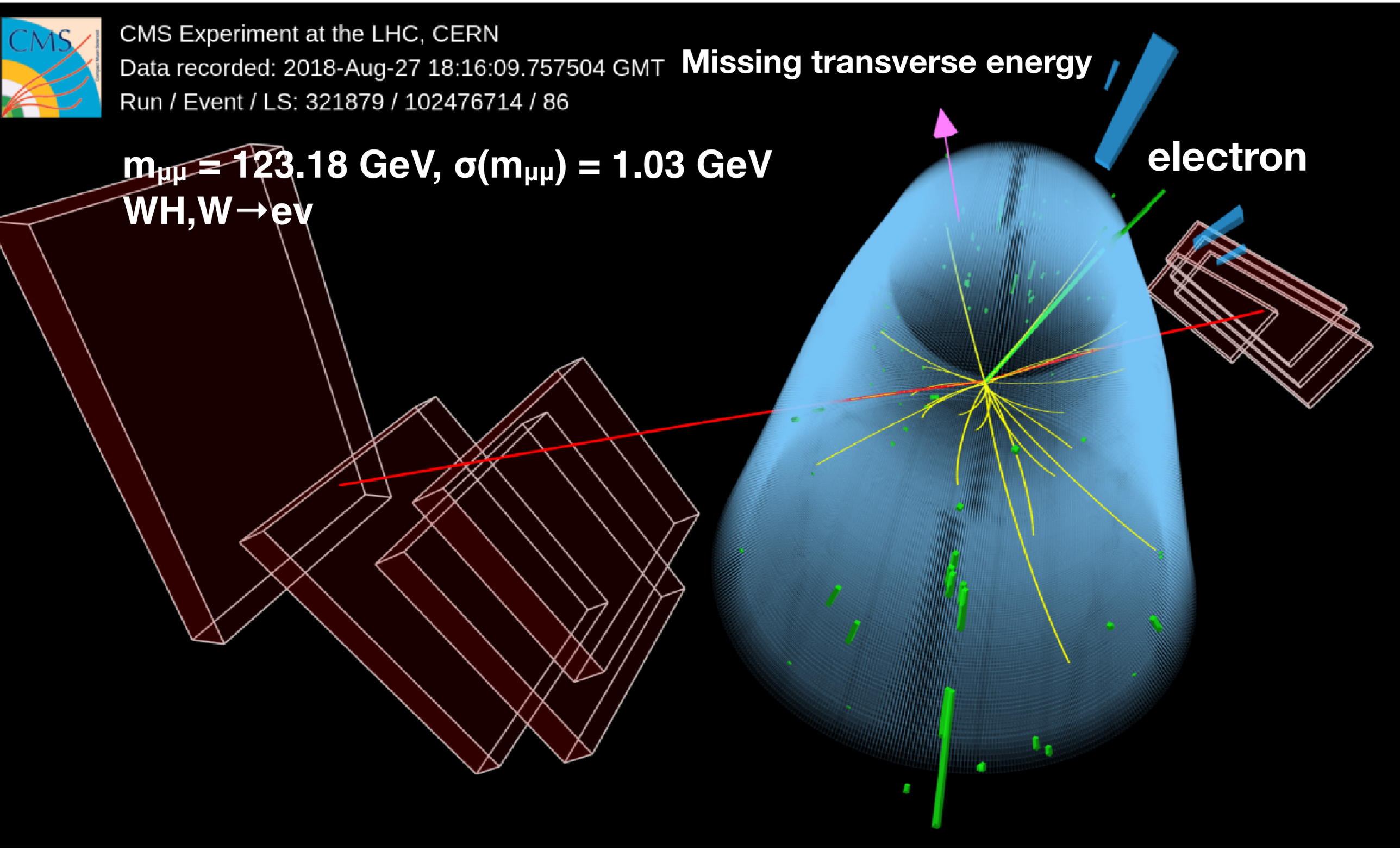

VBF: MC template fit method

VBF channel: overview

- Signal event yield in VBF categories is small: ~48 signal events expected
- New strategy based on MC:
  - good MC simulation precision in modeling VBF Higgs signal and relevant backgrounds: Drell-Yan Z→μμ + jets, electroweak Z + jets production
  - CMS has performed intensive measurements on main background DY and electroweak Z+2jets
  - sideband region to control the background prediction from MC

VBF Higgs signal

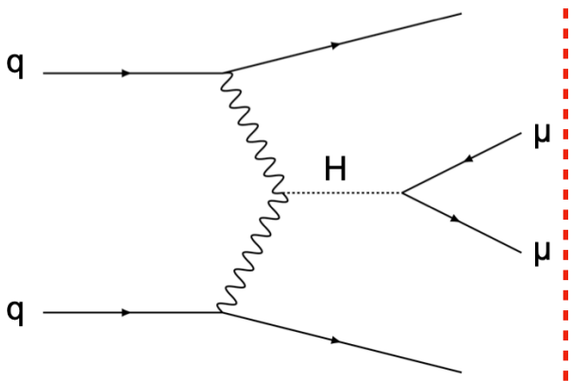

main background: electroweak production of two jets in association with a Z boson

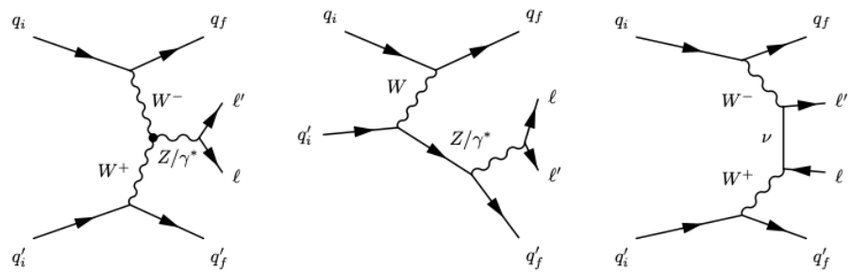

main background: Drell–Yan production with two jets

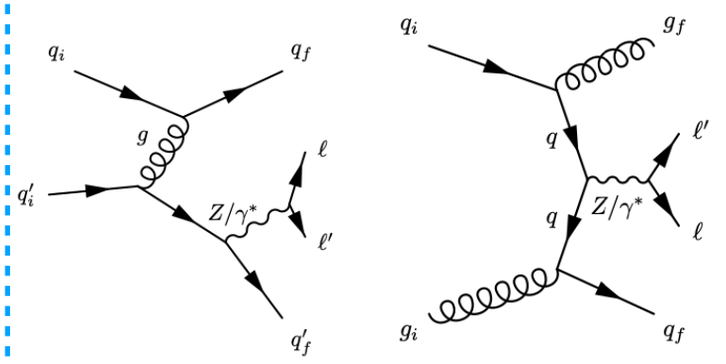

- Deep neural network (DNN) output score used as final discriminant
  - 20% improvement compared to mass fit method
  - Analysis strategy similar to the CMS study on electroweak Z+2jets production:
    - *JHEP 10 (2013) 101 (7 TeV), Eur. Phys. J. C 75 (2015) 66 (8 TeV observation), Eur. Phys. J. C 78 (2018) 589 (13 TeV measurement)*

VBF channel: Deep Neural Network

- DNN trained on kinematic information of the two muons and VBF signature (24 variables):
  - **Dimuon variables:** $m_{\mu\mu}$, $\sigma(m_{\mu\mu})$, $m_{\mu\mu}/\sigma(m_{\mu\mu})$, $p_{T\mu\mu}$, $\log(p_{T\mu\mu})$, $y_{\mu\mu}$, $\cos\theta^*$, ϕ^*
  - **Dijet variables:** pT, η, ϕ of jet_1, jet_2, $\log(m_{jj})$, m_{jj}, $\Delta\eta_{jj}$
  - **Soft track-jet variables:** $N_{\text{soft jet} > 5\text{ GeV}}$, $H_{T\text{ soft jet} > 2\text{ GeV}}$ (H_T: scalar sum of p_T):
    - jets reconstructed by charged tracks associated to the primary vertex
    - not associated with jet_1, jet_2 or the two muons
  - **Kinematic variable of the dimuon (μμ) and dijet system**
    - $\text{mim}(\Delta\eta(\mu\mu, jet_1), \Delta\eta(\mu\mu, jet_2))$
    - Zeppenfeld variable
    - pT balance ratio of μμ and jets $R(p_T) = \dfrac{|\vec{p}_T^{\,\mu\mu} + \vec{p}_T^{\,jj}|}{p_T^{\mu\mu} + p_T(j_1) + p_T(j_2)}$

most sensitive variable: $m_{\mu\mu}$

- **Quark/gluon likelihood:** jet_1, jet_2 (jets in DY process can originate from gluons)

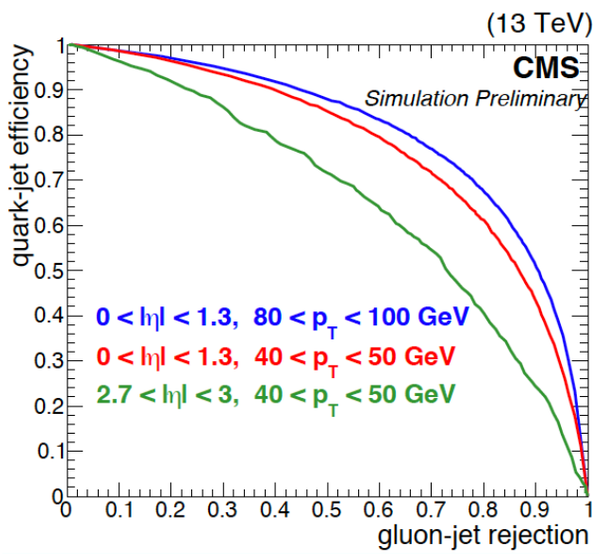

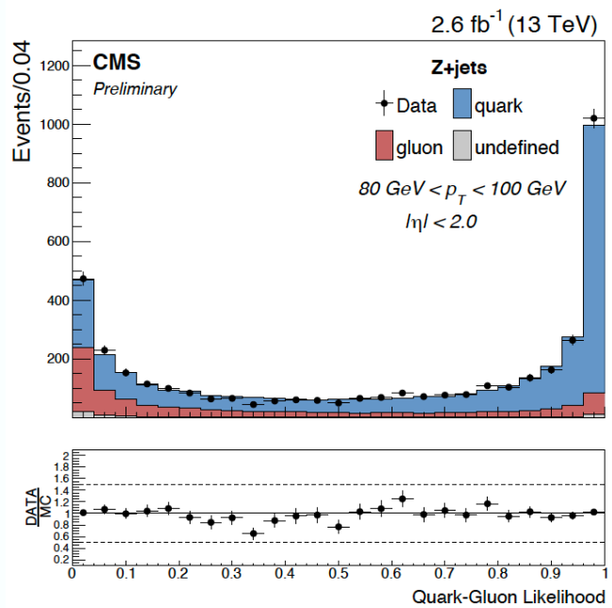

VBF channel: fitting strategy

Simultaneously fit in 6 VBF categories in total (signal and sideband regions in each year 2016, 17 and 18)

- DY separated into DY+2jet and DY+pileup/noise (for the latter: event yield is a free parameter in the fit)

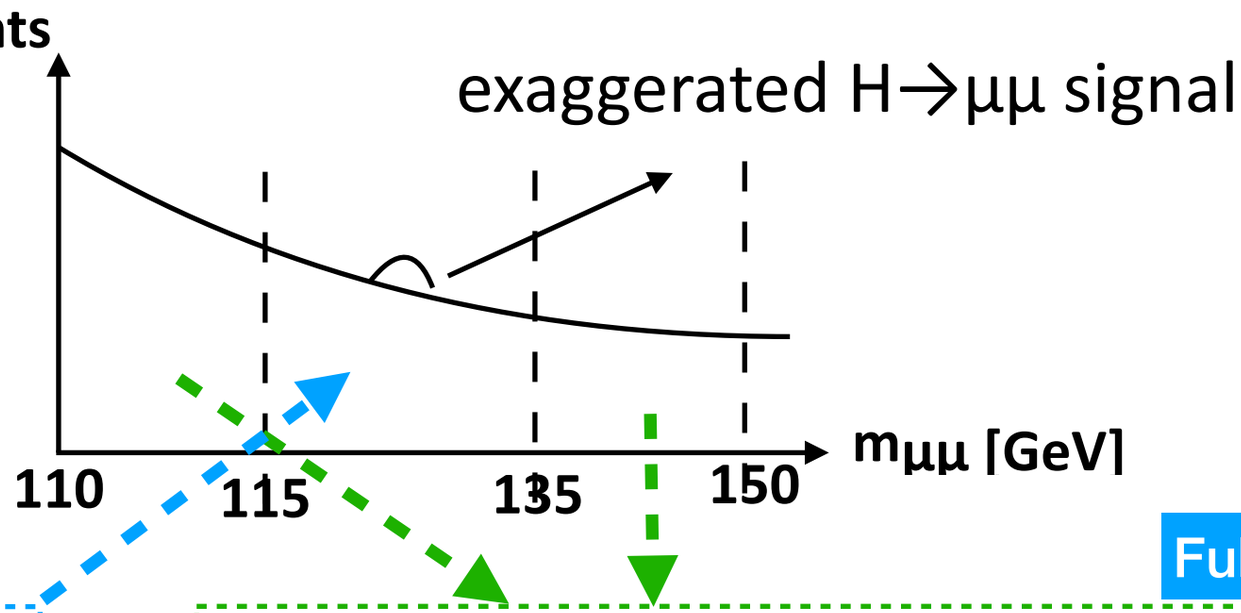

Full Run 2

signal region

115 < $m_{\mu\mu}$ < 135 GeV

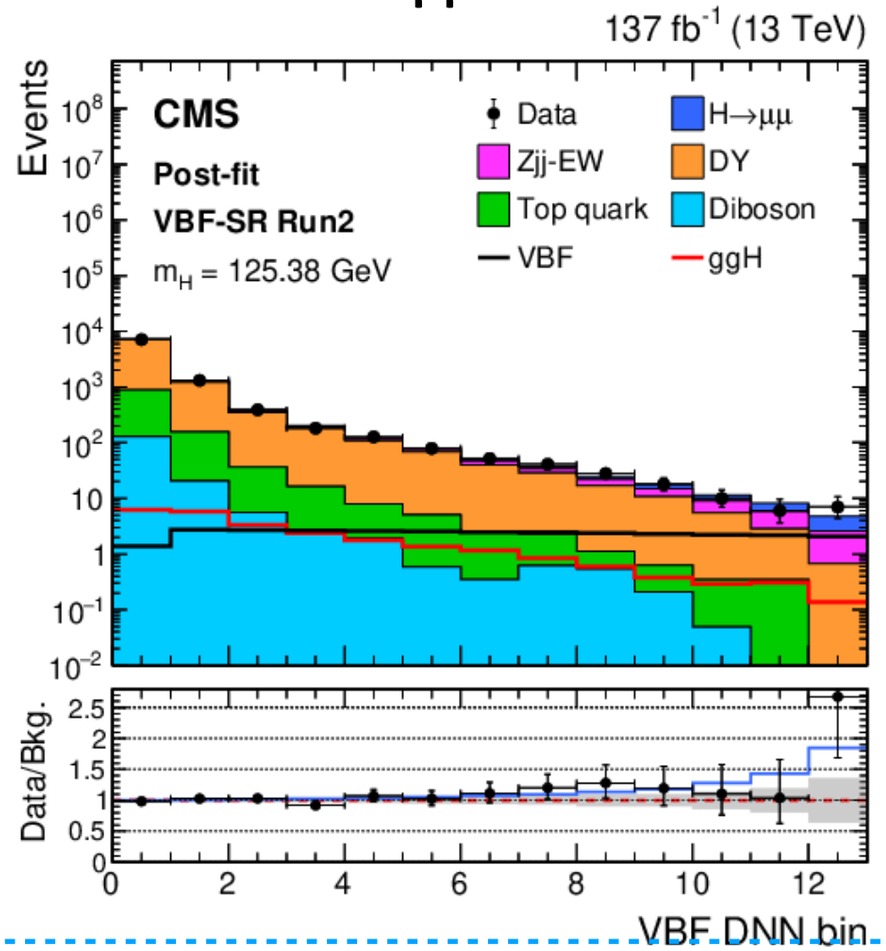

Full Run 2

sideband region: constraint background

110 < $m_{\mu\mu}$ < 115 GeV or 135 < $m_{\mu\mu}$ < 150 GeV

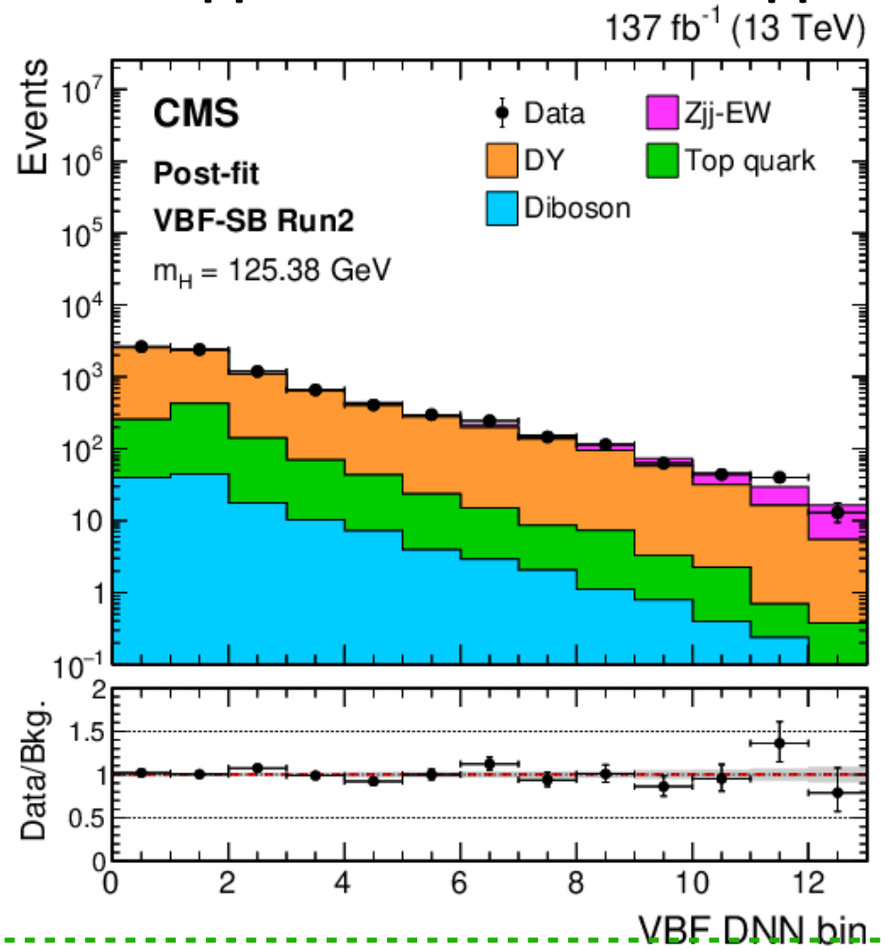

VBF channel: results

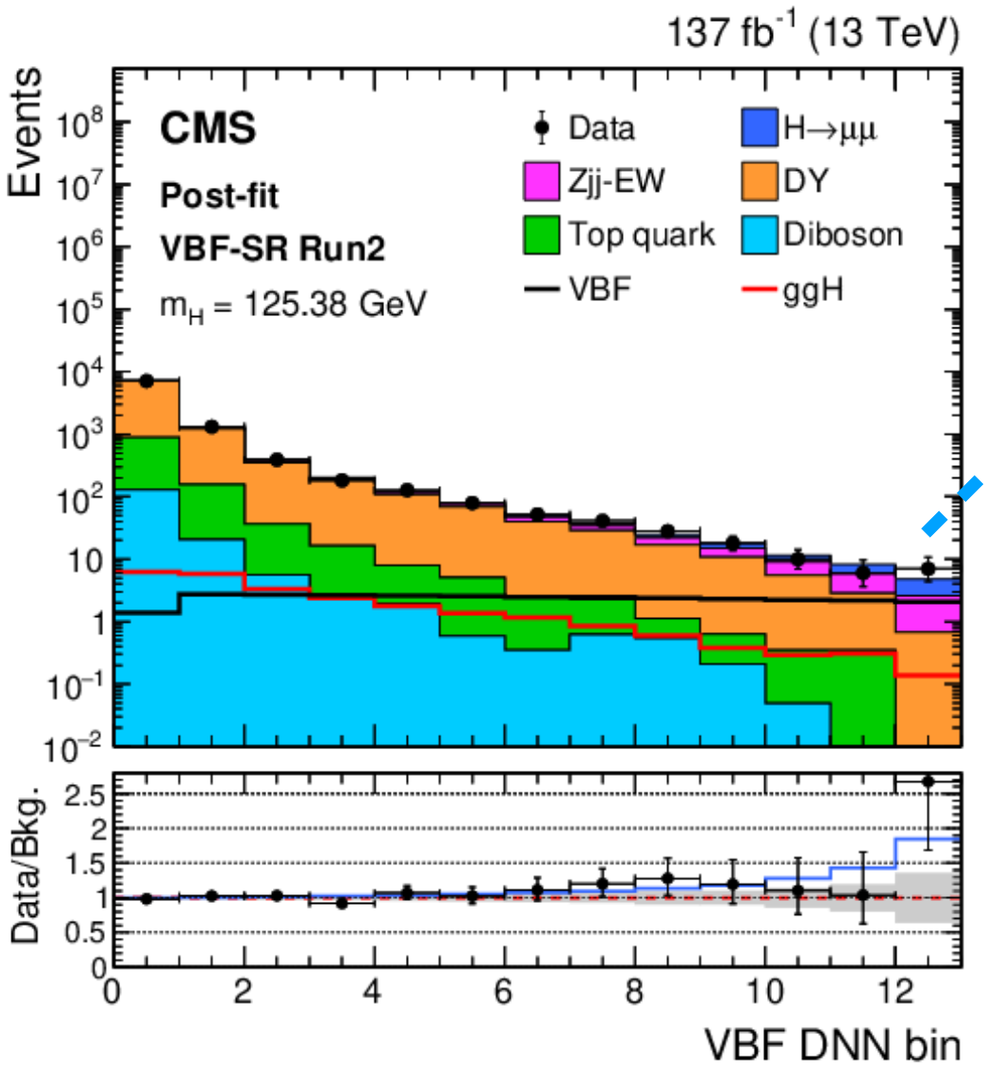

- Achieve unprecedented signal purity in high DNN bins
  - last DNN bin signal purity 42%
  - main background: electroweak Z+2jets, DY+2jets
- 20% improvement in sensitivity compared to $m_{\mu\mu}$ mass fit method
- Observed (expected) significance: 2.40σ (1.77σ), m_H = 125.38 GeV

DNN bin	Signal	VBF (%)	ggH (%)	Bkg. $\pm$ ΔB	S/(S + B) (%)	S/$\sqrt{B}$	Data
1–3	19.5	30	70	8894 $\pm$ 67	0.22	0.21	8815
4–6	11.6	57	43	394 $\pm$ 8	2.90	0.59	388
7–9	8.43	73	27	103 $\pm$ 4	7.66	0.84	121
10	2.30	85	15	15.1 $\pm$ 1.4	13.2	0.60	18
11	2.15	88	12	9.1 $\pm$ 1.2	19.2	0.72	10
12	2.10	87	13	5.8 $\pm$ 1.1	26.7	0.88	6
13	1.87	94	6	2.6 $\pm$ 0.9	41.8	1.18	7

VBF candidate event

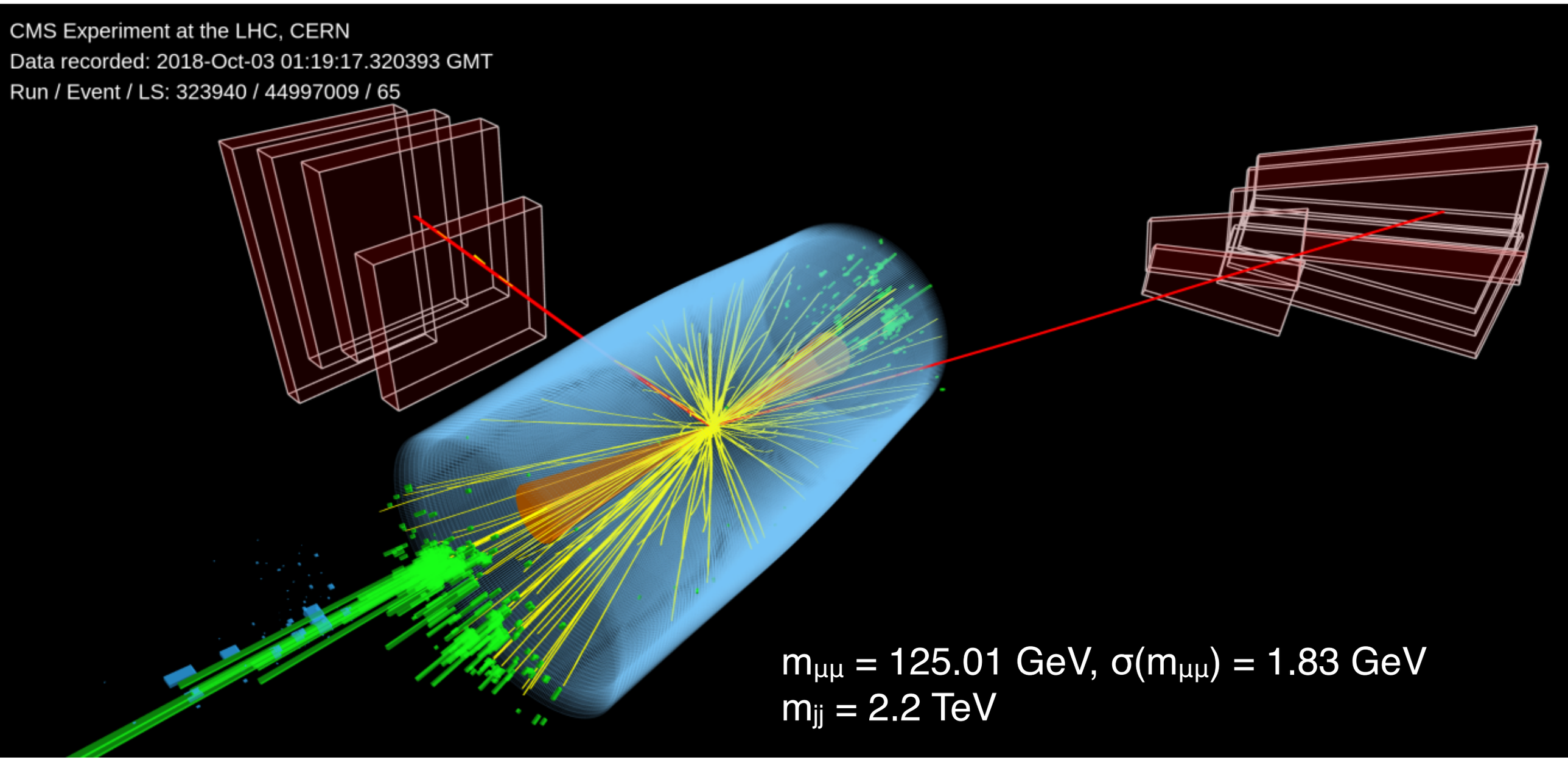

Evidence of H→μμ

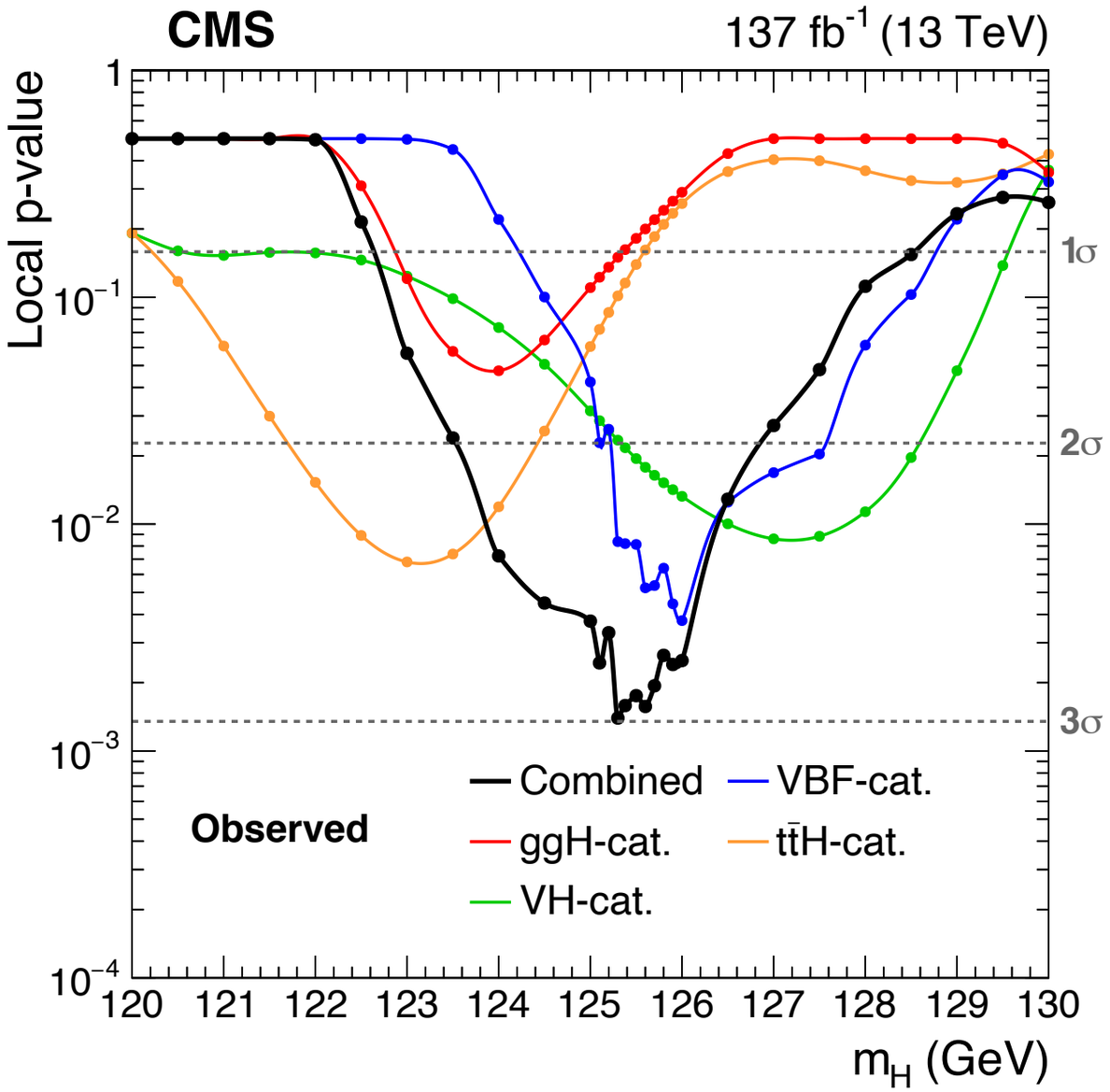

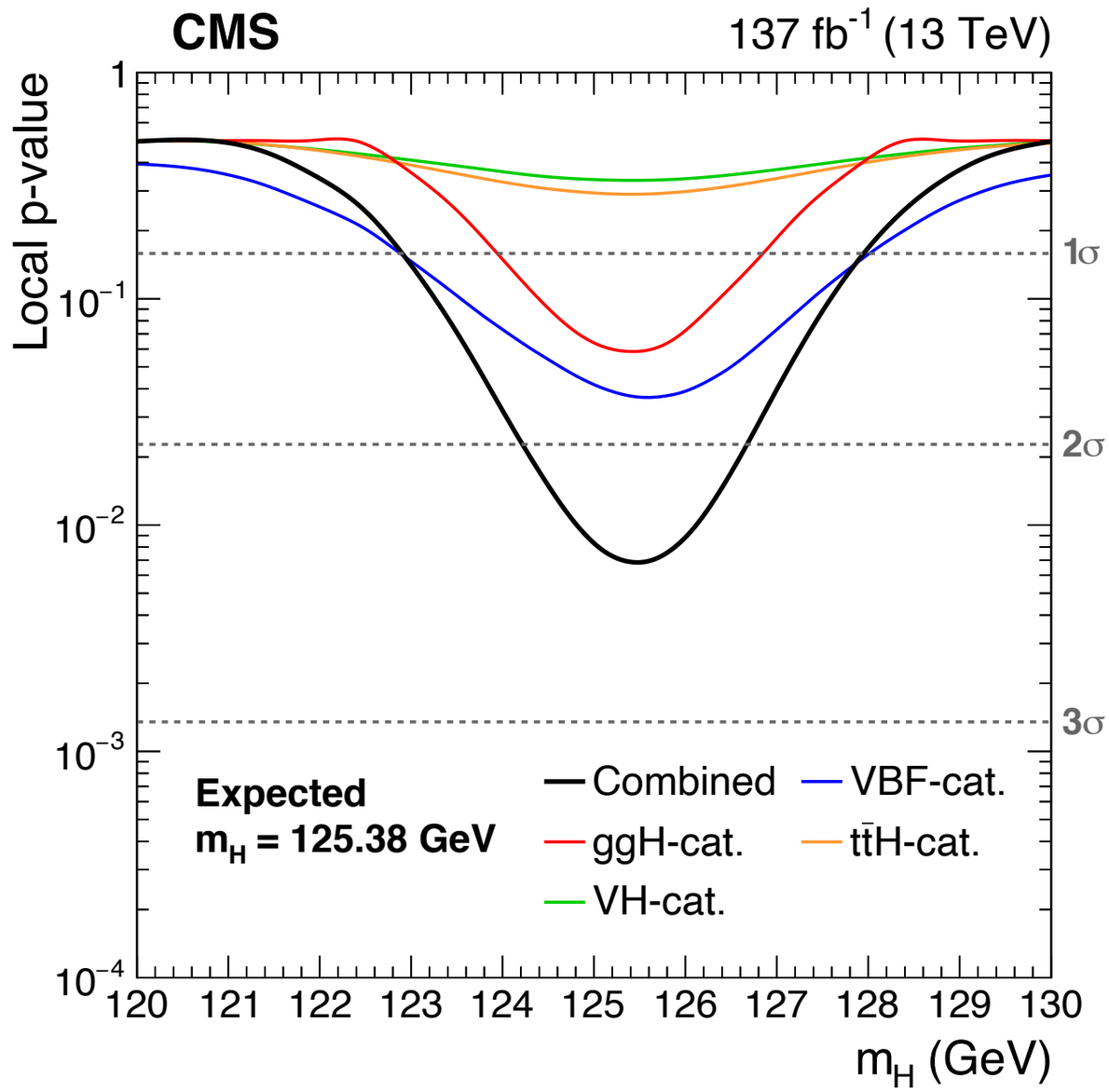

@m_H = 125.38 GeV:

- Run 2: observed (expected) significance 2.95σ (2.46σ)
- Run 2 + Run 1: observed (expected) significance 2.98σ (2.48σ), 1% improvement by adding Run 1 result

Signal strength measurement of H→μμ

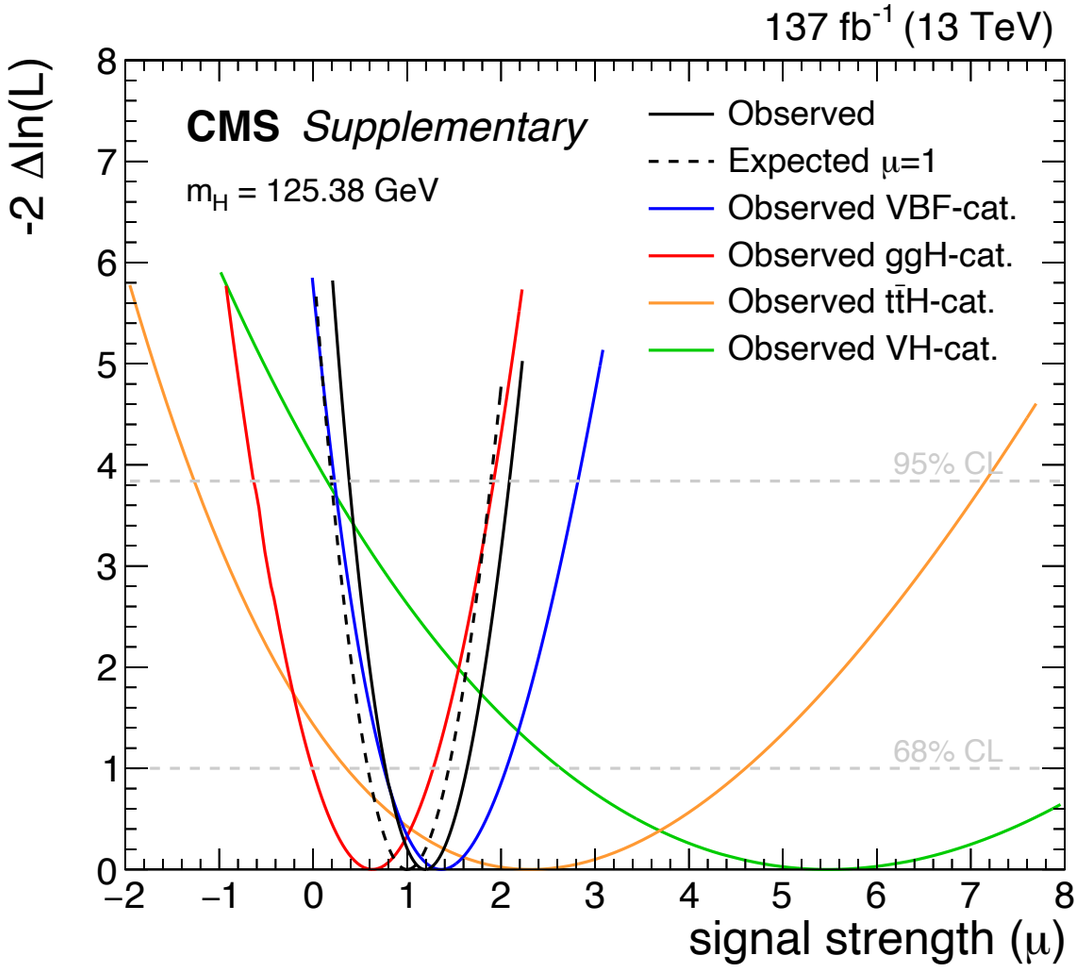

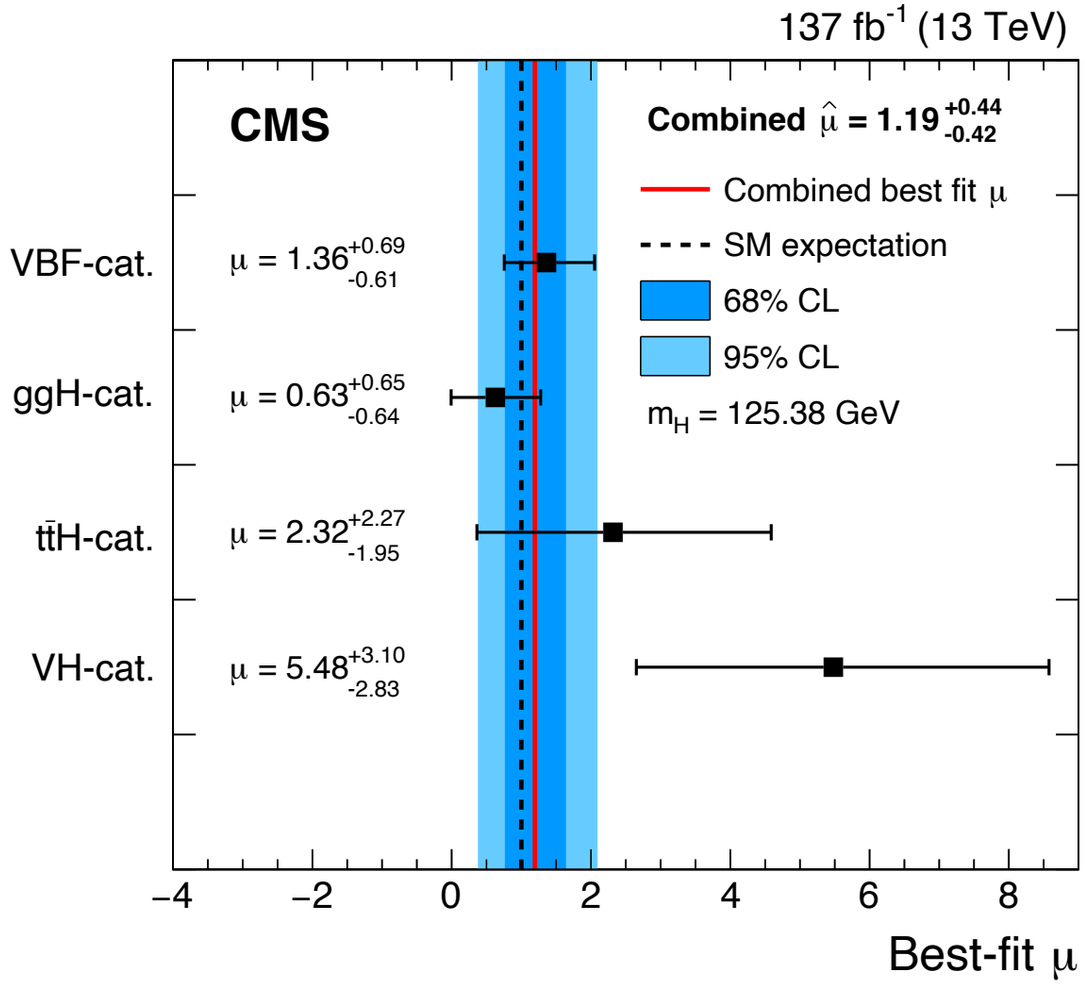

Combined signal strength of all channels : $\mu = \sigma B(H \to \mu\mu)_{obs} / \sigma B(H \to \mu\mu)_{SM}$

$$\mu = 1.19^{+0.44}_{-0.42} = 1.19^{+0.41}_{-0.39}(stats.)^{+0.10}_{-0.11}(theo.)^{+0.12}_{-0.10}(exp.)^{+0.07}_{-0.06}(MCstats.)$$

measurement dominated by statistical uncertainty in data

Boson and fermion-mediated production processes

Higgs production modes:

Fermion mediated

$$\mu^{\mu\mu}_{gg,ttH} = \mu^{\mu\mu}_{ggH} = \mu^{\mu\mu}_{ttH}$$

Boson mediated

$$\mu^{\mu\mu}_{VBF,VH} = \mu^{\mu\mu}_{VBF} = \mu^{\mu\mu}_{VH}$$

2D measurement signal strength in the vector boson vs fermion mediated production modes consistent with SM within 1σ

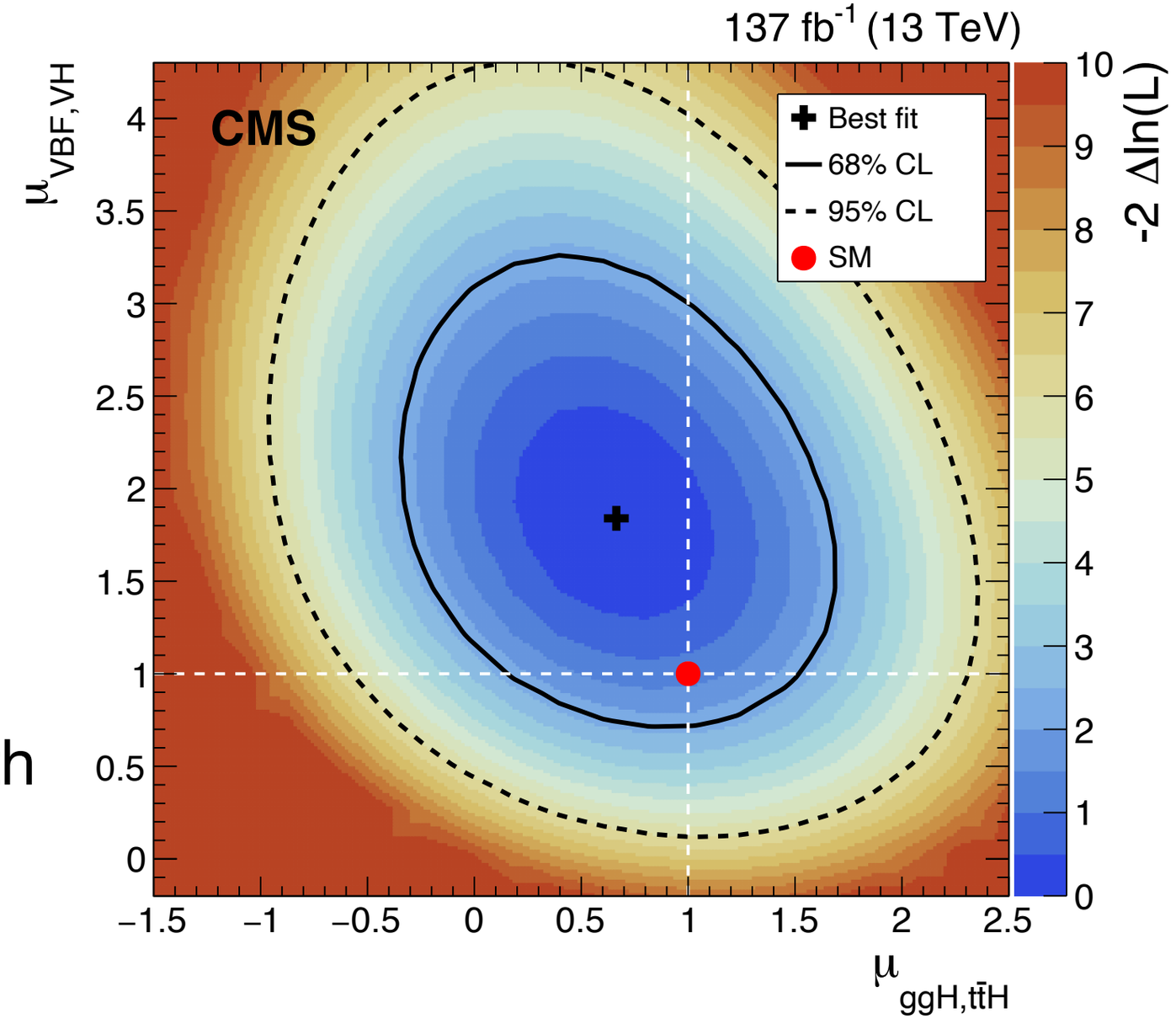

best-fit value:

$$(\hat{\mu^{\mu\mu}_{VBF,VH}},\ \hat{\mu^{\mu\mu}_{ggH,ttH}}) = (0.66,\ 1.84)$$

Higgs boson coupling to muons

- Precision of κ_μ improved from 89% to 19% in two years.
- 35% improvement in analysis strategy

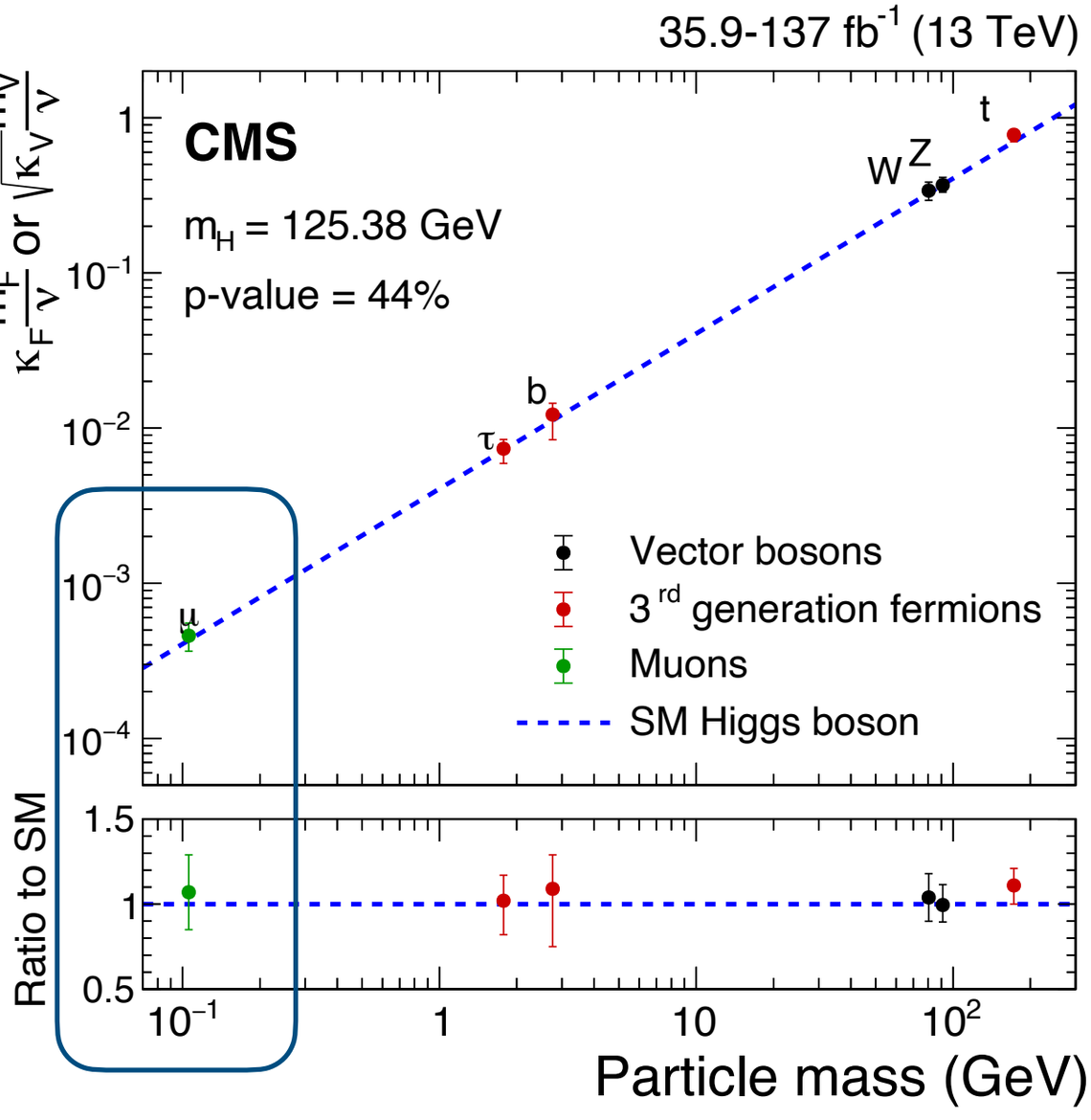

$\kappa_\mu = 1.13^{+0.21}_{-0.22}$ at 68% CL

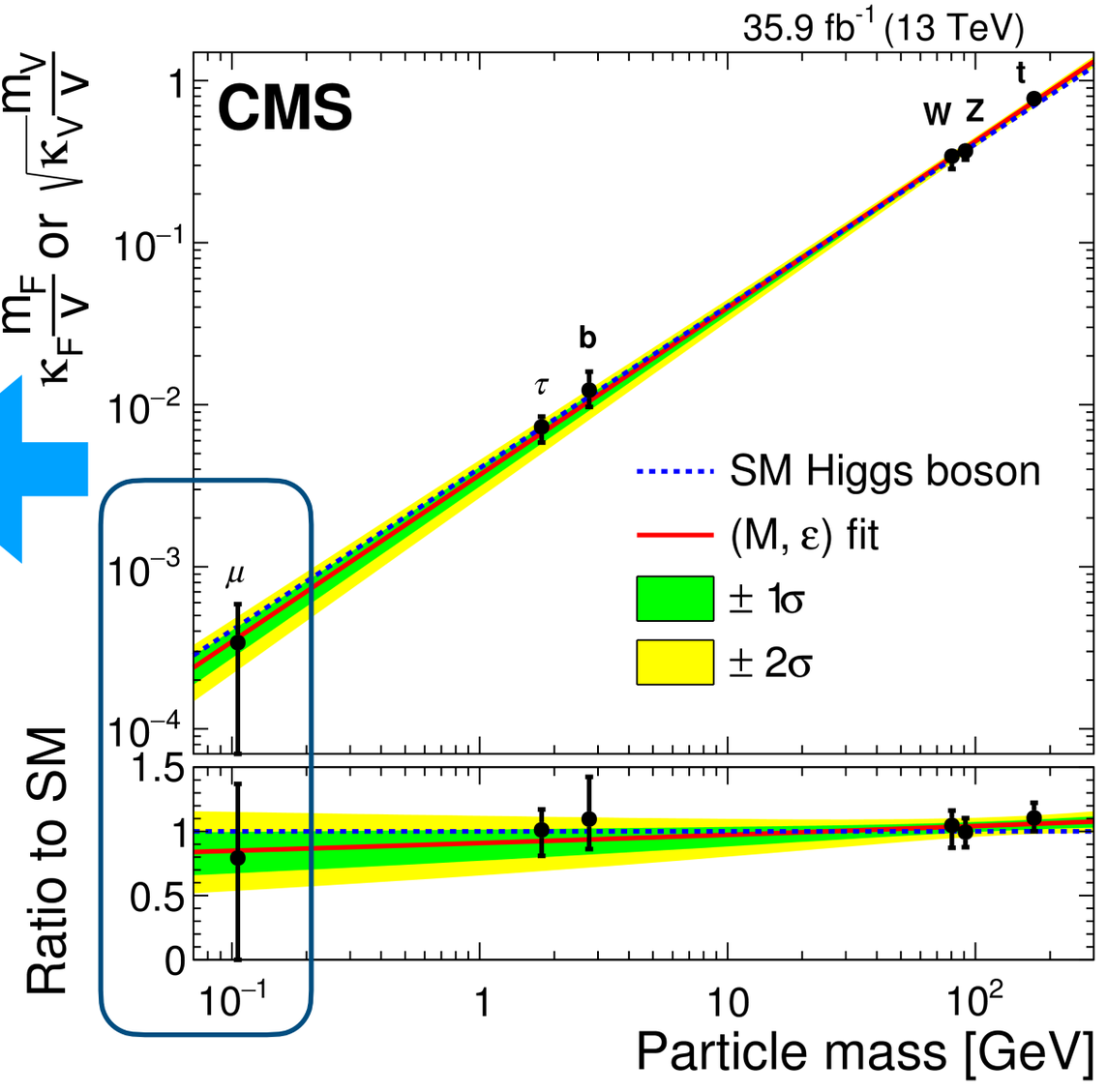

EPJC 79 (2019) 421

$\kappa_\mu = 0.79^{+0.58}_{-0.79}$ at 68% CL

Summary of improvements

- 2016 data analysis (Phys.Rev.Lett.122.021801):
  - bump hunt in m(μμ) spectrum targeting ggH and VBF signals
  - expected sensitivity with 2016 data of 36 fb^{-1}: 1.0σ
- Full Run 2 data analysis strategy has **35% improvement** wrt 2016 data analysis:
  - muon pT corrections: (1) final state radiation recovery (2) muon track momentum correction using interaction point position information
  - new analysis strategy for VBF channel: MC template fits to allow reaching unprecedented signal purity (42% in last DNN bin)
  - significantly improved analysis strategy for the ggH channel:
    - improved BDT, aware of the dimuon resolution
    - robust background modeling with less free parameters: core-pdf method
  - new categories for VH and ttH signals, less explored previously

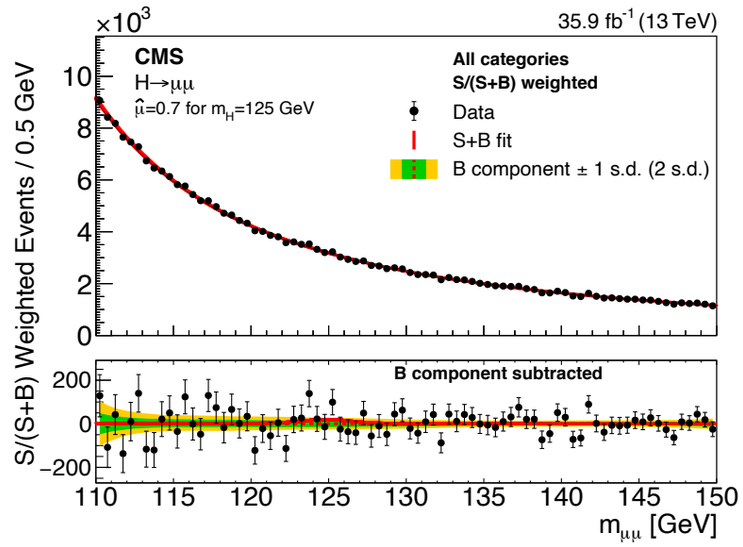

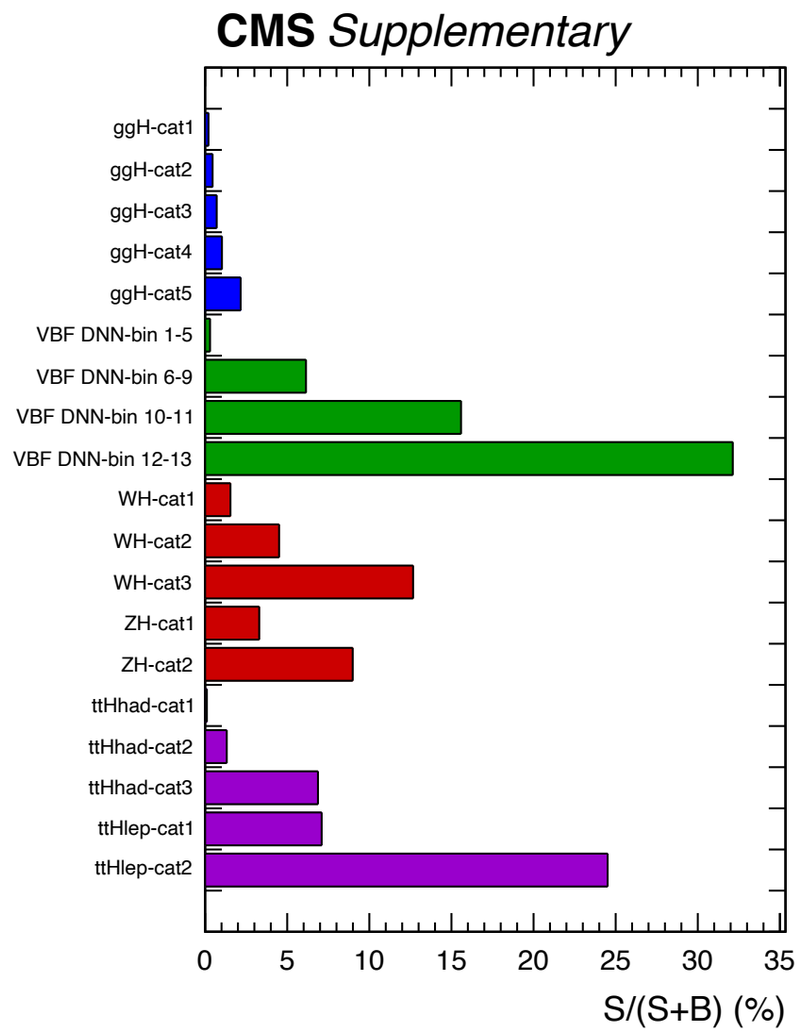

Comparison with ATLAS results

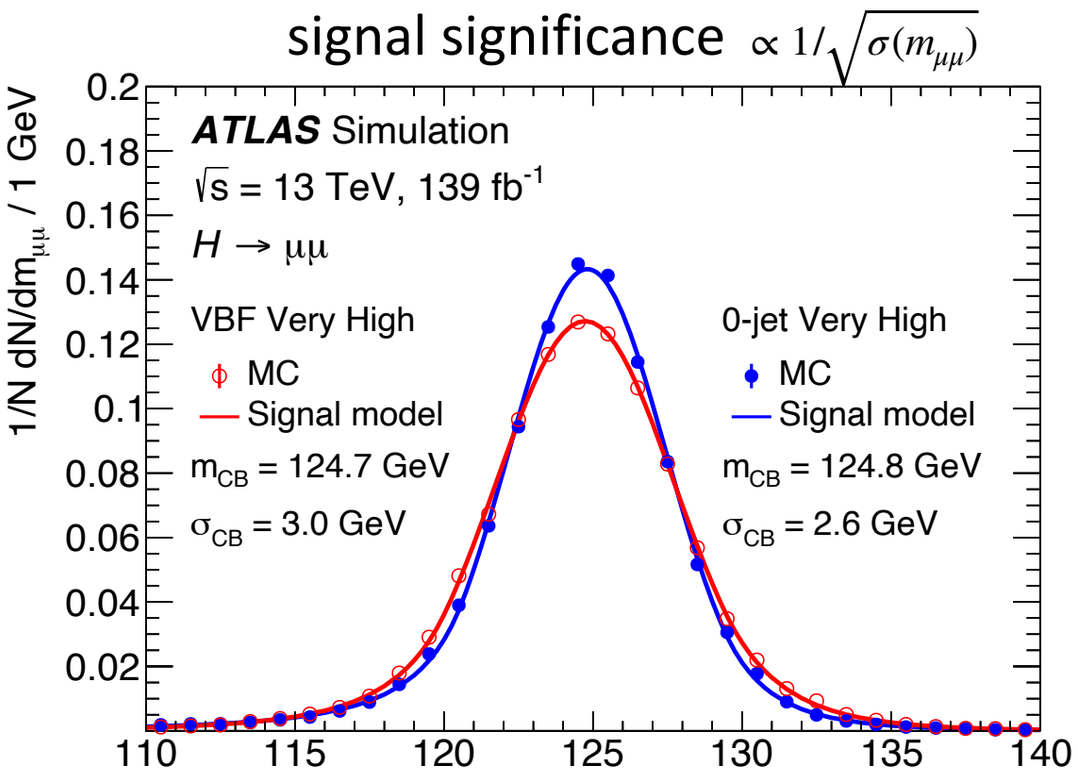

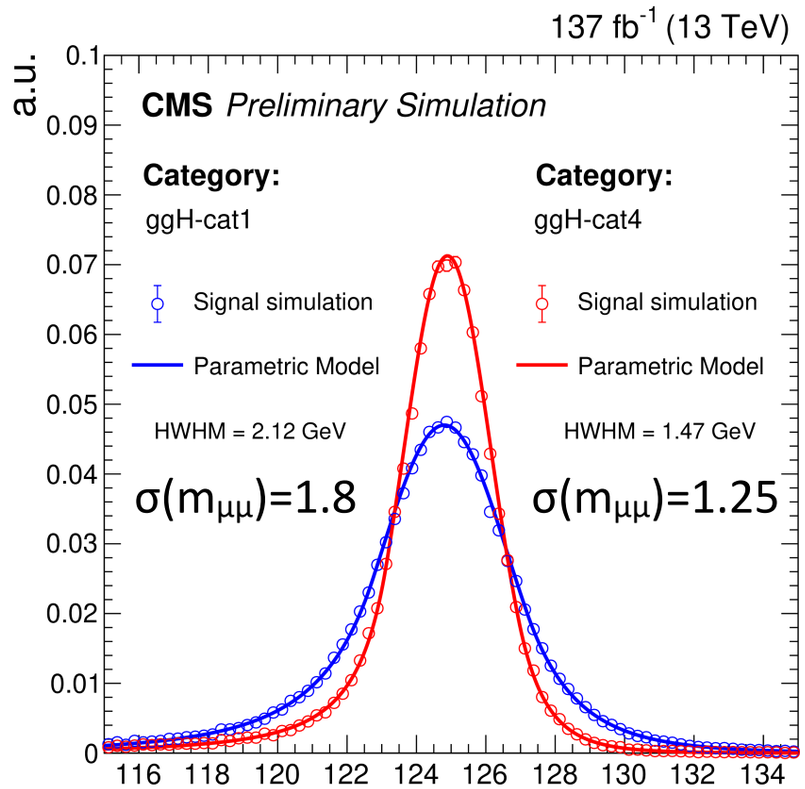

ATLAS:

ATLAS paper submitted to PLB

- Expected significance 1.7σ, observed 2.0σ
- Signal strength: $\mu = 1.2 \pm 0.58(stats.)^{+0.13}_{-0.08}(theory)^{+0.07}_{-0.03}(exp.) \pm 0.10(spurious)$

CMS:

- Expected significance 2.5σ, observed 3.0σ
- Signal strength: $\mu = 1.19^{+0.41}_{-0.39}(stats.)^{+0.10}_{-0.11}(theory)^{+0.12}_{-0.10}(exp.)^{+0.07}_{-0.06}(MCstats.)$

Main difference in the result of two experiments: $\sigma_{CMS}(m_{\mu\mu})/\sigma_{ATLAS}(m_{\mu\mu})$ = 48~60%

Analysis techniques employed by two experiments have rather similar performance

New possibilities in H→μμ with Phase-2 detector upgrades for HL-LHC

An intensive Phase-2 detector upgrade program on-going to meet the challenge of the HL-LHC:

- basic goal is to maintain the current CMS detector performance

pileup up to 140 (200) at HL-LHC

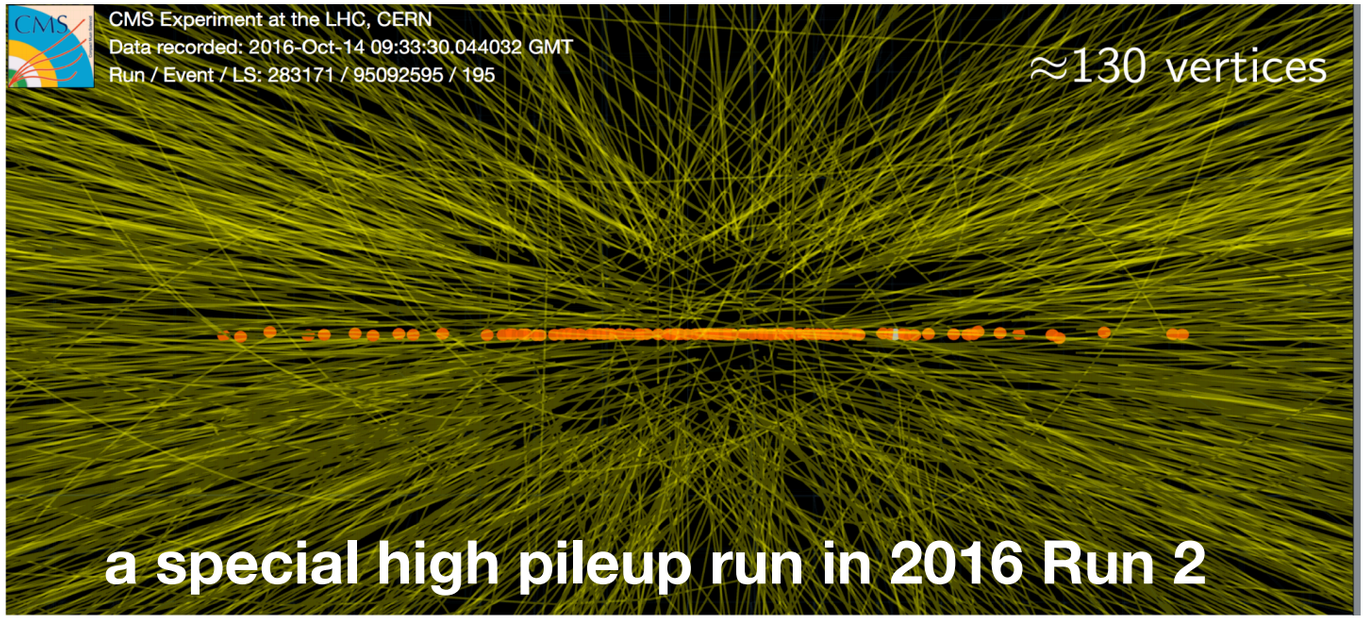

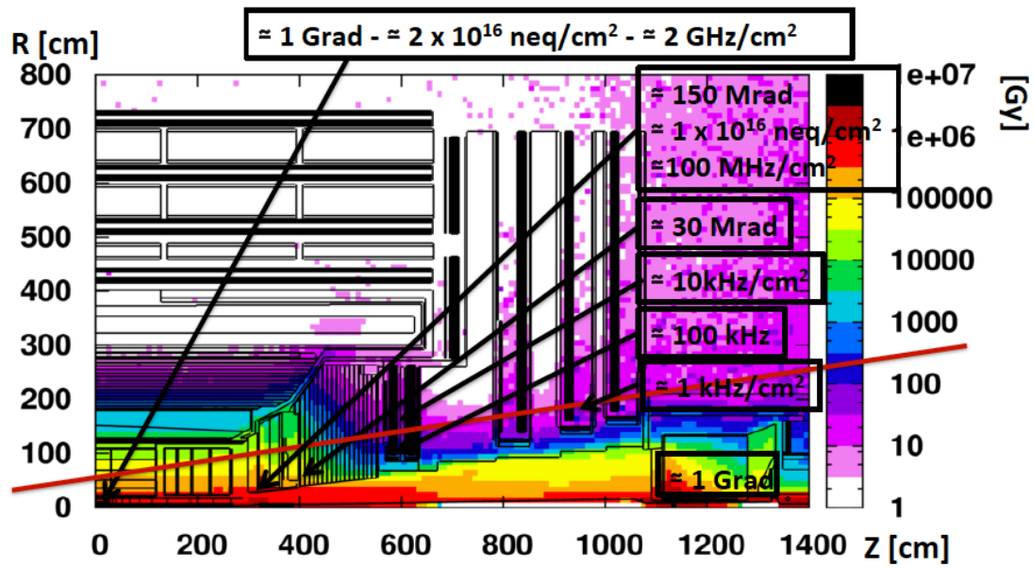

for today: selected areas related to muons

Tracking

- New full silicon detector: forward extension η ~ 4, finer granularity

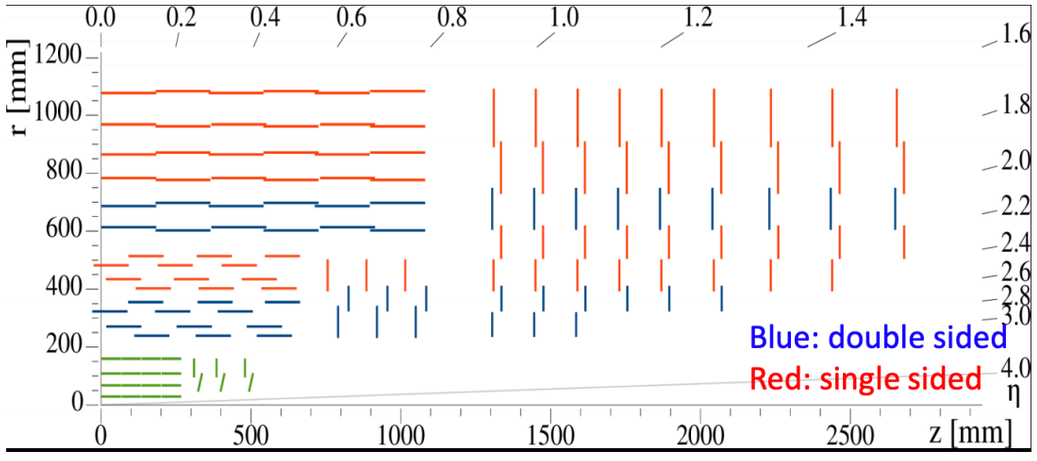

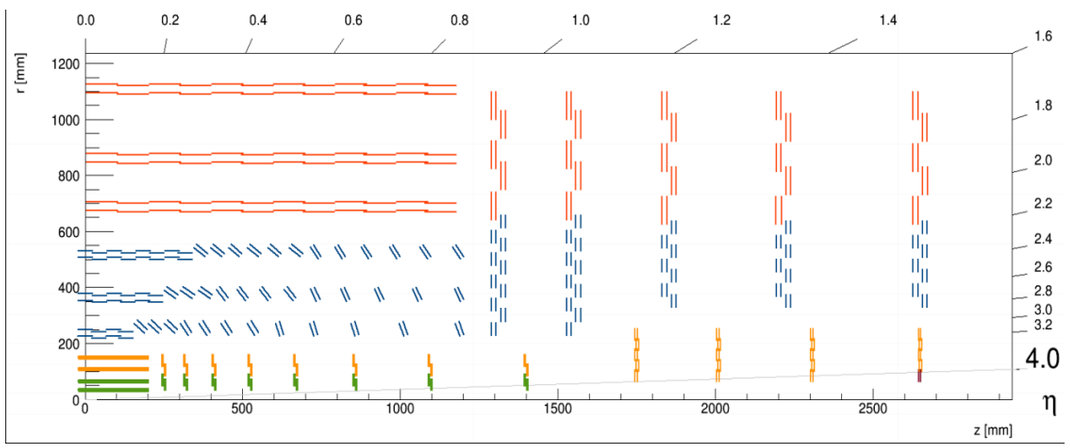

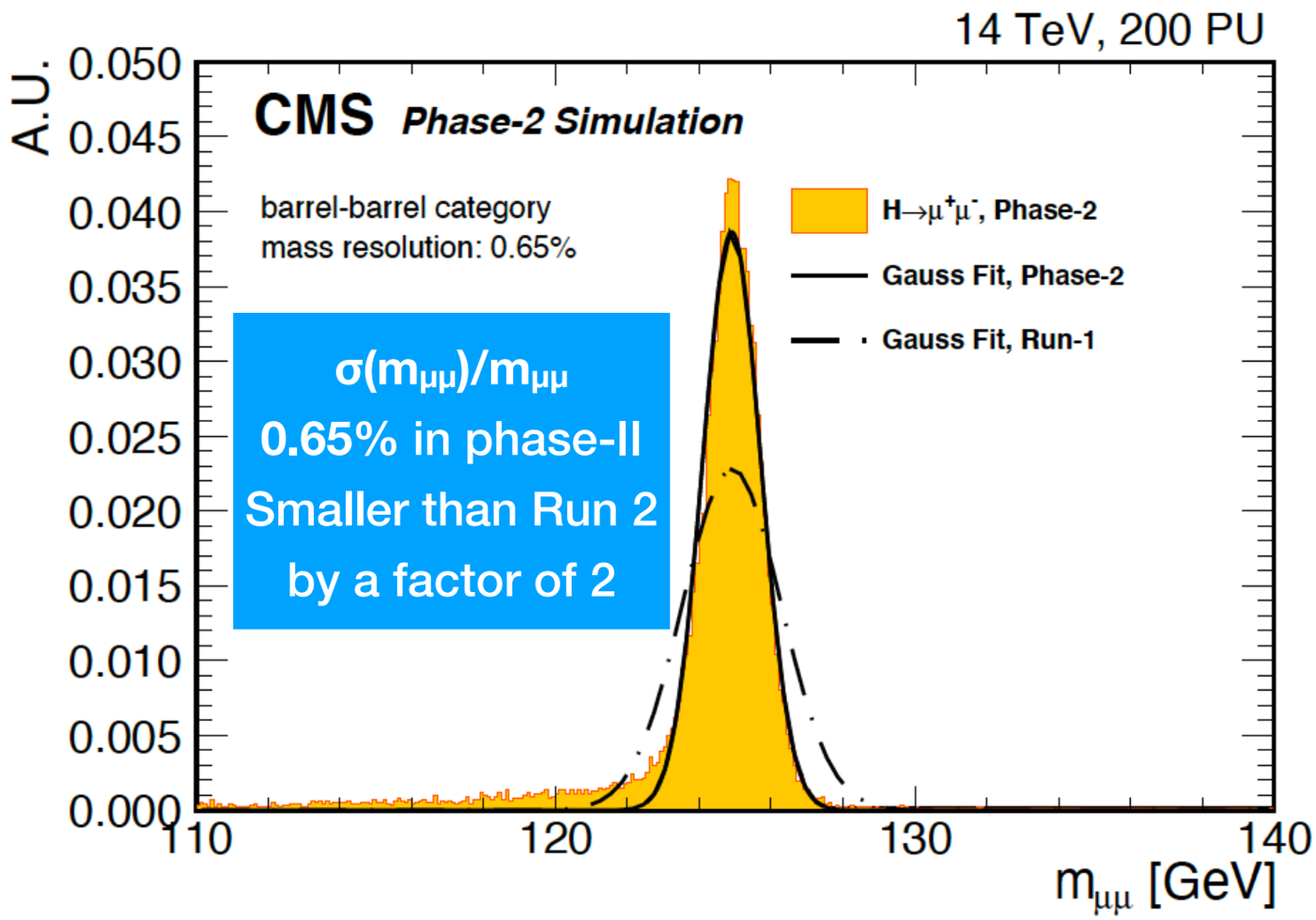

CMS-TDR-014

Muon system

- New muon chambers based on Gas Electron Multiplier and Resistive Plate Chamber technology
  - enhance muon trigger and measurement at high η
  - extends η coverage for global muons from 2.4 to 2.8 in HL-LHC

- Upgrades of the electronics

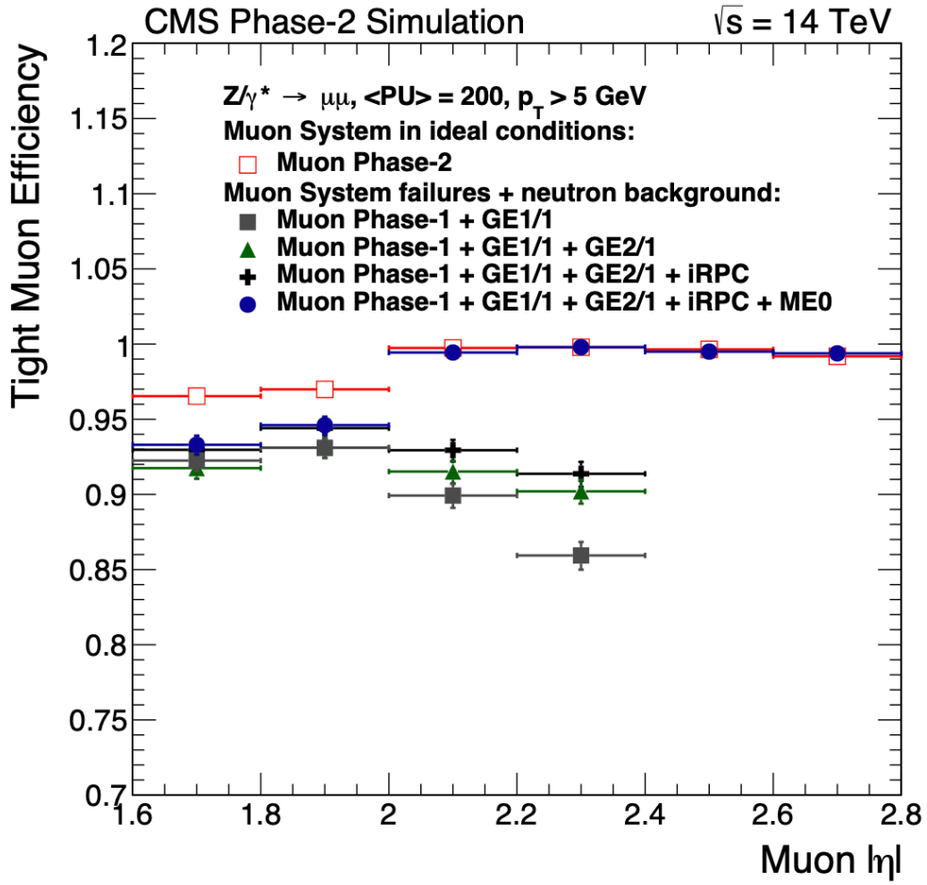

CMS-TDR-016

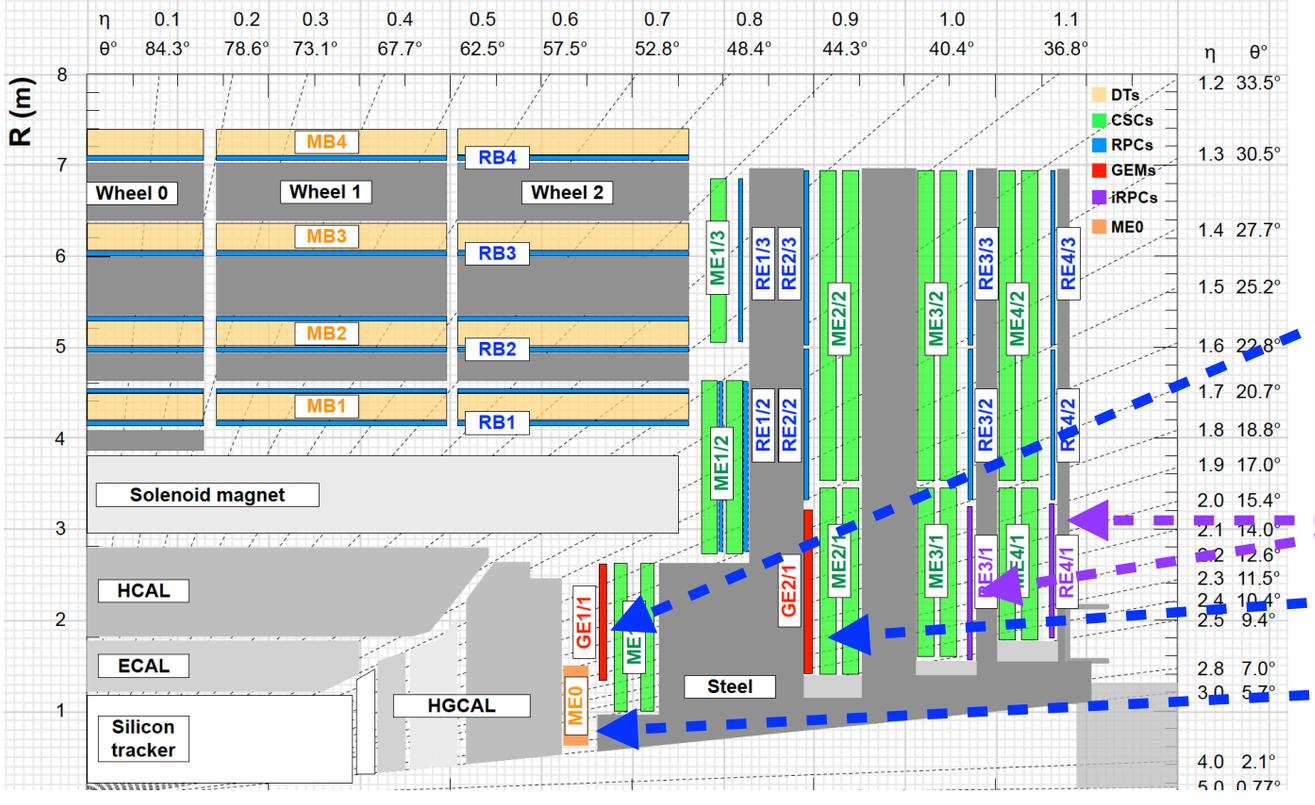

- Run 3 GE1/1: 1.6 < |η| < 2.18
- Phase-II HL-LHC
  - RE34/1: 1.8 < |η| < 2.4
  - GE2/1: 1.6 < |η| < 2.4
  - ME0: 2.0 < |η| < 2.8

First new Phase-2 detector installed in CMS

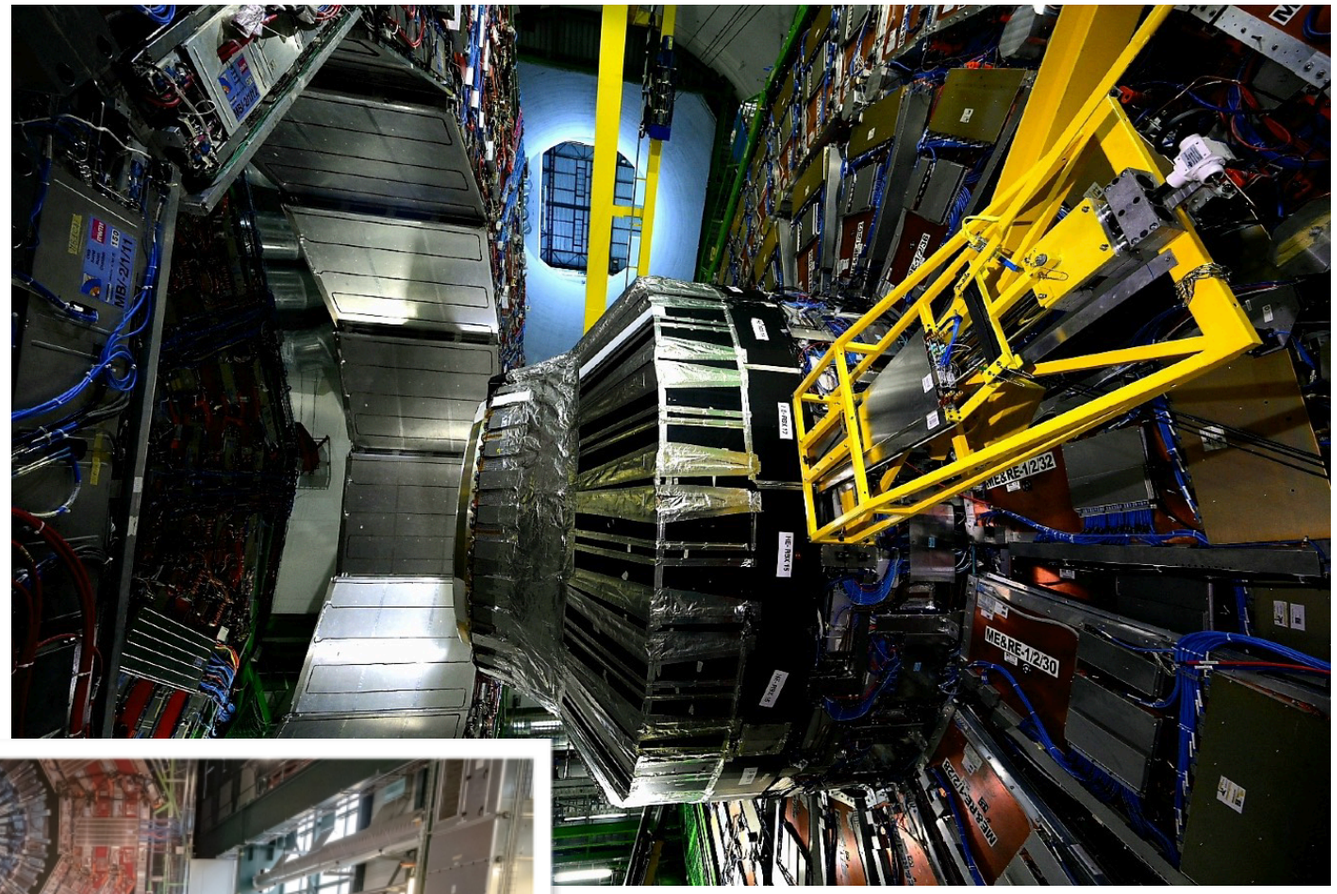

- Installation of the first GE1/1 disc (negative side) finished in October 2019
- Second GE1/1 disc (positive side) finished in September 2020

New timing dimension measurement at HL-LHC

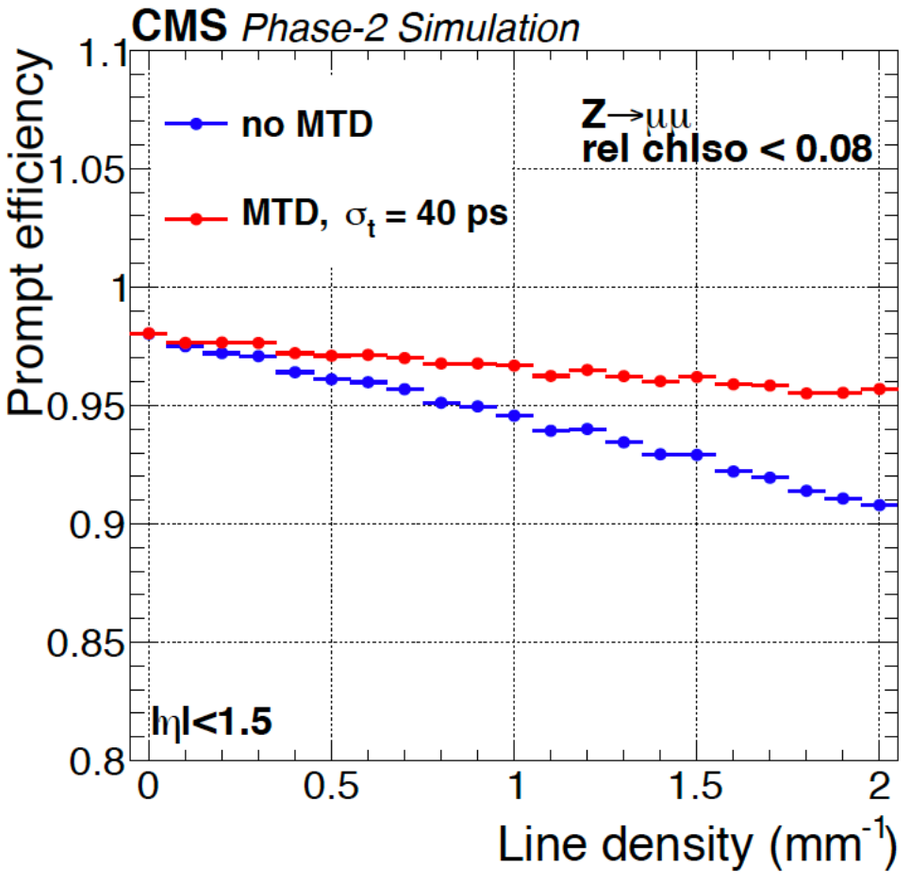

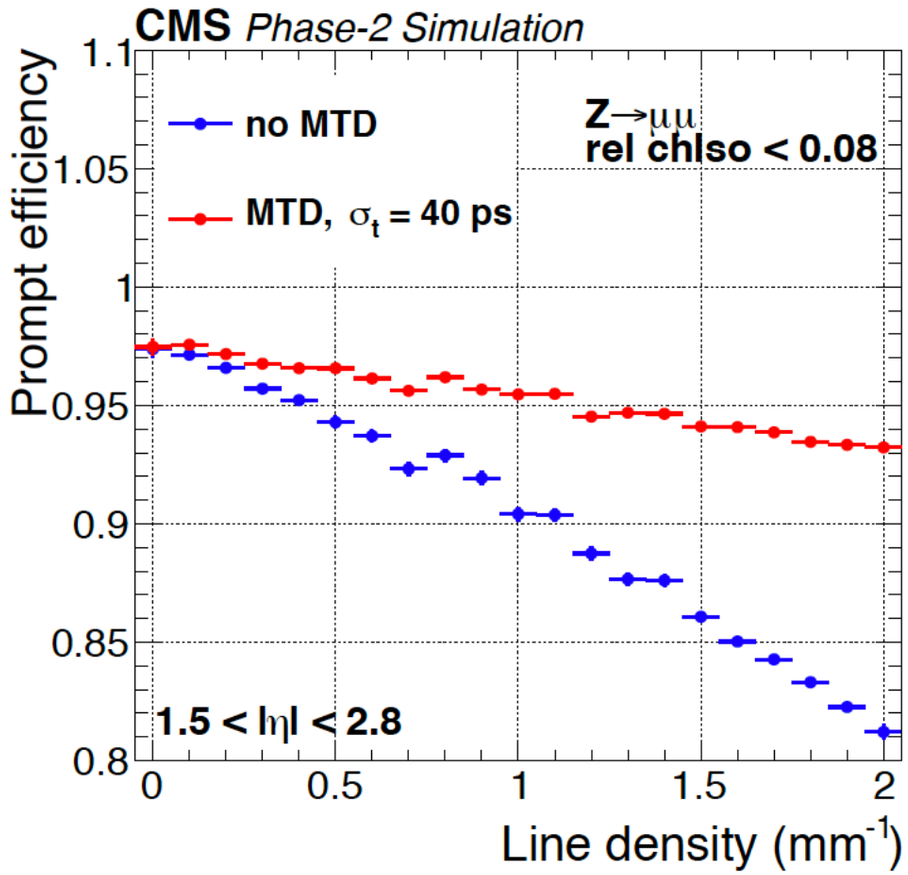

CMS MIP timing detector (30-50 ps time resolution for minimum ionizing particles) guards against adverse pileup effect on muon reconstruction at HL-LHC

CMS-TDR-020

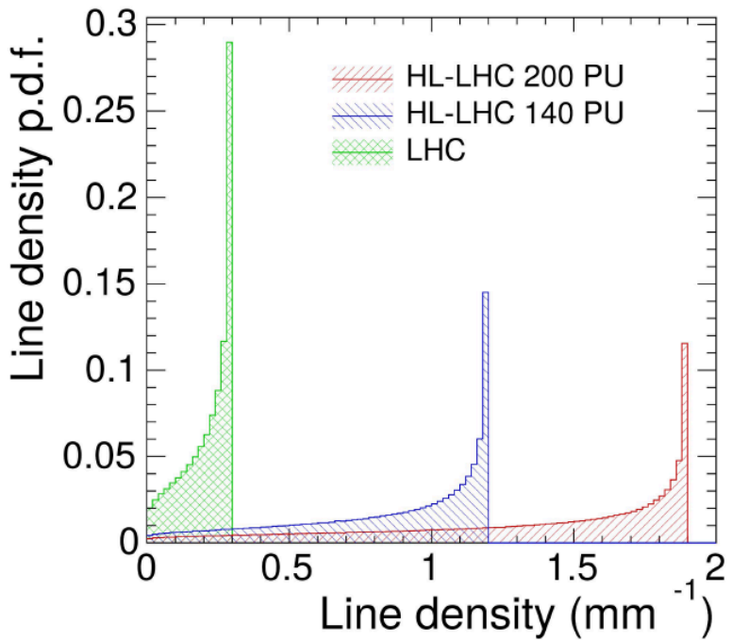

Prospect of precision measurement of Higgs coupling to muons

- Projection at HL-LHC combining ATLAS and CMS: 4.3% precision
- Complementary with proposed future Higgs factories

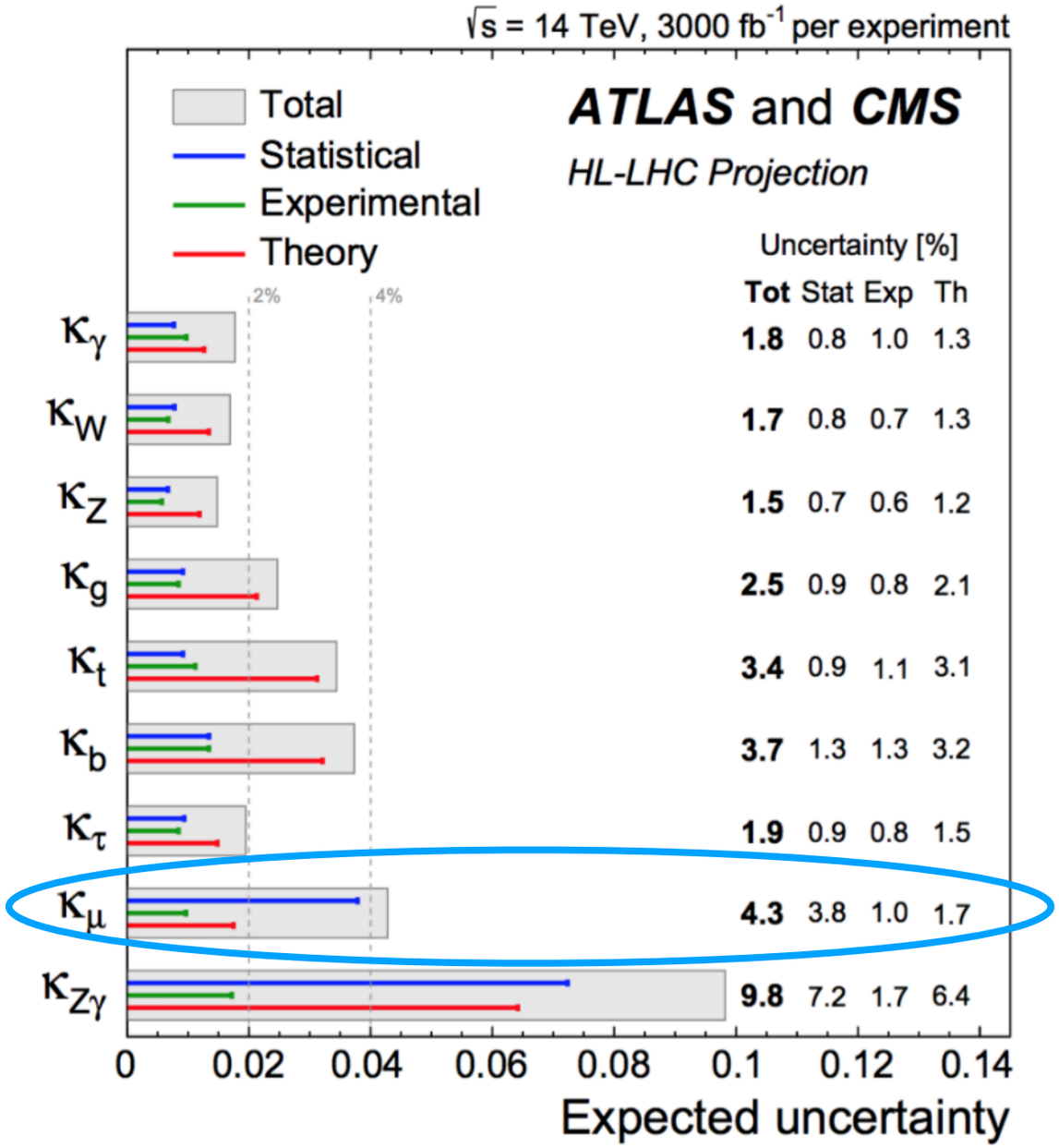

arxiv:1902.00134

Summary

- **CMS observed (expected) 3.0σ (2.5σ)** experimental evidence for H→μμ decay using full Run 2 data: (CERN press release, CMS paper submitted to JHEP) :

- Higgs boson coupling measured with 19% precision with CMS, **in agreement** with Standard Model prediction

$$\kappa_\mu = 1.13^{+0.21}_{-0.22} \text{ at 68\% CL}$$

- What's next: LHC data in **Run 3 and HL-LHC** will enable the **observation and a precise measurement** of κ_μ through H→μμ

Thank you!

backup slides

Particle Flow Algorithm and physics objects

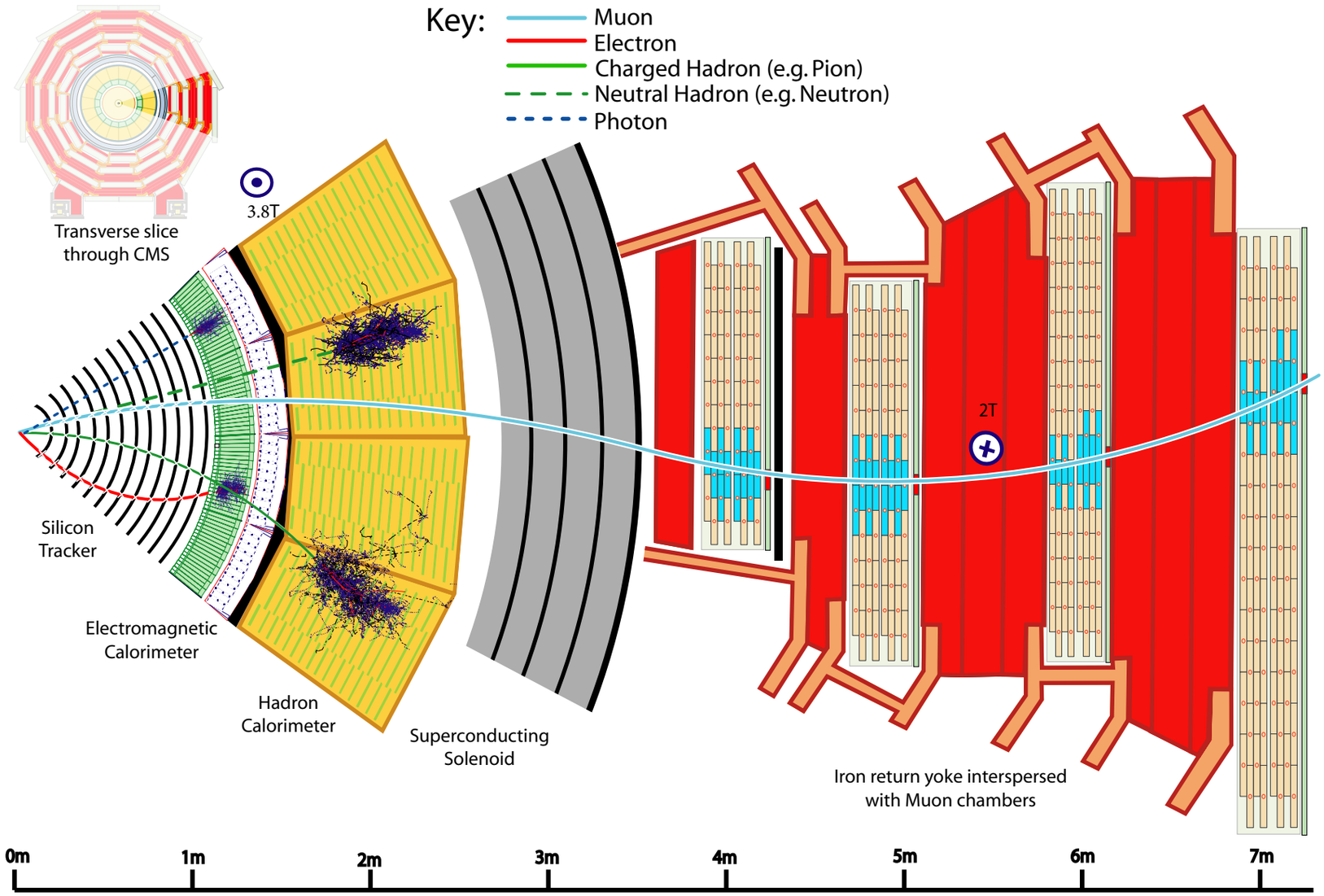

- Muons are well measured physics objects with high efficiency and purity, excellent resolution: combining tracks in the tracker and muon system

Higgs boson physics

The discovery of the Higgs boson by ATLAS and CMS experiments at LHC in 2012 started the era of precision Higgs boson property measurement:

- to test the SM, use Higgs as a tool to search for new physics beyond the SM
- one of the major physics goals at LHC and next generation colliders

(1) Any CP-mixing in Higgs couplings?

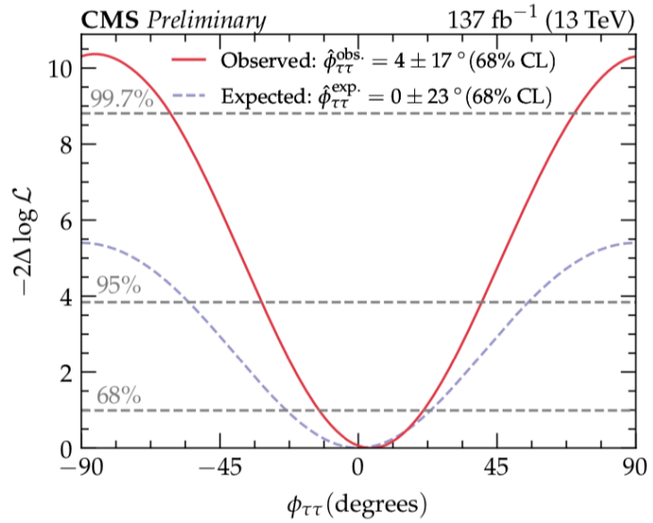

CMS HIG-20-006 PAS

(2) Is Higgs responsible for a possible 1st order phase transition inducing baryon asymmetry?

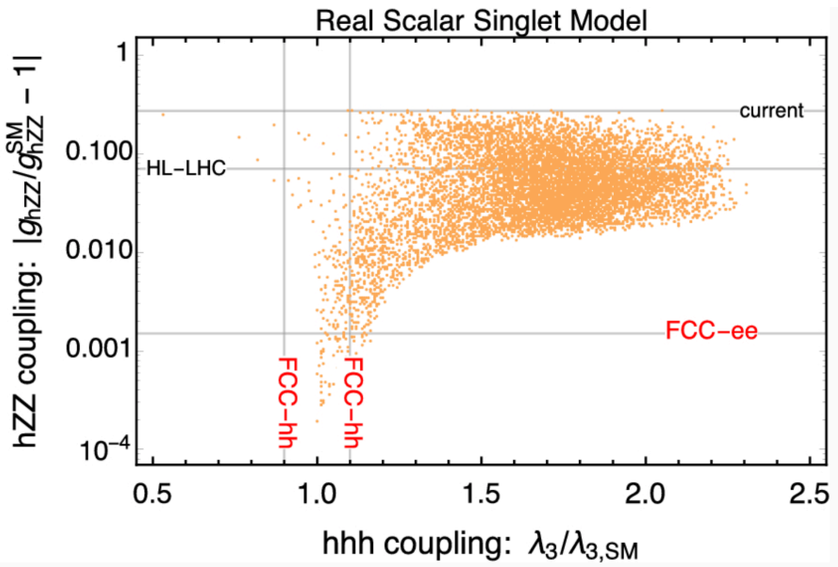

Fcc CDR

Higgs boson couplings probes Beyond the SM physics (examples):
(sub)percent level precision needed

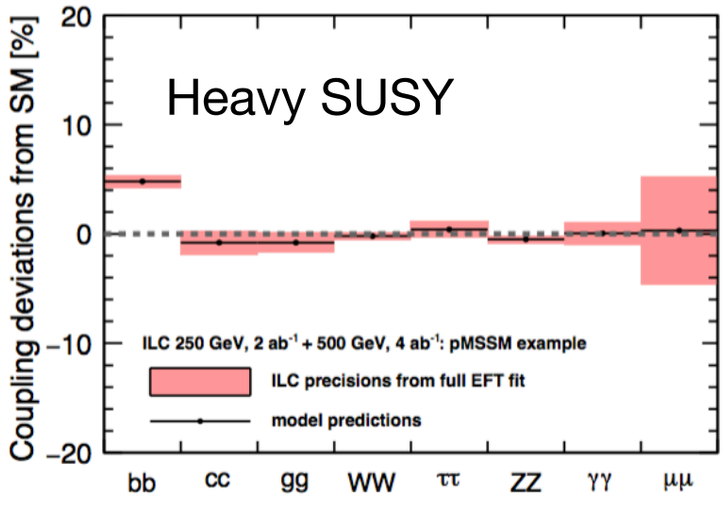

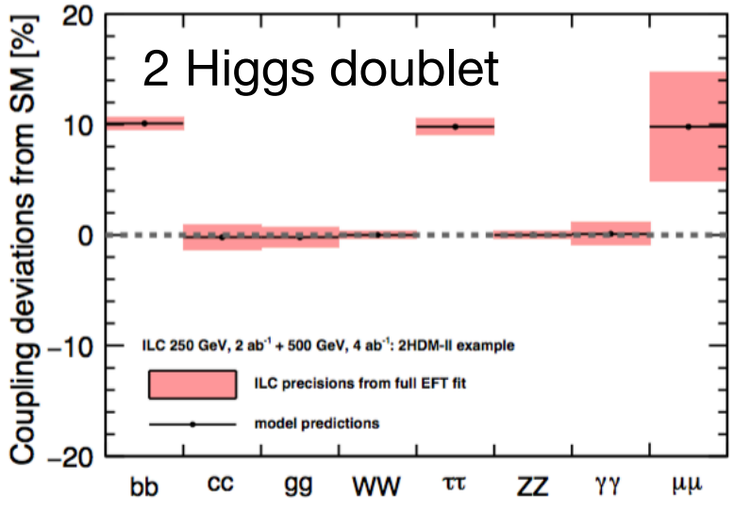

Peskin, ICHEP2020

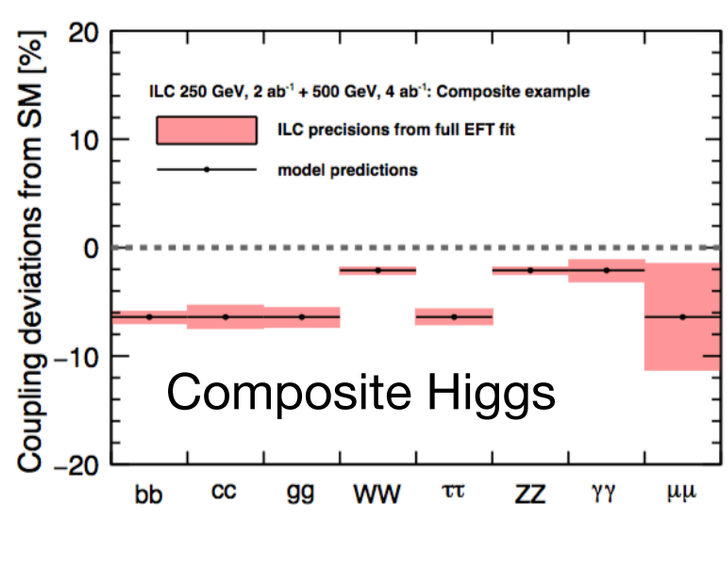

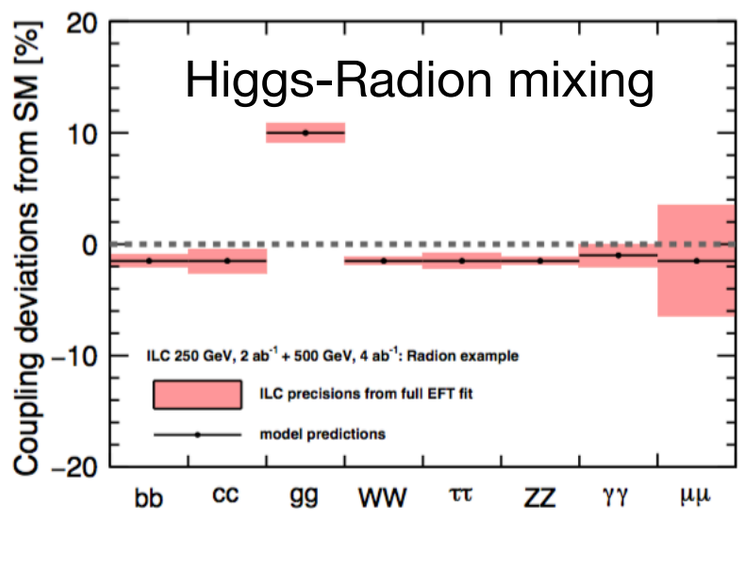

Possible scenarios of future colliders

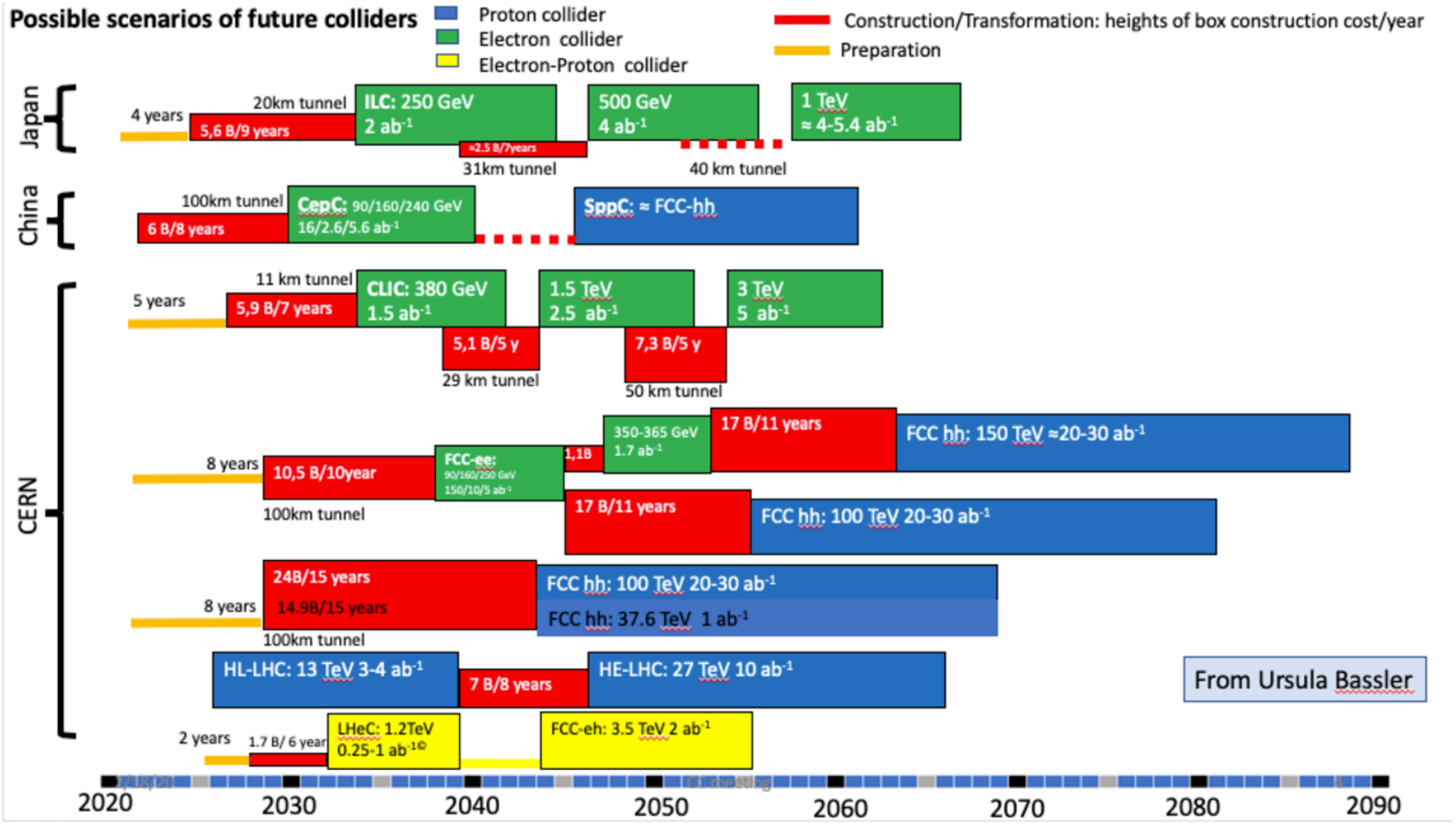

Higgs boson main production mechanism at the LHC

125.38 GeV Higgs boson production cross section @13 TeV

Gluon-fusion (ggH)
48.3 pb ~88%

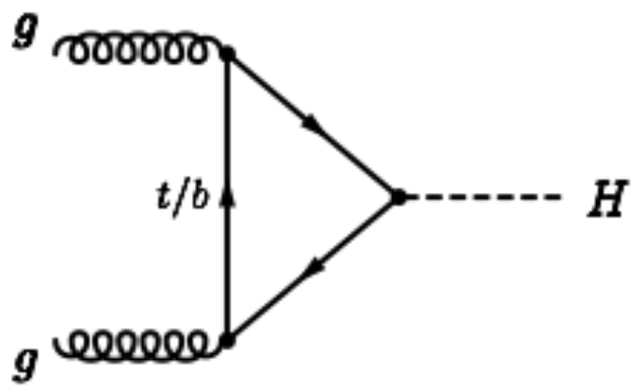

Vector boson fusion (VBF)
3.8 pb ~7%

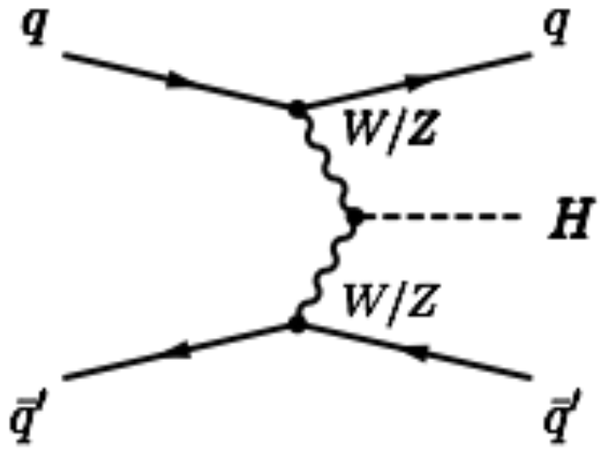

Associated Higgs production with a W or Z boson (VH): 2.2 pb ~ 4%

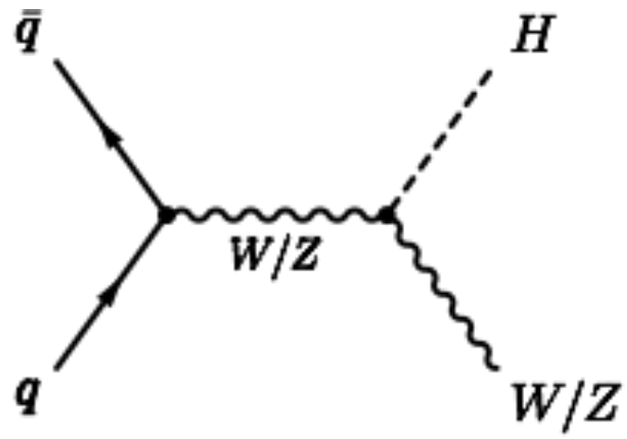

Associated Higgs production with a top quark pair (ttH): 0.5 pb ~1%

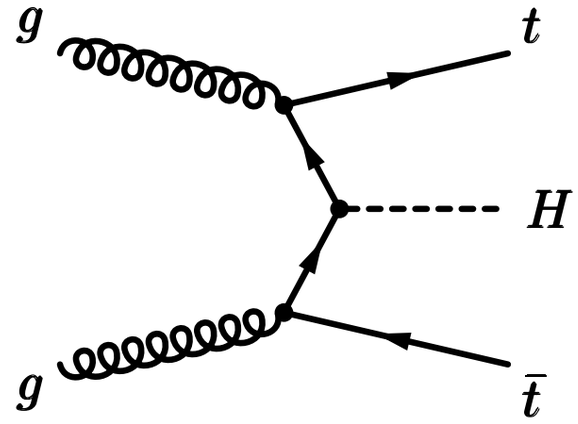

Framework for coupling-strength measurements

Leading order tree-level motivated framework with assumptions:

- Signal observed in different channels originate from a single resonance $m_H \sim 125.36$ GeV
- Narrow width approximation.
- Lagrangian tensor structure: SM hypothesis $J^{CP} = 0^{++}$

Yield for the production and decay $i \to H \to f$ parametrized in terms of coupling scale factors scaling the SM cross sections and widths

Coupling scale factors:

$$\sigma \cdot B(i \to H \to f) = \frac{\sigma_i \cdot \Gamma_f}{\Gamma_H} = \frac{\sigma_i^{SM} \cdot \Gamma_f^{SM}}{\Gamma_H^{SM}} \cdot \left(\frac{\kappa_i^2 \kappa_f^2}{\kappa_H^2} \right)$$

Coupling scale factors:

$$\kappa_i^2 = \frac{\sigma_i}{\sigma_i^{SM}} \qquad \kappa_f^2 = \frac{\Gamma_f}{\Gamma_f^{SM}} \qquad \kappa_H^2 = \frac{\sum \Gamma_f}{\sum \Gamma_f^{SM}}$$

Production **Decay** **Total width**

Higgs boson width Γ_H not experimentally constrained to a meaningful precision at the LHC:

- No assumptions on Γ_H: Ratios of coupling strength can be measured
- Make assumption on Γ_H: absolute coupling strengths can be measured.

Higgs boson mass measurements

- *m_H precision exceeding Run 1 result: ~0.11% precision by CMS, 0.19% by ATLAS*

Phys. Lett. B 805 (2020) 135425

Phys. Lett. B 784 (2018) 345

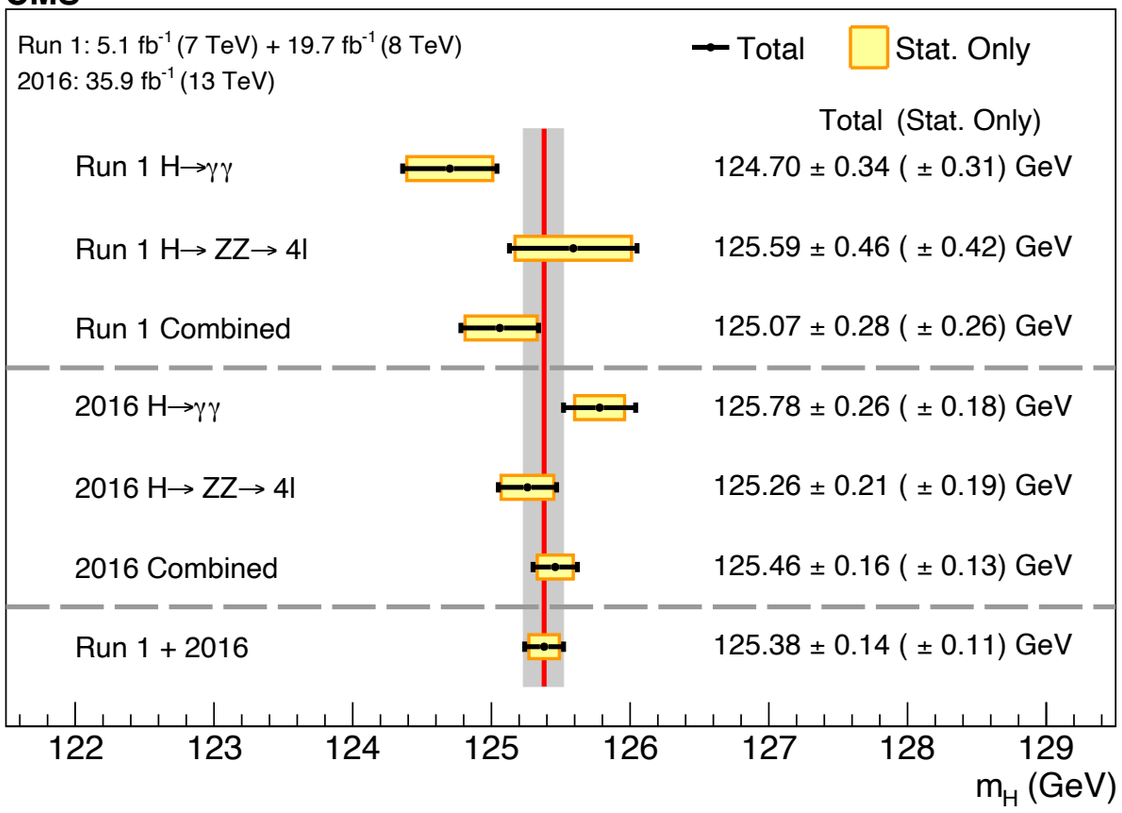

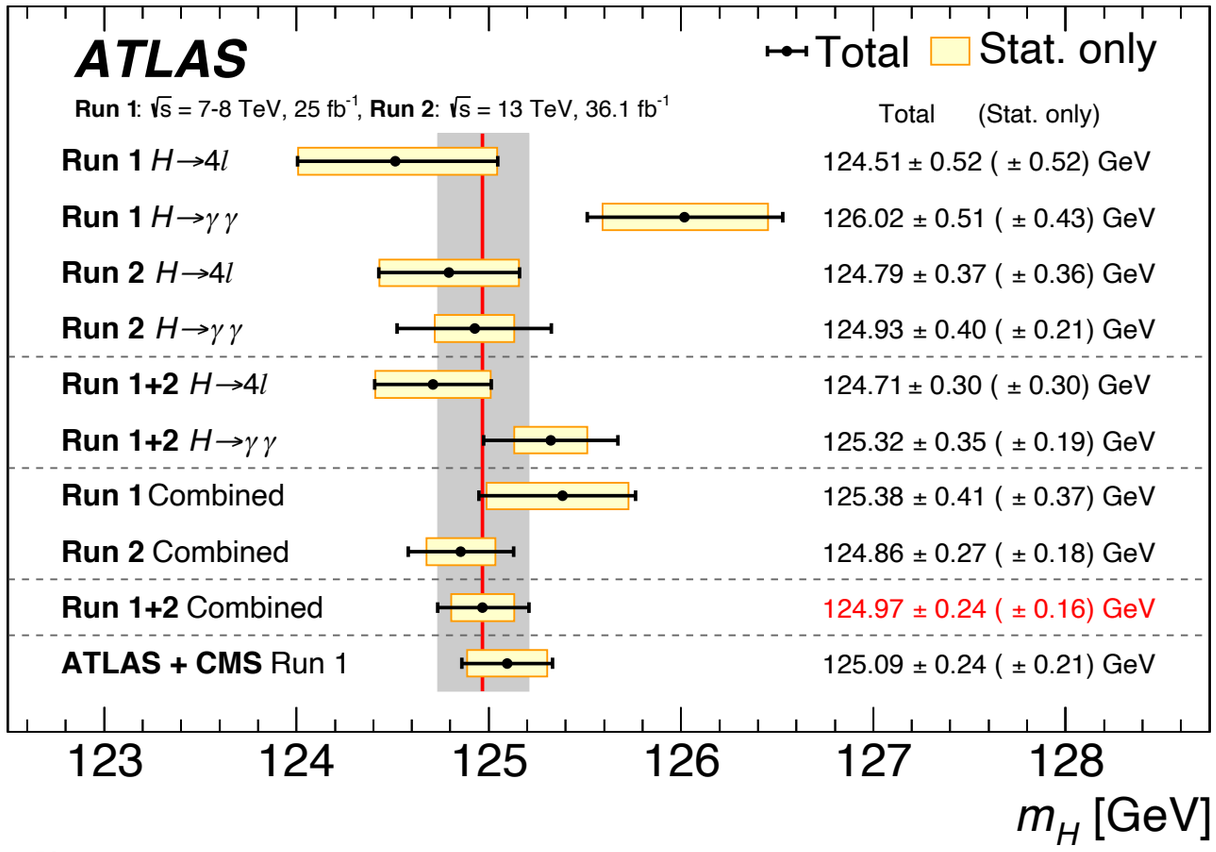

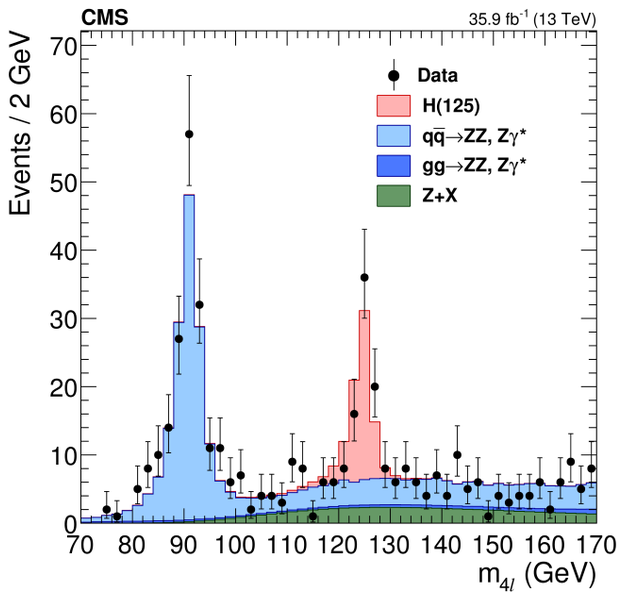

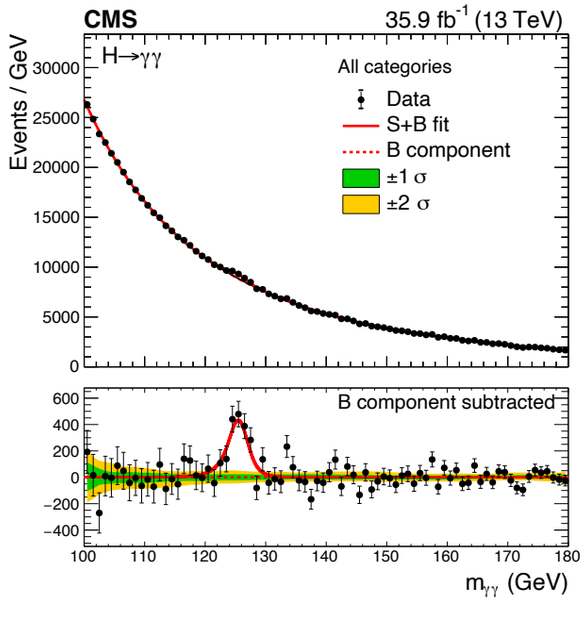

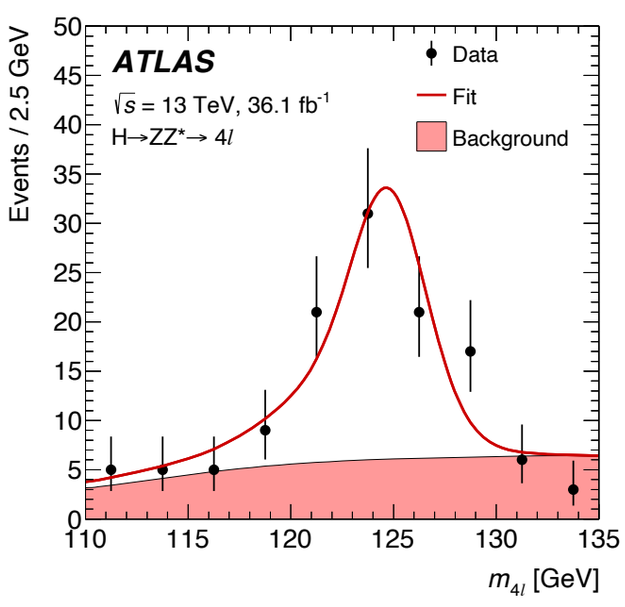

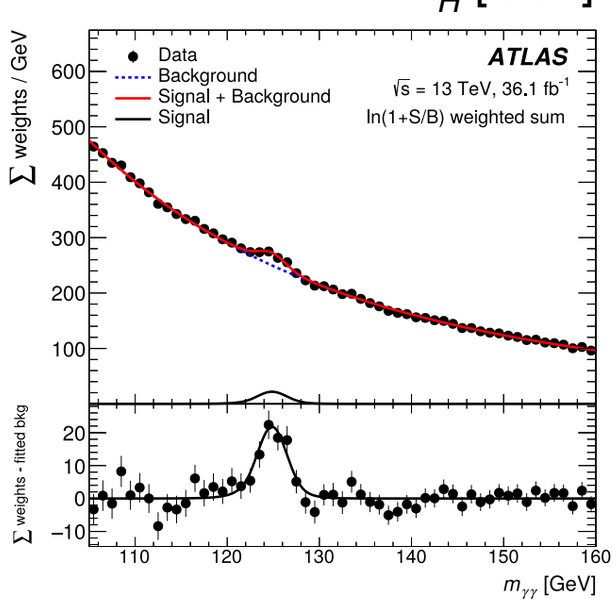

H→cc

- Currently best 95% CL limit on **σ**(VH)xB(H→cc): < 70 (expected: 37) ×SM, based on 36.1 /fb CMS data at 13 TeV

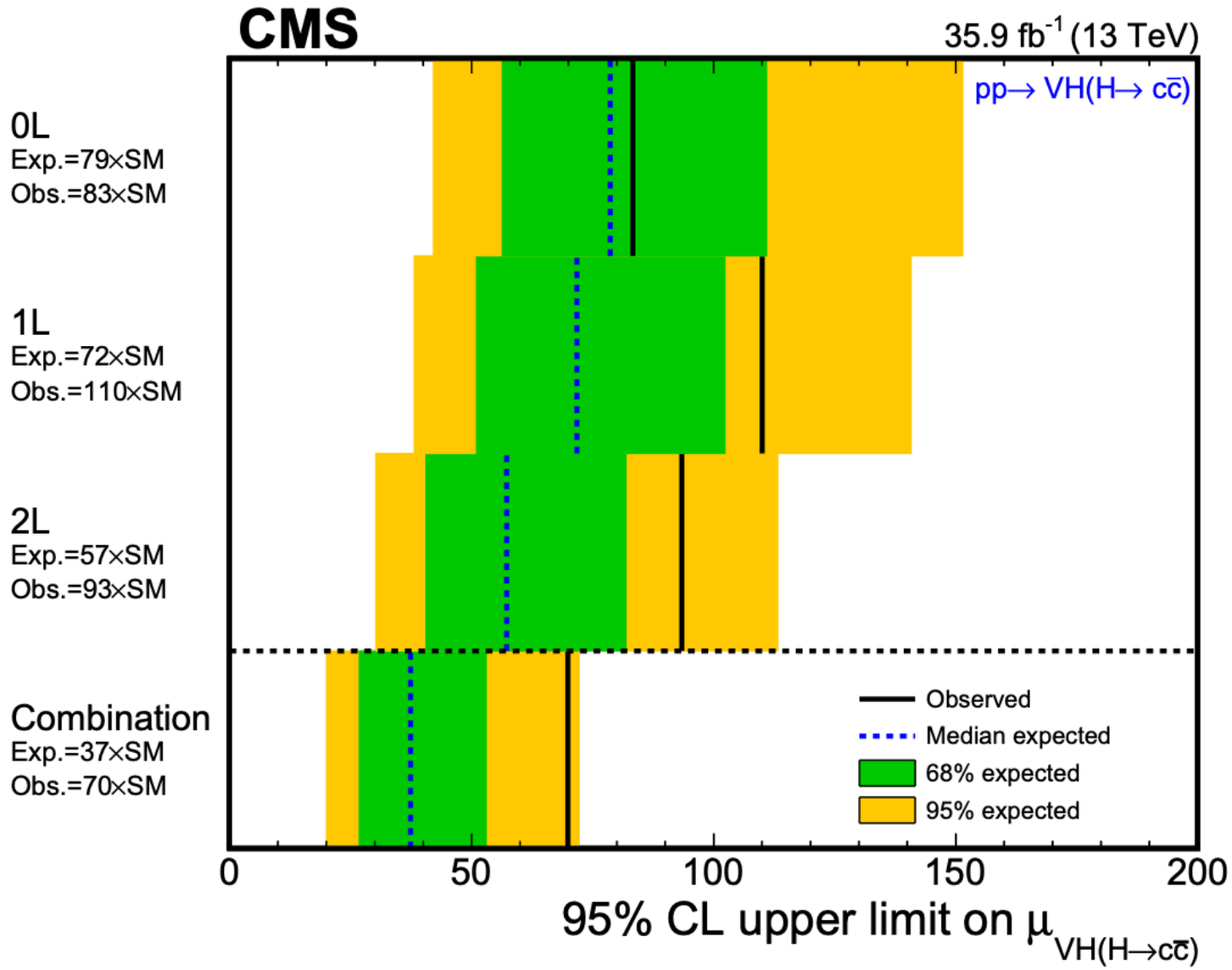

JHEP 03 (2020) 131

Physics objection selection

muons:

- $|\eta|<2.4$
- leading muon pT>26 (2016, 2018)/29 (2017)
- sub-leading muon pT>20 GeV
- loose isolation criteria
- medium muon ID
- global muon
- correction to the muon pT: final state photon recovery and geo-fit correction

Top tagging

- Only used in the ttH category
- MVA-based resolved hadronic top tag with 3 jets [PRL **122**, 011803 (2019)]

Jets:

- pT > 25 GeV, $|\eta| < 4.7$
- reject jets originate from pileup
  - MVA pile-up jet identification
- Calibration on jet energy

B-jet tagging

- pT > 25 GeV and $|\eta|< 2.5$ within tracker coverage
- DeepCSV b-tagging algorithm
  - Loose (85% efficiency, 10% mis-ID)
  - medium (70% efficiency, 1% mis-ID)

Event simulation

Monte Carlo (MC) simulation samples:

Process		Generator (Perturbative order)	Parton shower	Cross section	Additional corrections
ggH	signal	MADGRAPH5_aMC@NLO (NLO QCD)	PYTHIA	N3LO QCD, NLO EW	$p_T(H)$ from NNLOPS
VBF		POWHEG (NLO QCD)	PYTHIA dipole shower	NNLO QCD, NLO EW	—
$qq \to VH$		POWHEG (NLO QCD)	PYTHIA	NNLO QCD, NLO EW	—
$gg \to ZH$		POWHEG (LO)	PYTHIA	NNLO QCD, NLO EW	—
$t\bar{t}H$		POWHEG (NLO QCD)	PYTHIA	NLO QCD, NLO EW	—
$b\bar{b}H$		POWHEG (NLO QCD)	PYTHIA	NLO QCD	—
tHq		MADGRAPH5_aMC@NLO (LO)	PYTHIA	NLO QCD	—
tHW		MADGRAPH5_aMC@NLO (LO)	PYTHIA	NLO QCD	—
Drell–Yan	bkg	MADGRAPH5_aMC@NLO (NLO QCD)	PYTHIA	NNLO QCD, NLO EW	—
Zjj-EW		MADGRAPH5_aMC@NLO (LO)	HERWIG++/HERWIG 7	LO	—
$t\bar{t}$		POWHEG (NLO QCD)	PYTHIA	NNLO QCD	—
Single top quark		POWHEG/MADGRAPH5_aMC@NLO (NLO QCD)	PYTHIA	NLO QCD	—
Diboson (VV)		POWHEG/MADGRAPH5_aMC@NLO (NLO QCD)	PYTHIA	NLO QCD	NNLO/NLO K factors
$gg \to ZZ$		MCFM (LO)	PYTHIA	LO	NNLO/LO K factors
$t\bar{t}V$, $t\bar{t}VV$		MADGRAPH5_aMC@NLO (NLO QCD)	PYTHIA	NLO QCD	—
Triboson (VVV)		MADGRAPH5_aMC@NLO (NLO QCD)	PYTHIA	NLO QCD	—

ggH:

- Higgs pT distribution reweighted to match POWHEG NNLOPS predictions

Drell-Yan:

- Madgraph5_amc@NLO generator with up to two partons in the final state at the ME level
- Dedicated sample targeting the VBF phase-space created to reduce MC stats uncertainty

Collins - Soper angles

- θ_{CS}: the angle between the collinear muons (μ) in the dimuon rest frame and the line that bisects the acute angle between the colliding partons (p)

- ϕ_{CS}: the angle between the dimuon plane and the plane of the colliding partons

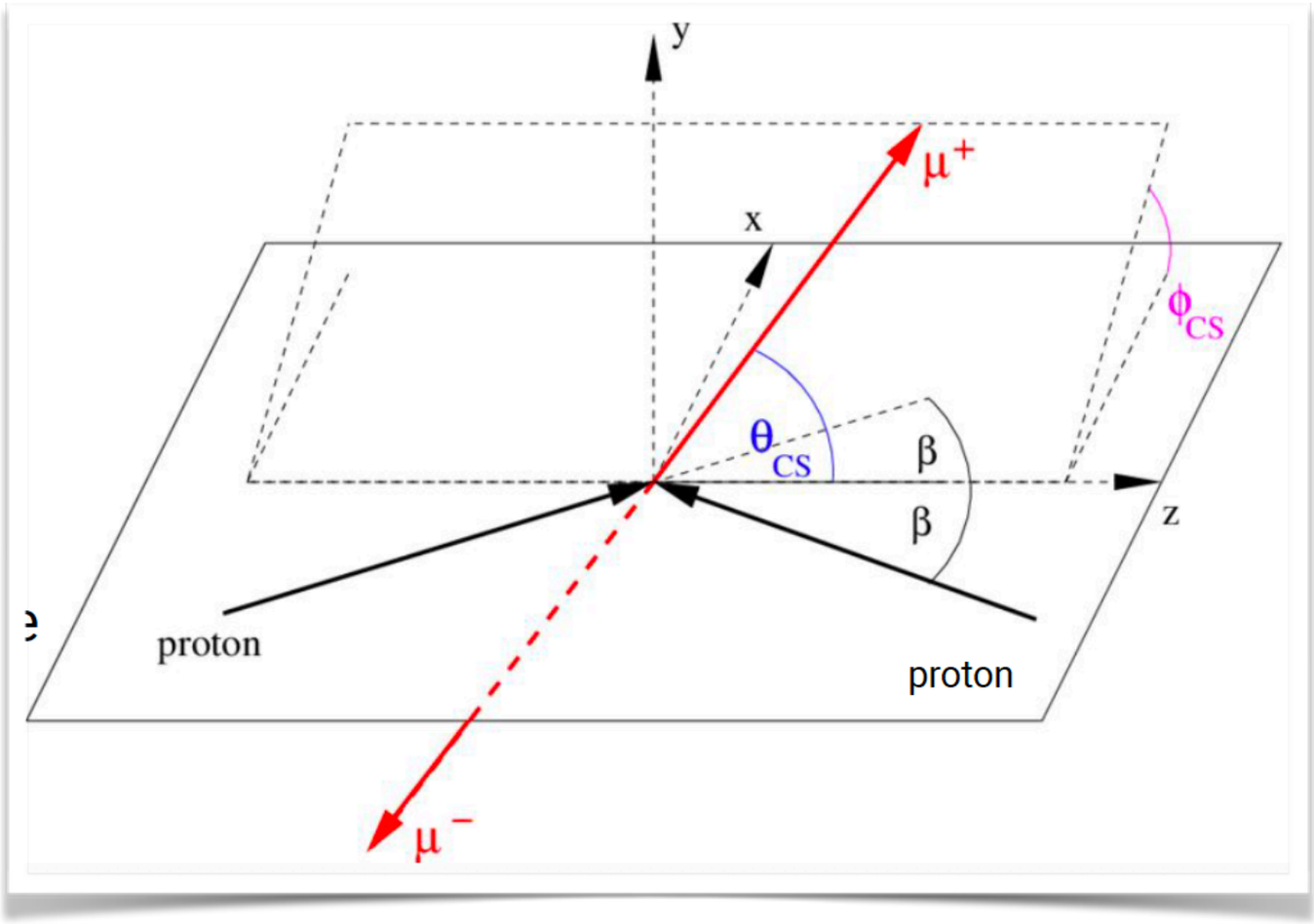

Image credit : Jens Kessler

Ranking of systematic uncertainties

- Leading systematic uncertainty: VBF signal parton shower uncertainty
- No strong shifts from central values or constraint on the size of systematic uncertainty

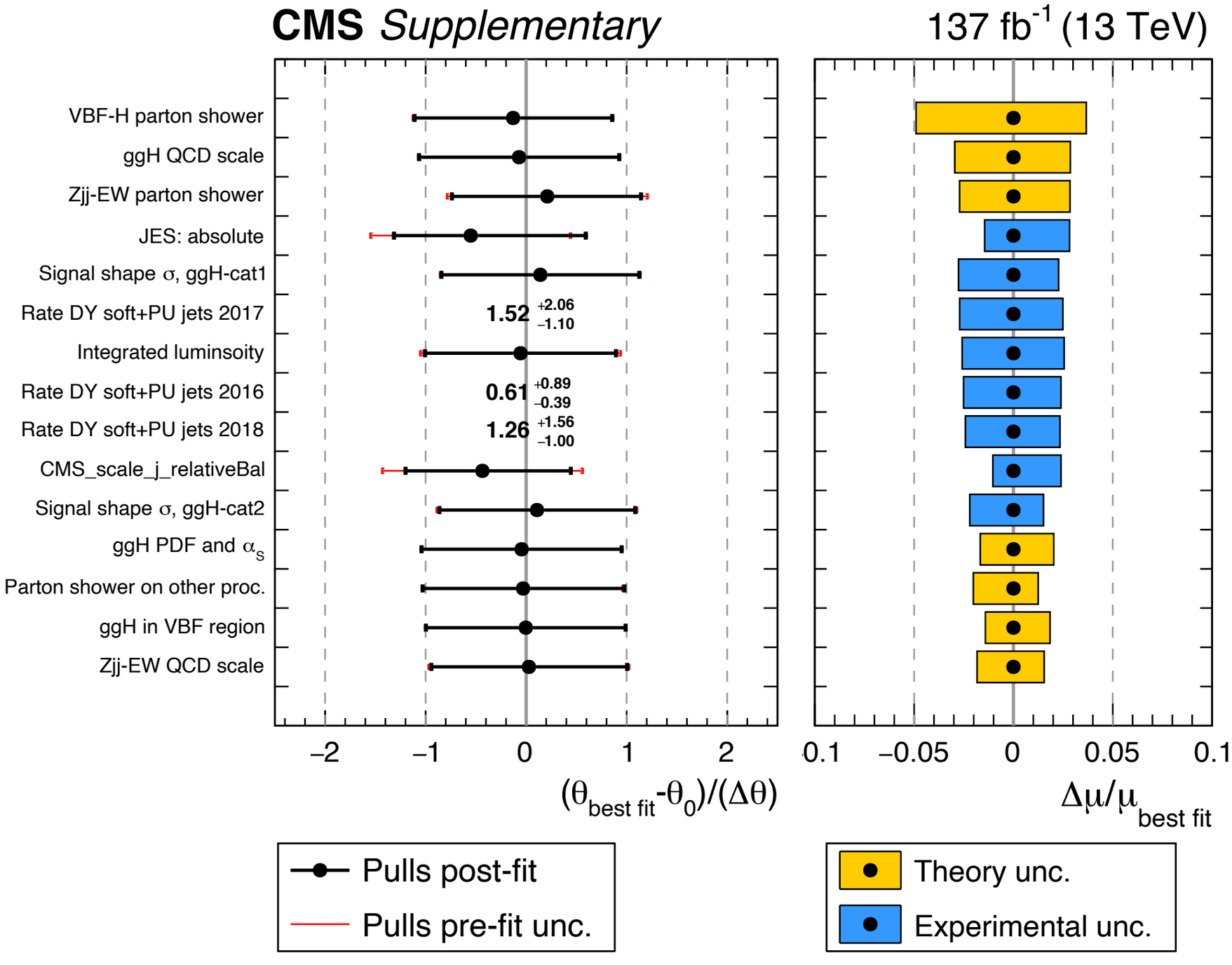

VBF: 2016 signal and sideband region

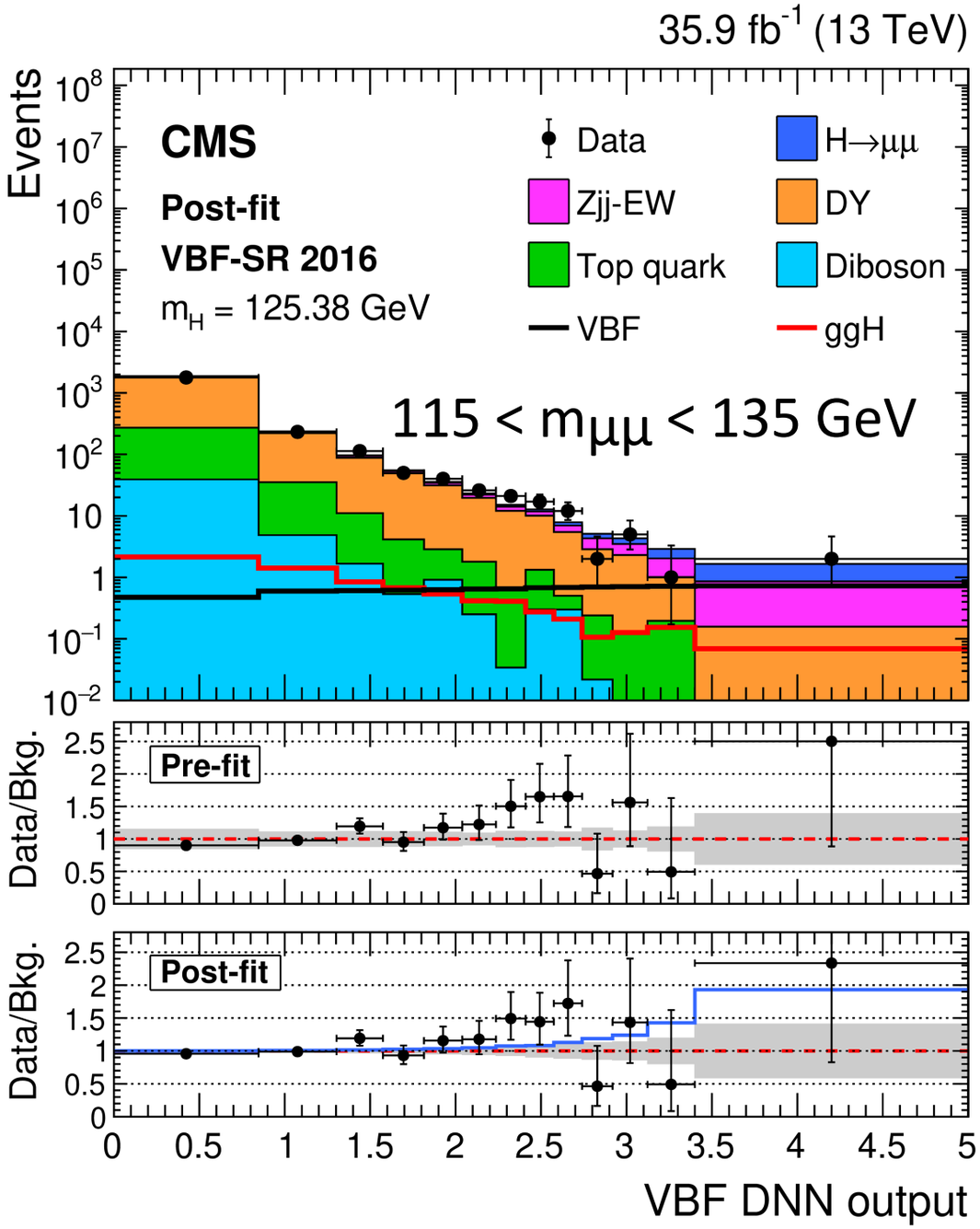

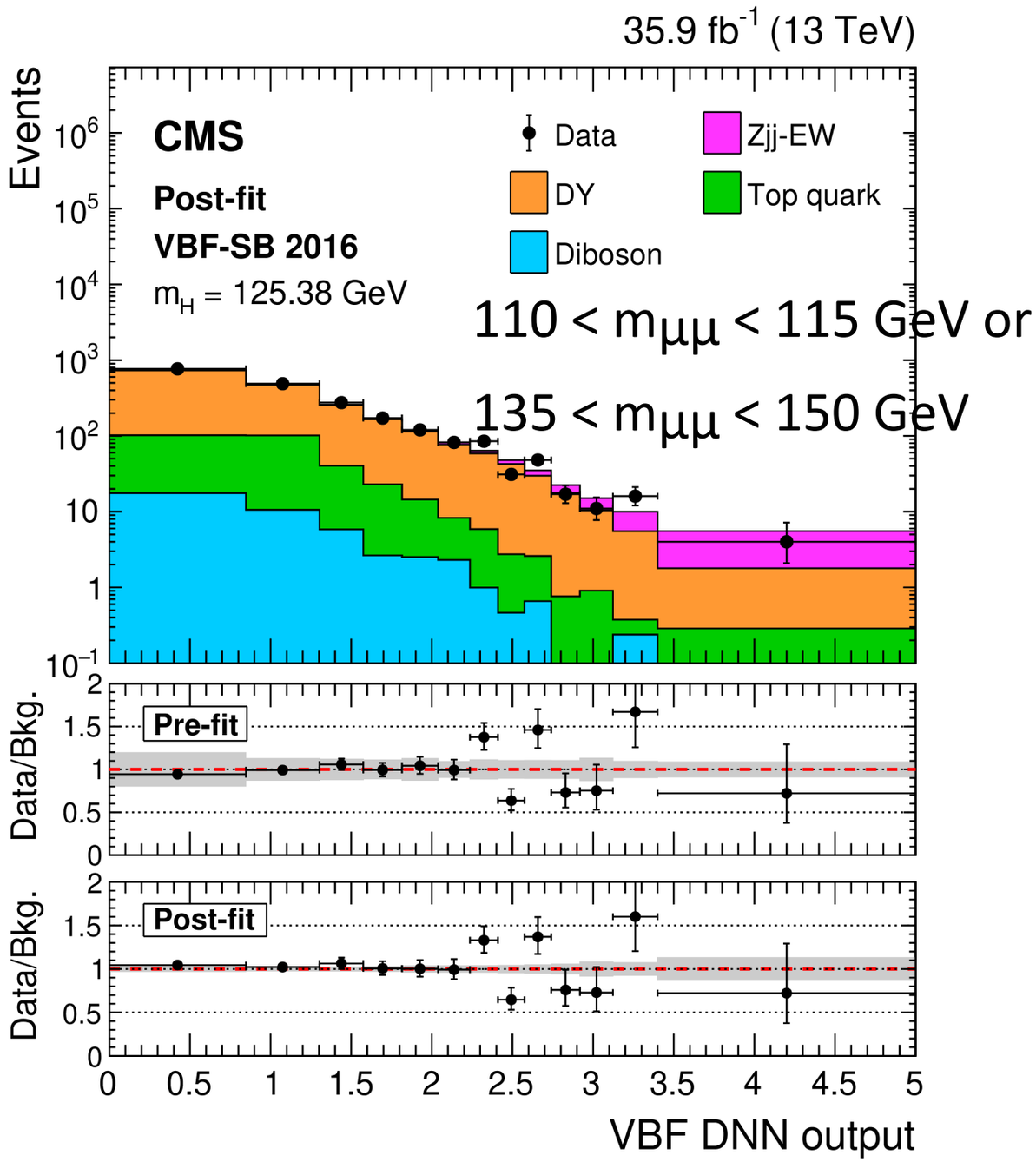

VBF: 2017 signal and sideband region

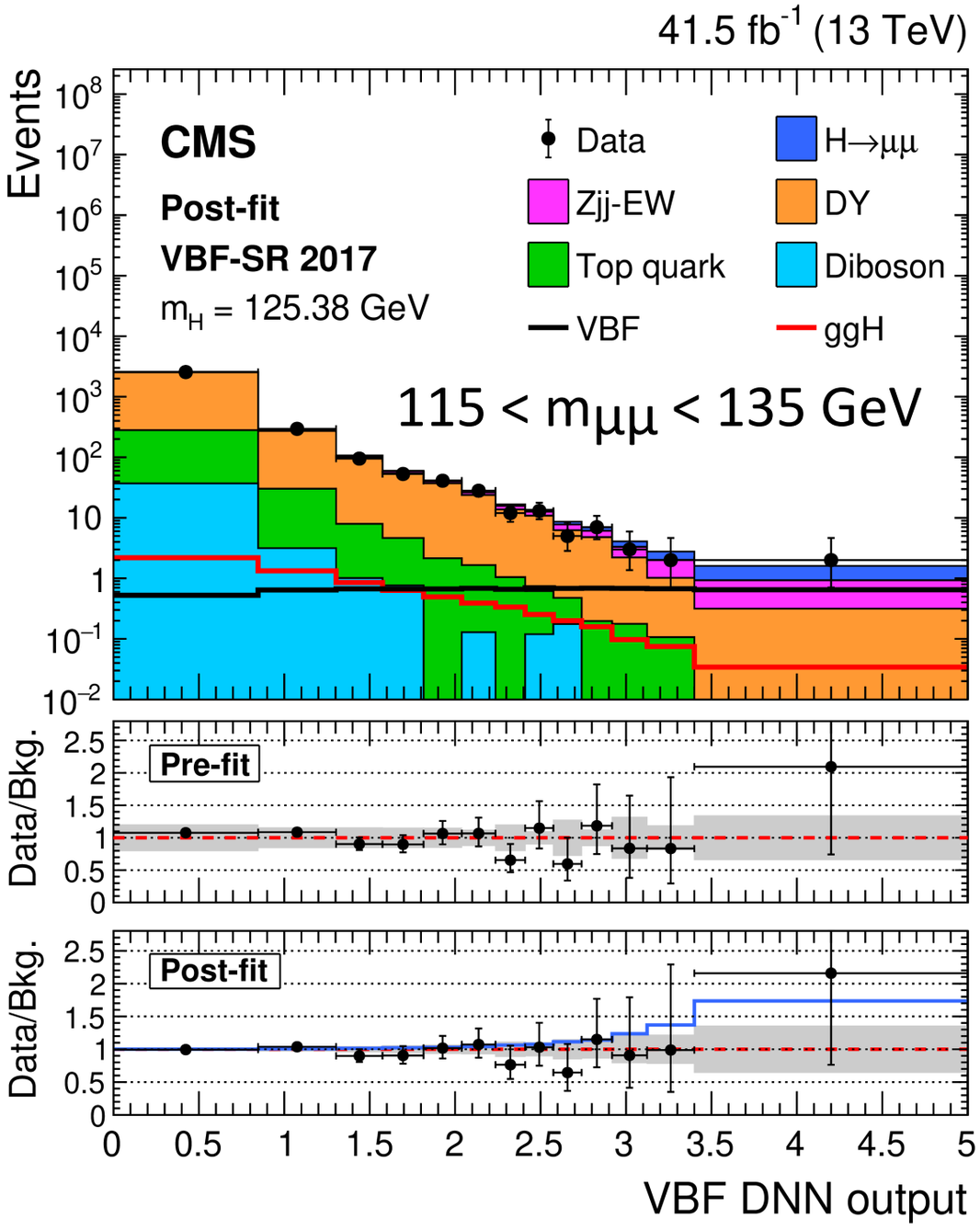

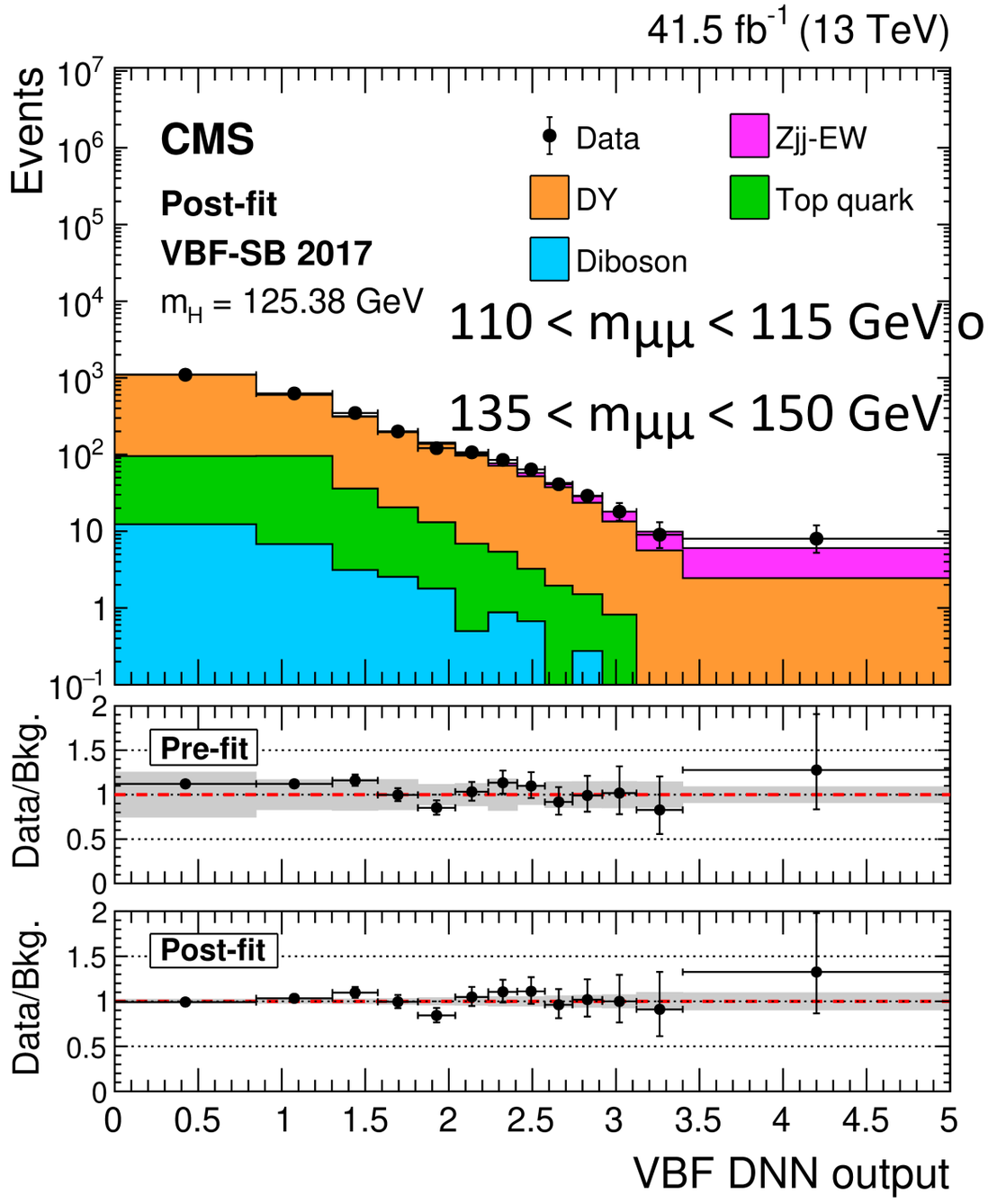

VBF: 2018 signal and sideband region

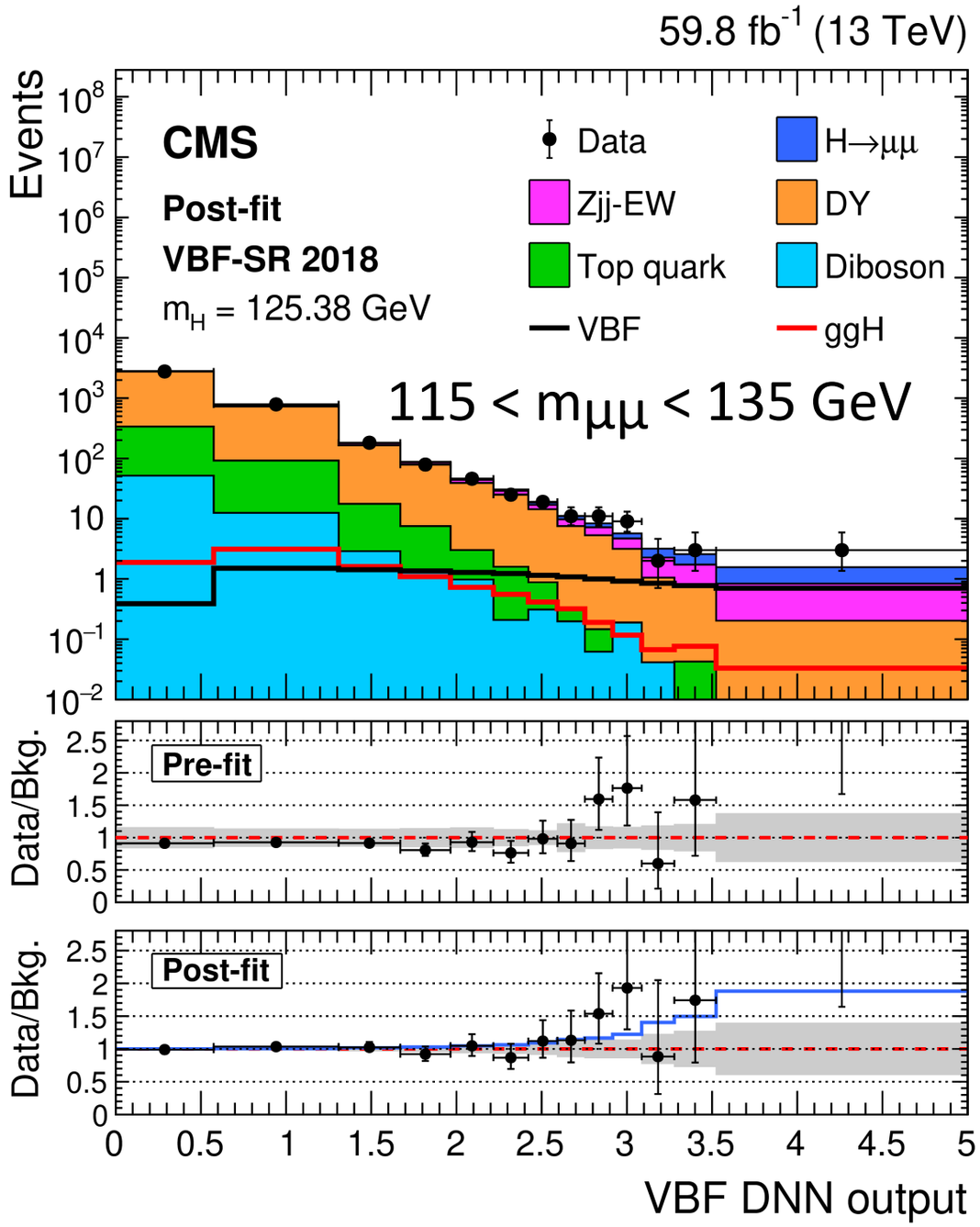

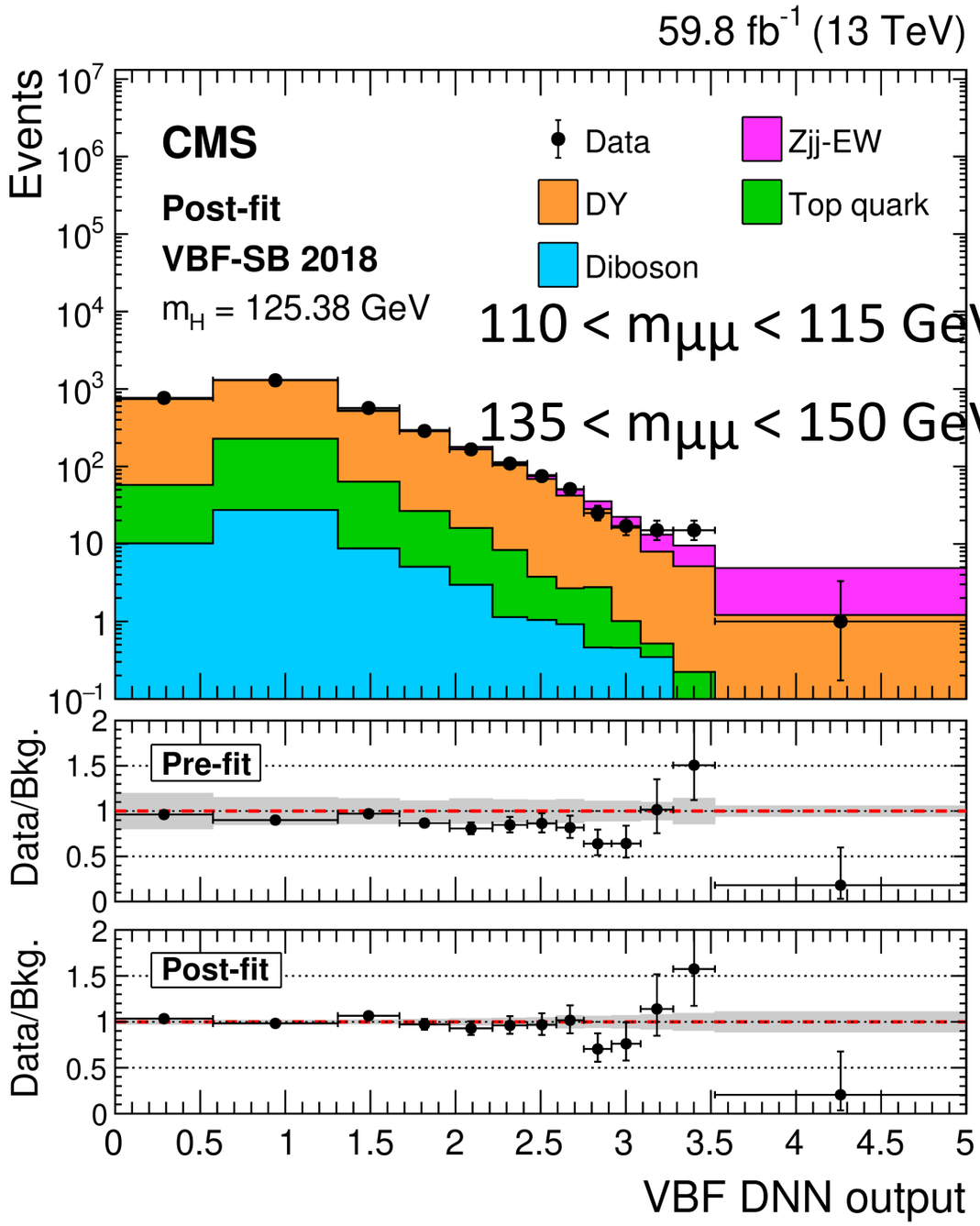

Sources of systematic uncertainties and correlation

Source of uncertainty	Categories and processes	Type	Correlation vs cat.	Correlation vs year
		Experimental uncertainties		
Integrated luminosity	Sig. in all cat., bkg. in VBF	Rate	Correlated	Partial
Muon efficiency	Sig. in all cat., bkg. in VBF	Rate	Correlated	Correlated
Electron efficiency	Sig. in $t\bar{t}H$ and VH	Rate	Correlated	Correlated
Muon trigger	Sig. in all cat., bkg. in VBF	Rate	Correlated	Correlated
Muon p_T scale	Sig. in all cat., bkg. in VBF	Shape in VBF, rate in others	Correlated	Correlated
Nonprompt leptons	Sig. in $t\bar{t}H$ and VH	Rate	Correlated	Correlated
Pileup model	Sig. in all cat., bkg. in VBF	Shape in VBF, rate in others	Correlated	Uncorrelated
L1 inefficiency	Sig. in all cat., bkg. in VBF	Shape in VBF, rate in others	Correlated	Uncorrelated
B-tagging efficiency	Sig. in all cat., bkg. in VBF	Shape in VBF, rate in others	Correlated	Correlated
Jet energy scale	Sig. in all cat., bkg. in VBF	Shape in VBF, rate in others	Correlated	Partial
Jet energy resolution	Sig. in all cat., bkg. in VBF	Shape in VBF, rate in others	Correlated	Uncorrelated
		Theoretical uncertainties		
μ_R and μ_F for ggH	ggH in all cat.	Rate	Correlated	Correlated
μ_R and μ_F for VBF	VBF in all cat.	Rate	Correlated	Correlated
μ_R and μ_F for $t\bar{t}H$	$t\bar{t}H$ in all cat.	Rate	Correlated	Correlated
μ_R and μ_F for VH	VH in all cat.	Rate	Correlated	Correlated
PDF for ggH	ggH in all cat.	Rate	Correlated	Correlated
PDF for VBF	VBF in all cat.	Rate	Correlated	Correlated
PDF for $t\bar{t}H$	$t\bar{t}H$ in all cat.	Rate	Correlated	Correlated
PDF for VH	VH in all cat.	Rate	Correlated	Correlated
ggH accept. vs (p_T(H),N_j,m_{jj})	ggH in all cat.	Shape in VBF, rate in others	Correlated	Correlated
VBF accept. vs (p_T(H),N_j,m_{jj})	VBF in all cat.	Shape in VBF, rate in others	Correlated	Correlated
$t\bar{t}H$ accept. from μ_R and μ_F	$t\bar{t}H$ in all cat.	Rate	Correlated	Correlated
VH accept. from μ_R and μ_F	VH in all cat.	Rate	Correlated	Correlated
$t\bar{t}H$ accept. from PDF	$t\bar{t}H$ in all cat.	Rate	Correlated	Correlated
VH accept. from PDF	VH in all cat.	Rate	Correlated	Correlated
PYTHIA ISR and FSR	Sig. in all cat., bkg. in VBF	Shape in VBF, rate in others	Correlated	Correlated
PYTHIA vs HERWIG)	VBF and Zjj-EW in VBF cat.	Shape	Correlated	Correlated
μ_R and μ_F for Drell–Yan	VBF cat.	Shape	Correlated	Correlated
μ_R and μ_F for Zjj-EW	VBF cat.	Shape	Correlated	Correlated
μ_R and μ_F for top bkgs.	VBF cat.	Shape	Correlated	Correlated
μ_R and μ_F for diboson	VBF cat.	Shape	Correlated	Correlated
PDF for Drell–Yan	VBF cat.	Shape	Correlated	Correlated
PDF for Zjj-EW	VBF cat.	Shape	Correlated	Correlated
PDF for top bkgs.	VBF cat.	Shape	Correlated	Correlated
PDF for dibosons	VBF cat.	Shape	Correlated	Correlated
Size of simulated samples	VBF cat.	Bin-by-bin	—	Uncorrelated

Signal composition

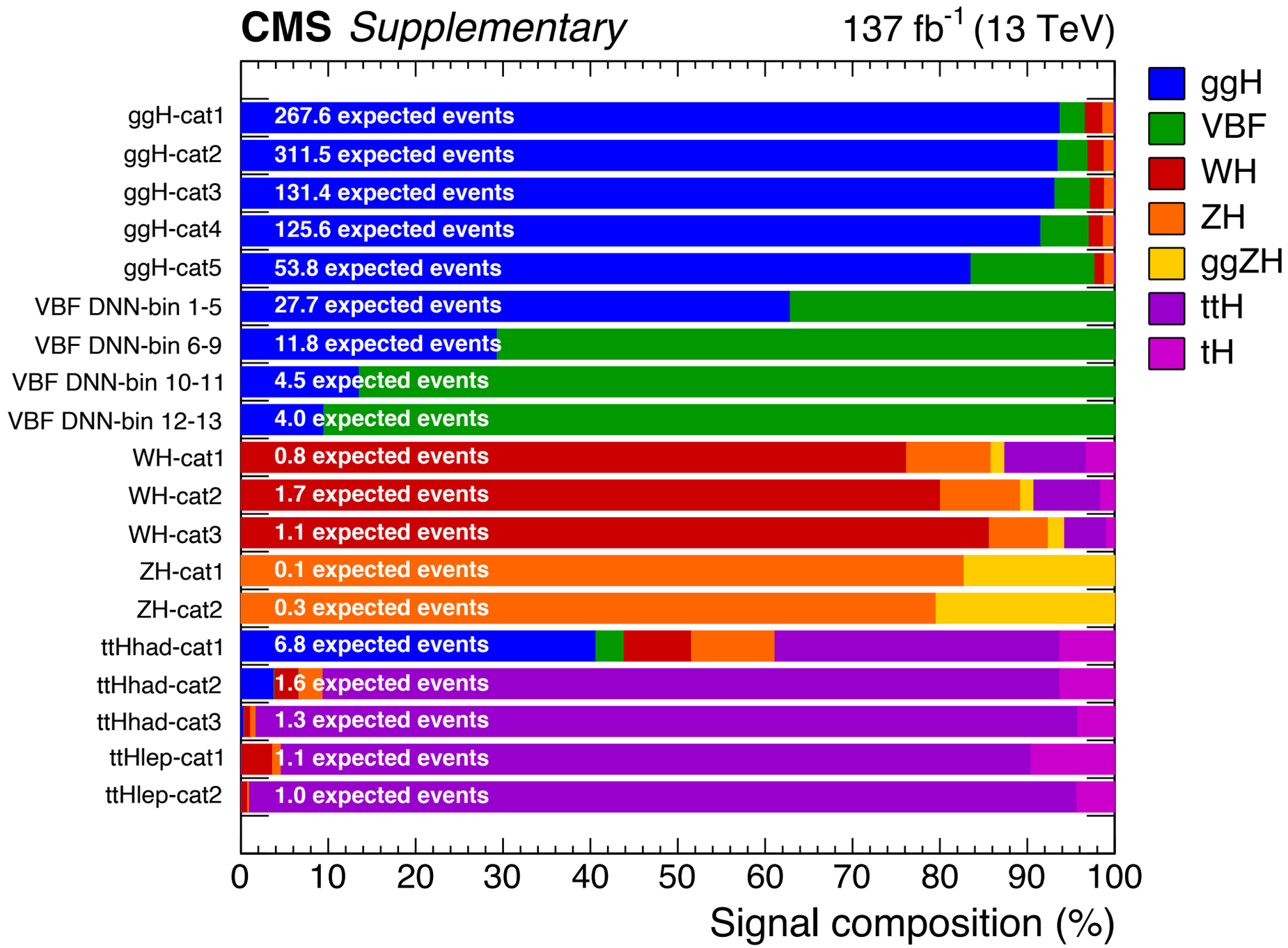

H→μμ: Run 1 and Run 2 combination

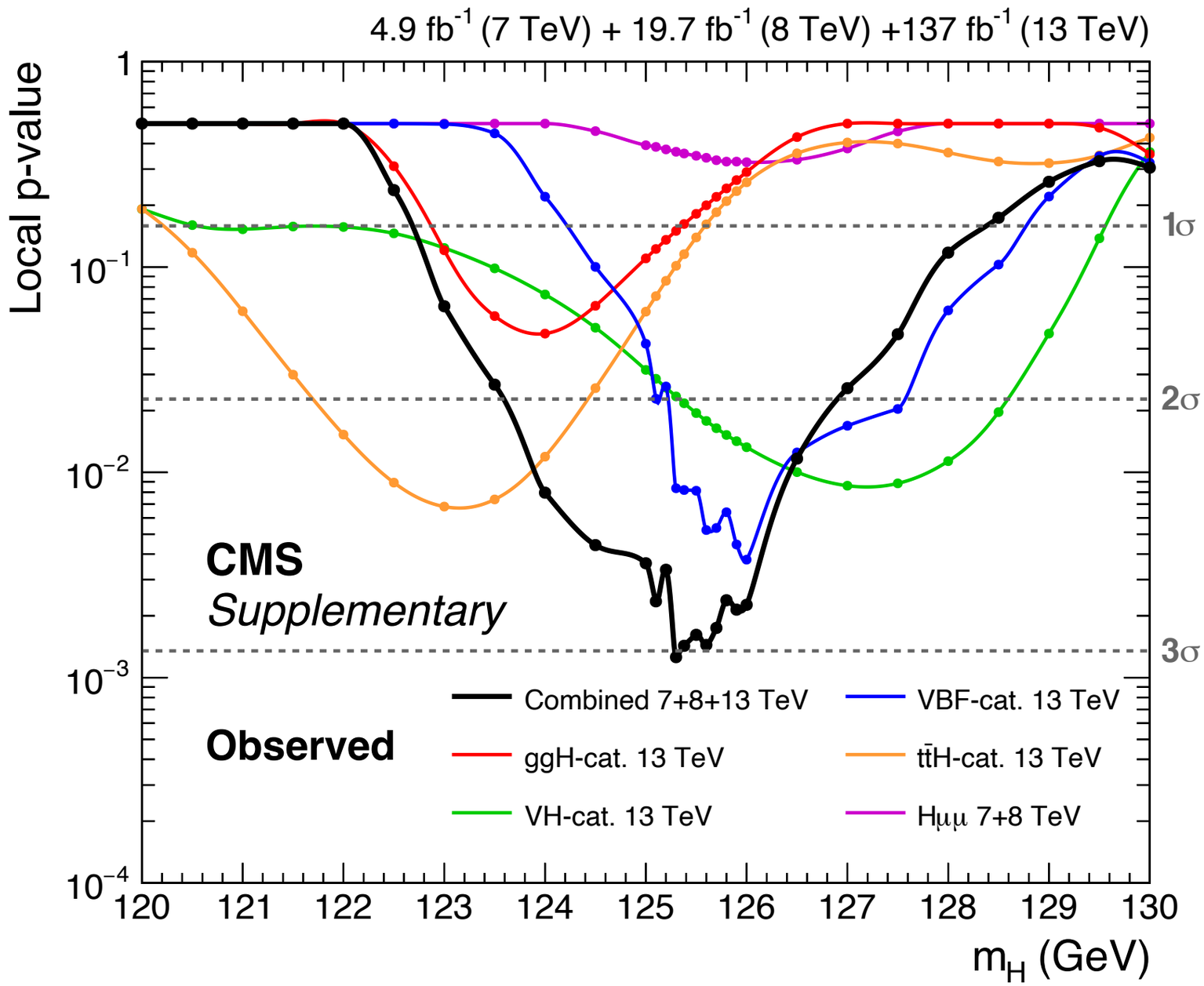

H→μμ: Higgs boson coupling to muons

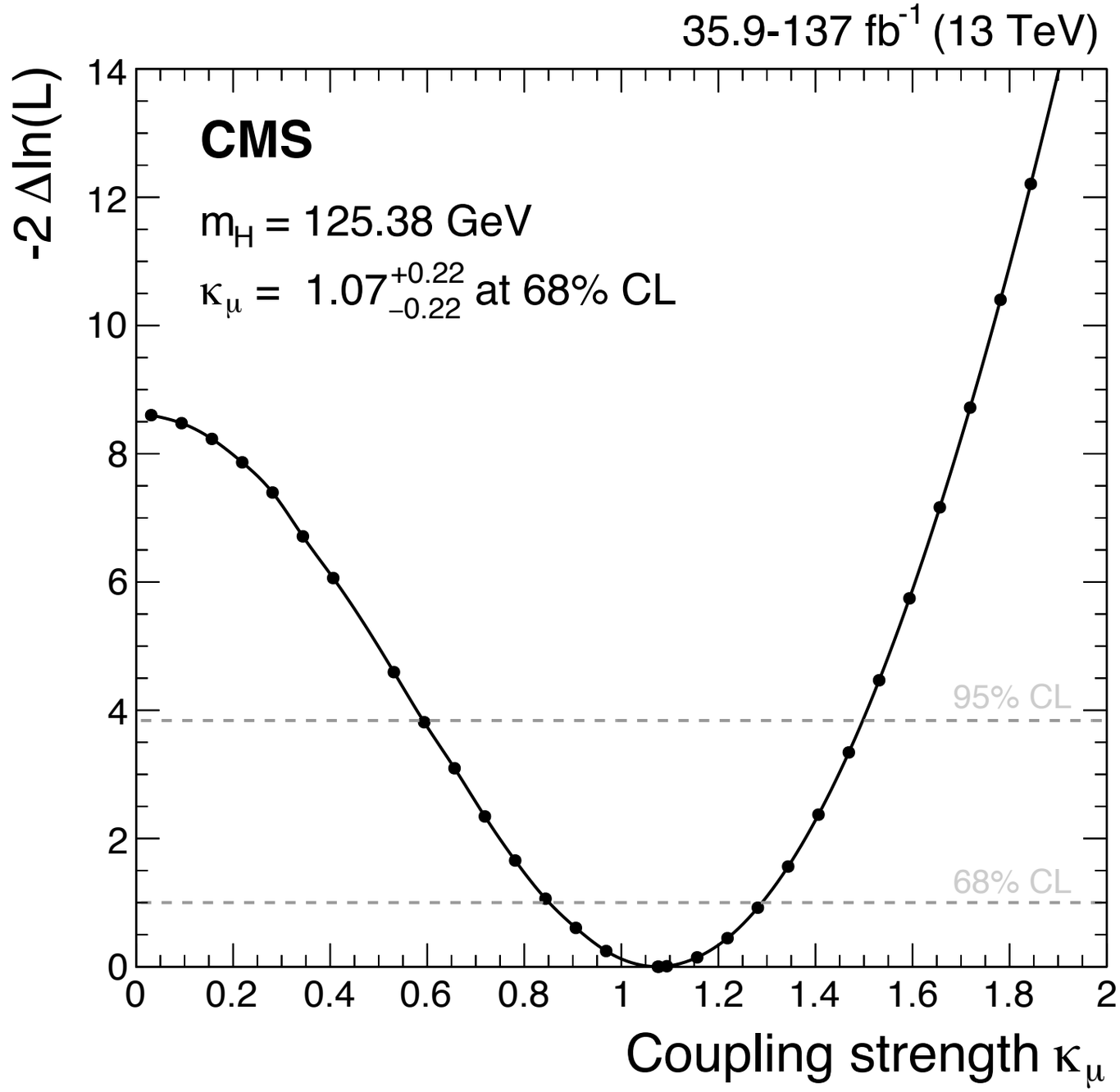

ttH channel selection

Selection	$t\bar{t}H$ hadronic	$t\bar{t}H$ leptonic
Number of b quark jets	> 0 medium or > 1 loose b-tagged jets	
Number of leptons	2	3 or 4
Lepton charge	$\sum q(\ell) = 0$	$\mathrm{N}(\ell) = 3\ (4) \rightarrow \sum q(\ell) = \pm 1\ (0)$
Jet multiplicity ($p_{\mathrm{T}} > 25\,\mathrm{GeV}$, $\lvert\eta\rvert < 4.7$)	≥ 3	≥ 2
Leading jet p_{T}	$> 50\,\mathrm{GeV}$	$> 35\,\mathrm{GeV}$
Jet triplet mass	$100 < m_{jjj} < 300\,\mathrm{GeV}$	—
Z mass veto	—	$\lvert m_{\ell\ell} - m_{\mathrm{Z}}\rvert > 10\,\mathrm{GeV}$
Low mass resonance veto	—	$m_{\ell\ell} > 12\,\mathrm{GeV}$

VH-leptonic channel

Observable	WH leptonic		ZH leptonic	
	$\mu\mu\mu$	$\mu\mu$e	4μ	2μ2e
Number of loose (medium) b-tagged jets	$\leq$1 (0)	$\leq$1 (0)	$\leq$1 (0)	$\leq$1 (0)
Number of selected muons	$=$3	$=$2	$=$4	$=$2
Number of selected electrons	$=$0	$=$1	$=$0	$=$2
Lepton charge ($q(\ell)$)	$\sum q(\ell) = \pm 1$		$\sum q(\ell) = 0$	
Low-mass resonance veto	$m_{\ell\ell} > 12\,\text{GeV}$			
N($\mu^+\mu^-$) pairs with $110 < m_{\mu\mu} < 150\,\text{GeV}$	$\geq$1	$=$1	$\geq$1	$=$1
N($\mu^+\mu^-$) pairs with $\lvert m_{\mu\mu} - m_Z \rvert < 10\,\text{GeV}$	$=$0	$=$0	$=$1	$=$0
N(e^+e^-) pairs with $\lvert m_{ee} - m_Z \rvert < 20\,\text{GeV}$	$=$0	$=$0	$=$1	$=$1

Functional forms:

WH-cat1

$$\text{BWZGamma}(m_{\mu\mu}; a, f, m_Z, \Gamma_Z) = f \times \text{BWZ}(m_{\mu\mu}; a, m_Z, \Gamma_Z) + (1-f) \times \frac{e^{a m_{\mu\mu}}}{m_{\mu\mu}^2}$$

Other categories

$$\text{BWZ}(m_{\mu\mu}; a, m_Z, \Gamma_Z) = \frac{\Gamma_Z e^{a m_{\mu\mu}}}{(m_{\mu\mu} - m_Z)^2 + (\Gamma_Z/2)^2}$$

H→μμ: mass spectra

Note: this spectra is not from the fit, because VBF channel does not use mass fit method

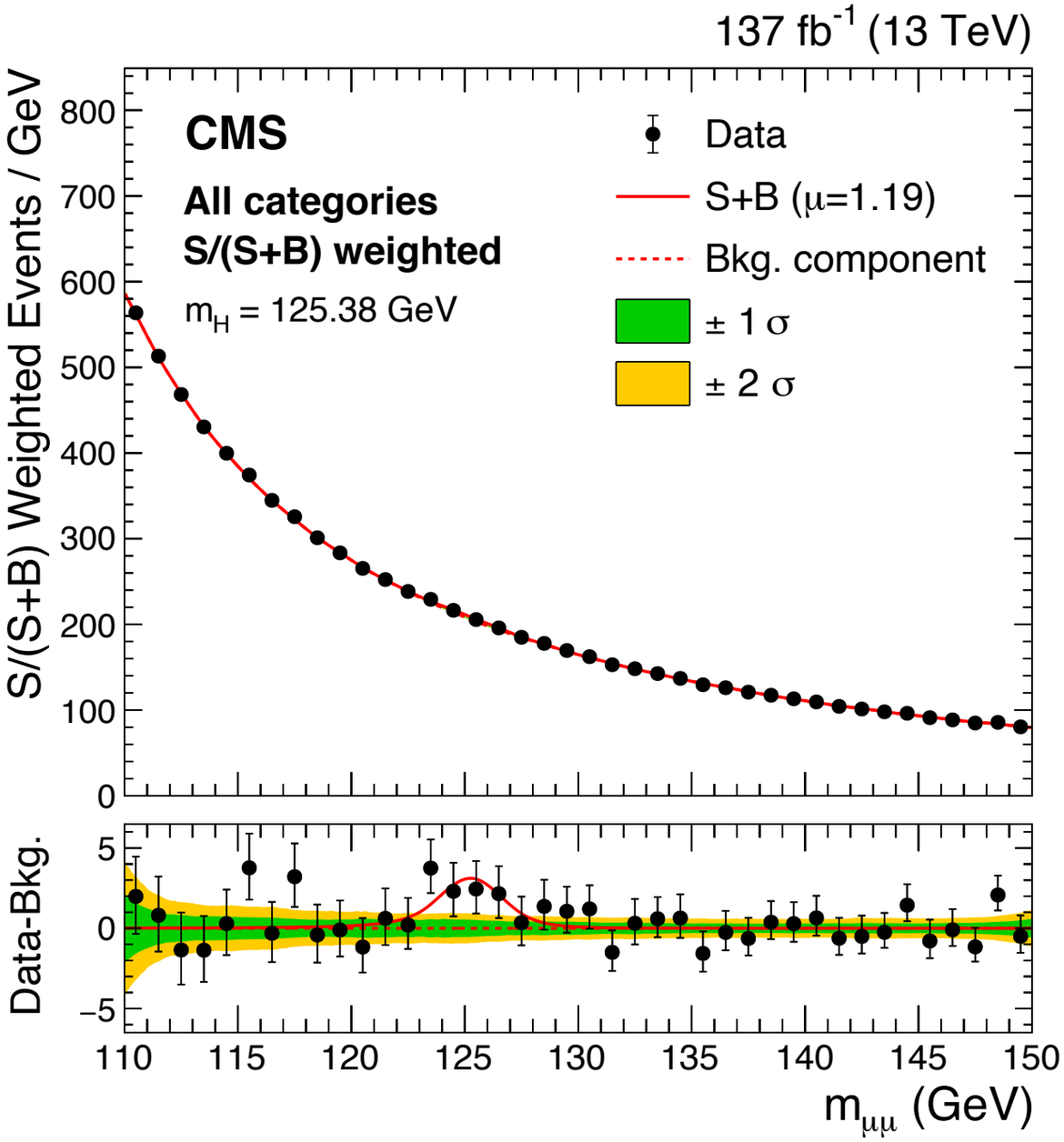

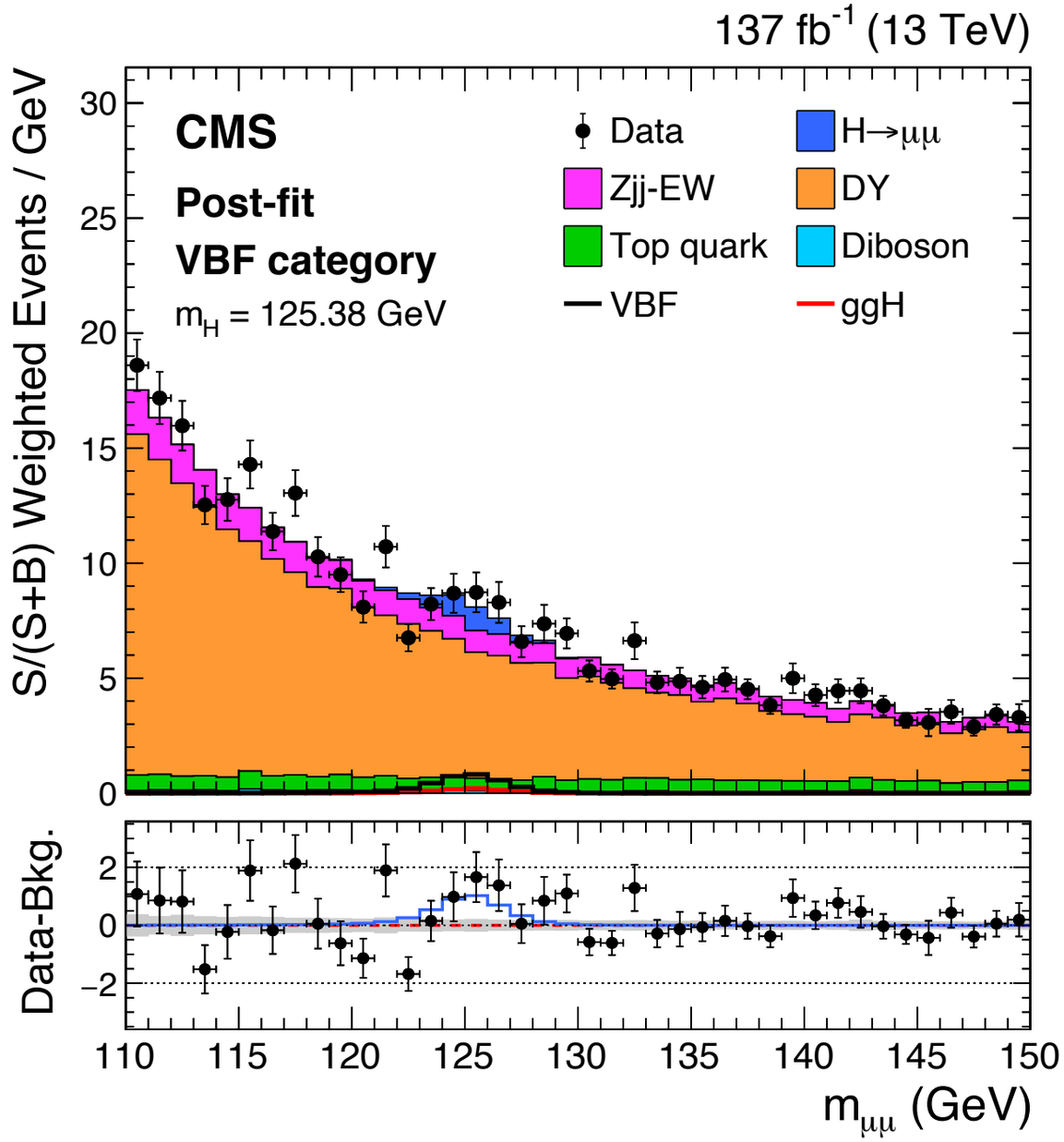

Muon momentum resolution

$\sigma/p_T \approx 1\%$ @ 50GeV to 10% @ 1TeV

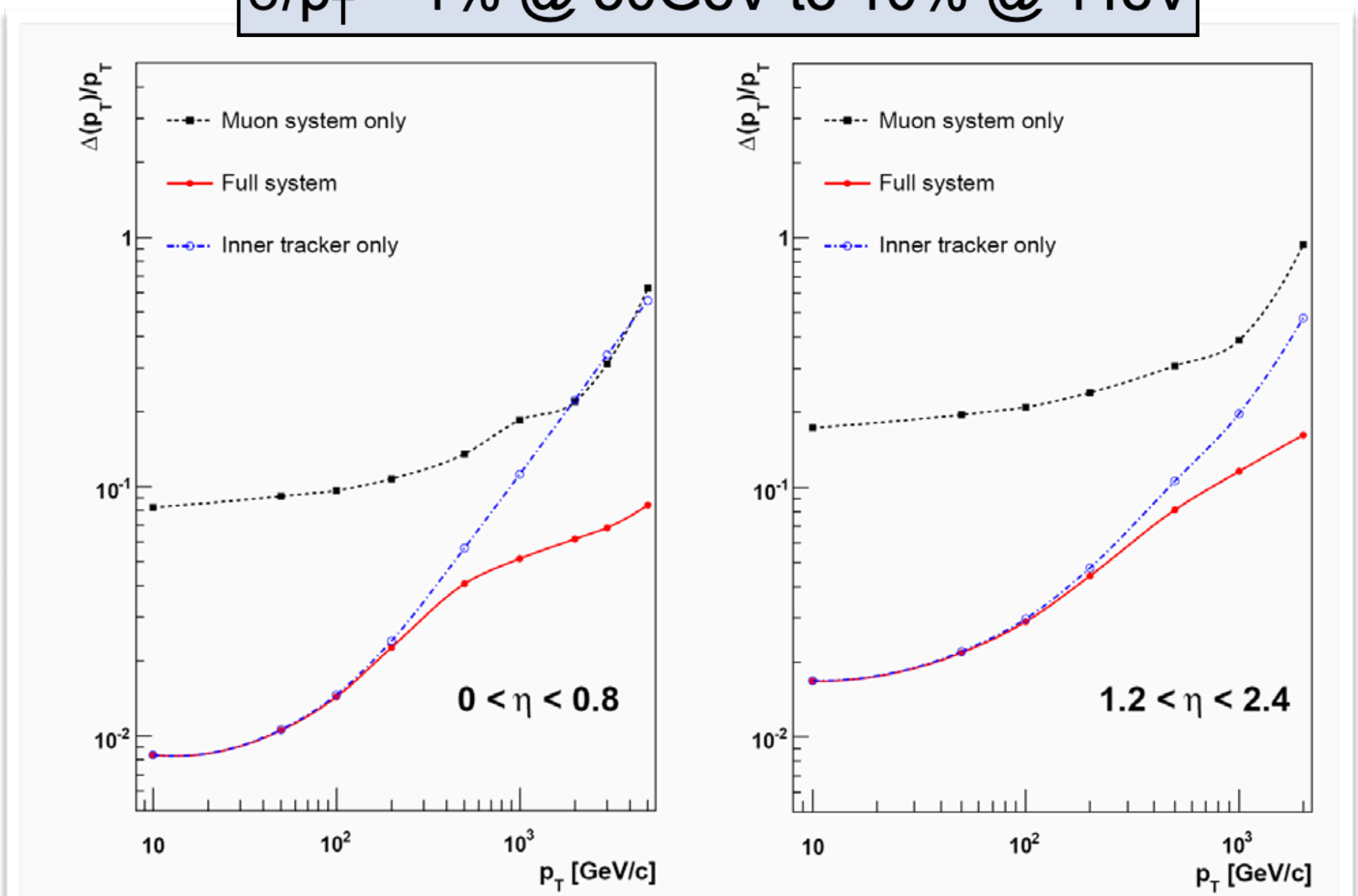

H→μμ events:

- typical p_T of muons: 50~60 GeV
- muon p_T resolution $\sigma(p_T)/p_T$ dominated by measurements by tracker

Rochester Correction

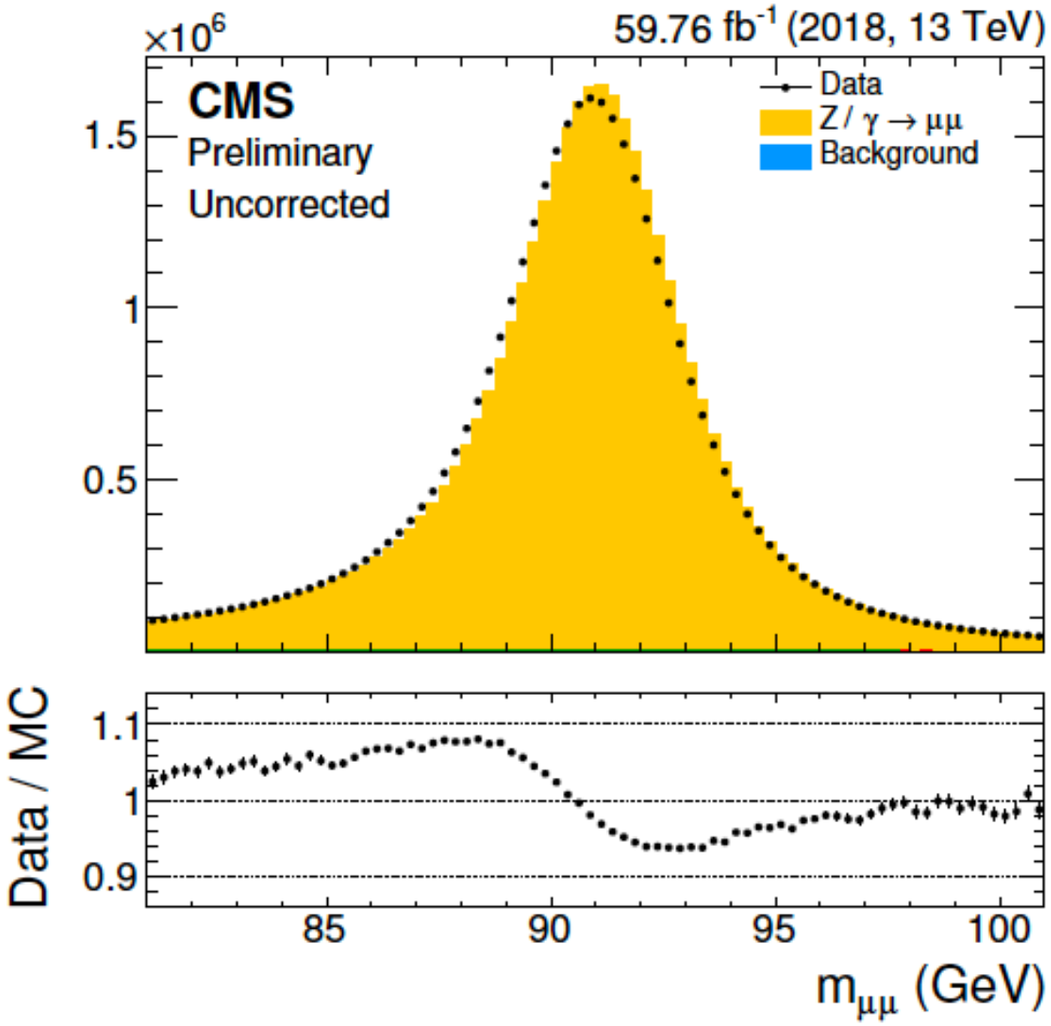

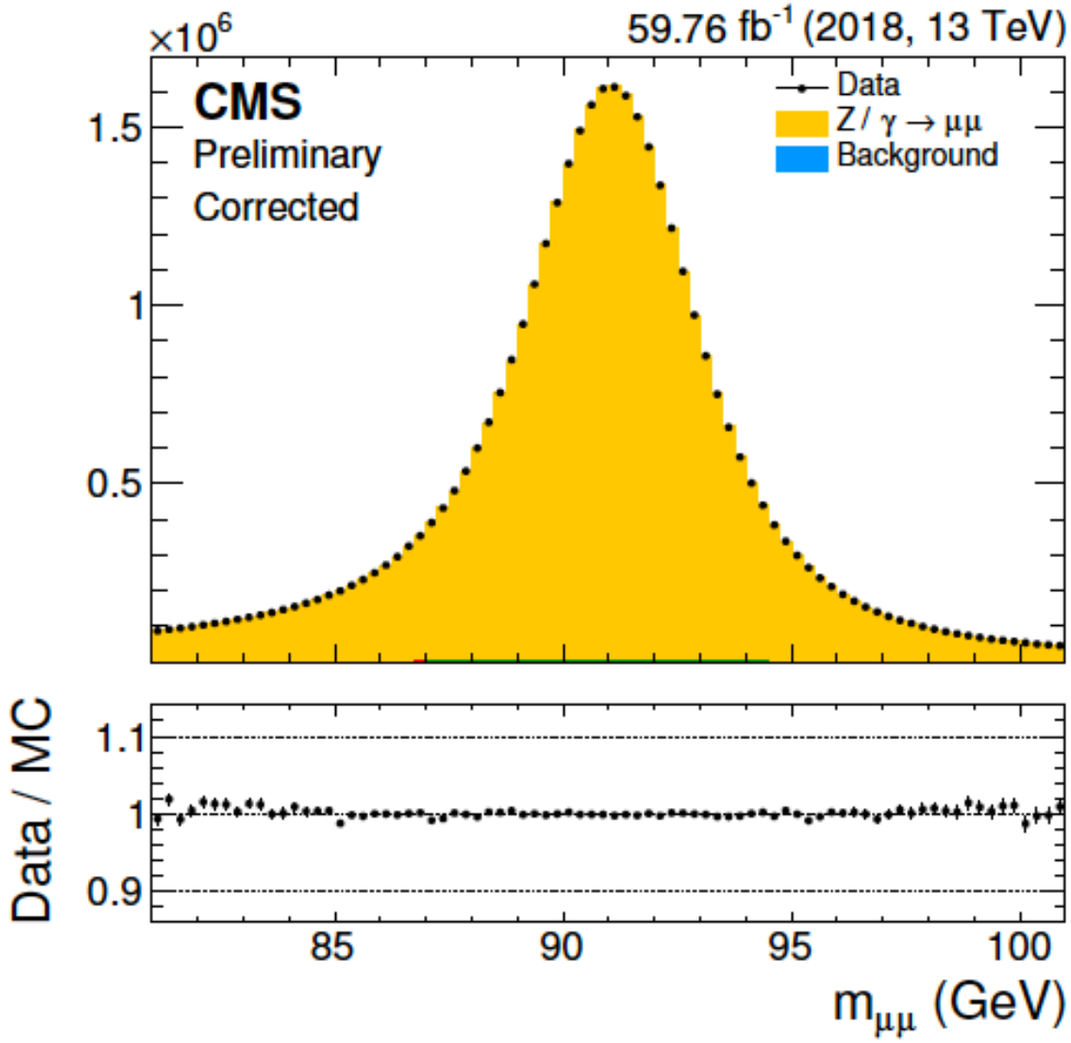

Muon resolution in Z peak region

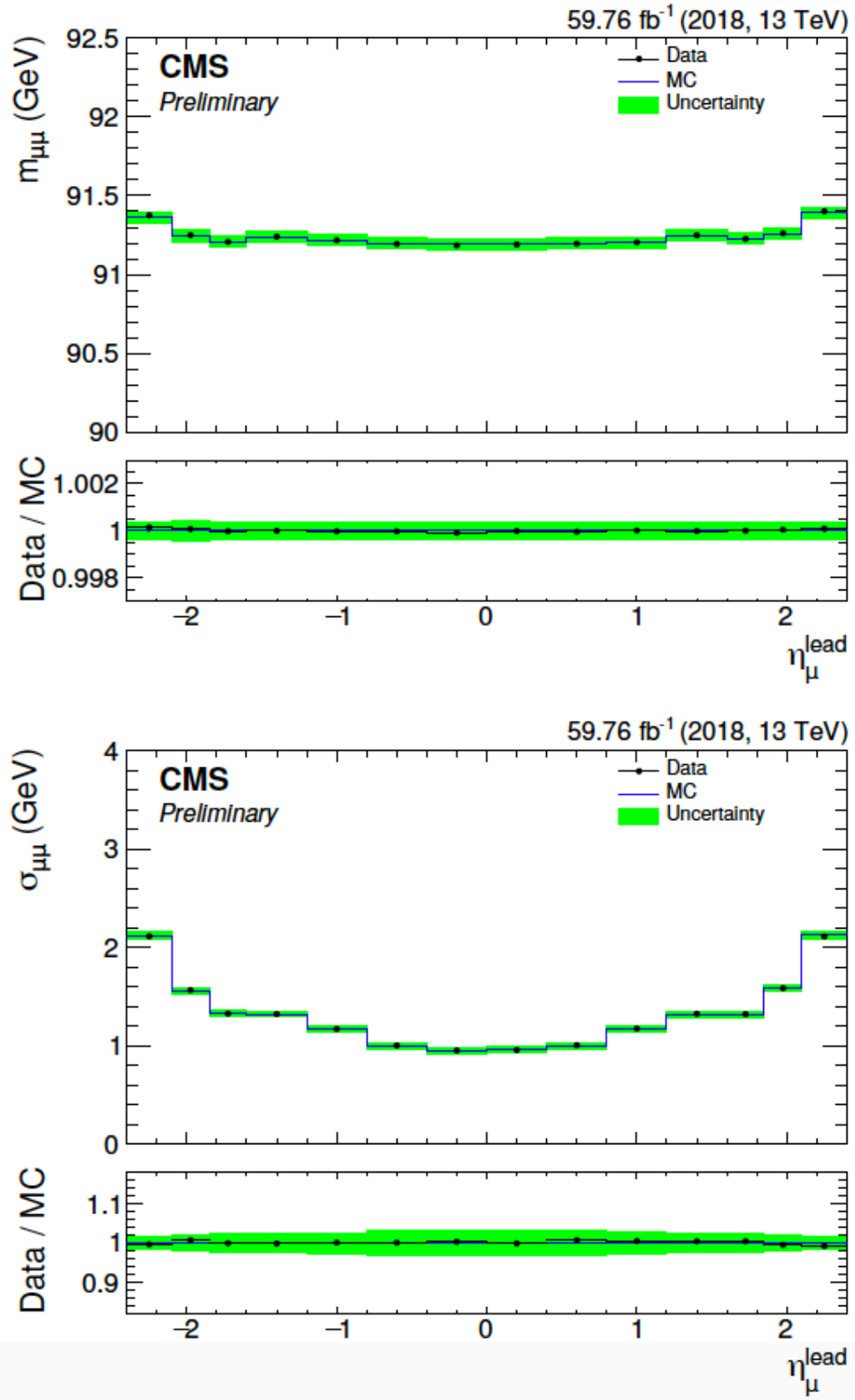

New timing dimension measurement at HL-LHC

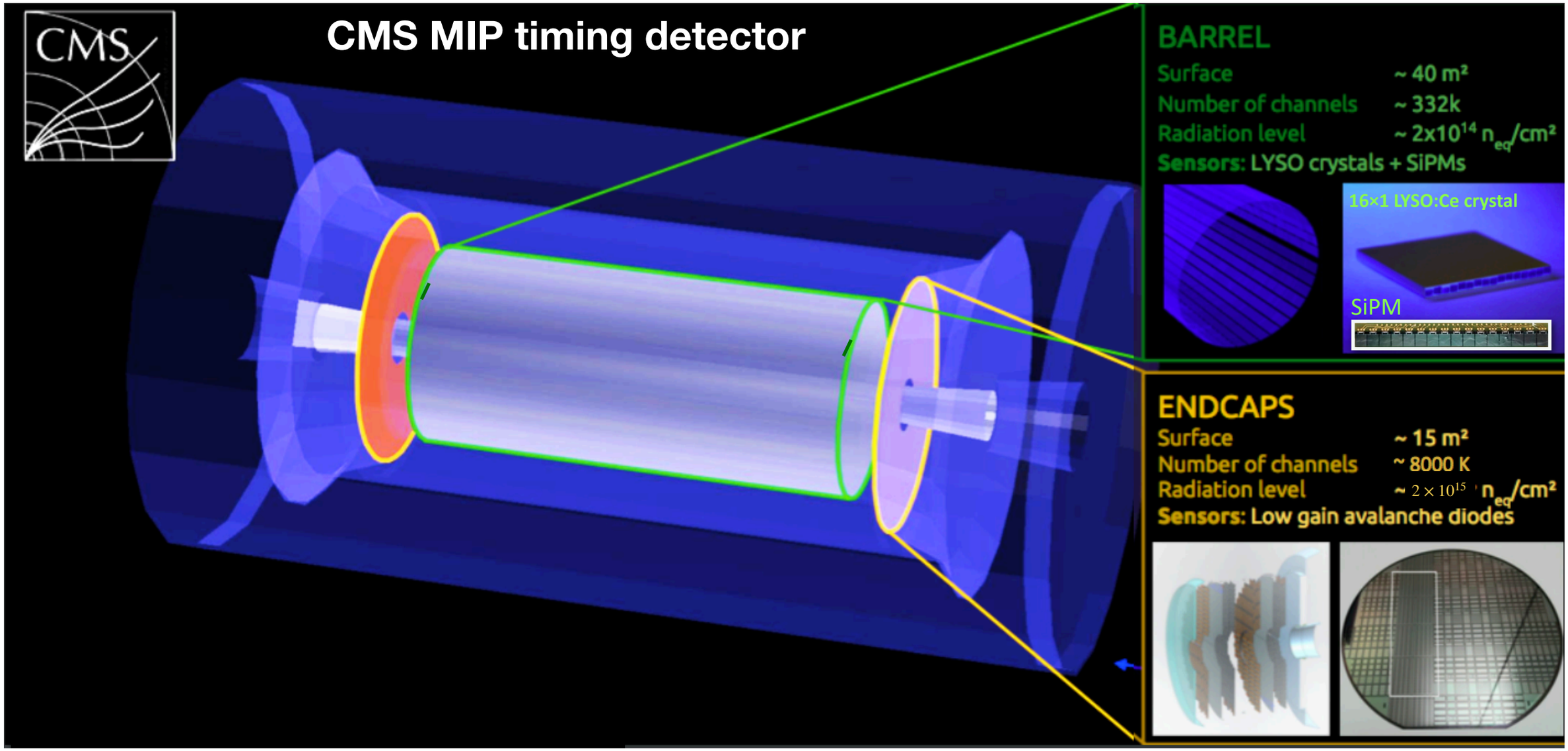

CMS-TDR-020

- Time resolution of 30-50 ps for minimum ionizing particles (MIPs)
- Thin layer between tracker and calorimeters, covering $|\eta|<3$

BTL sensor design - LYSO:Ce

Lutetium-yttrium orthosilicate crystals activated with cerium (LYSO:Ce) as scintillator $3 \times 3 \times 57\ mm^3$.

LYSO:Ce matrix 1x16

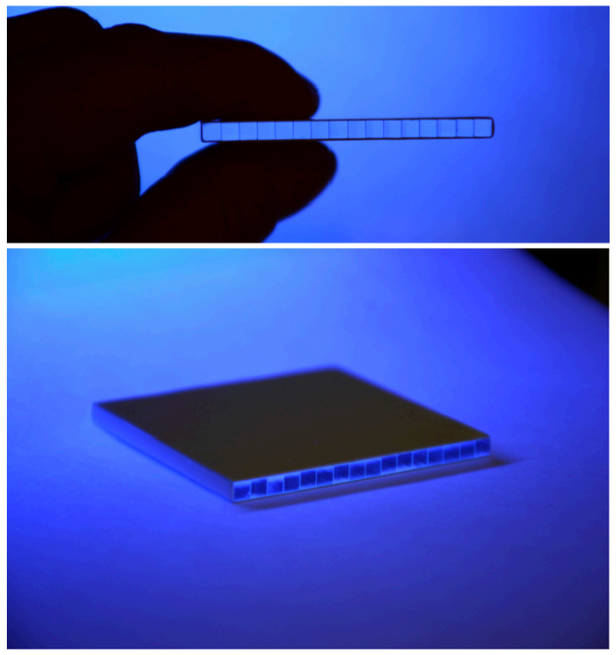

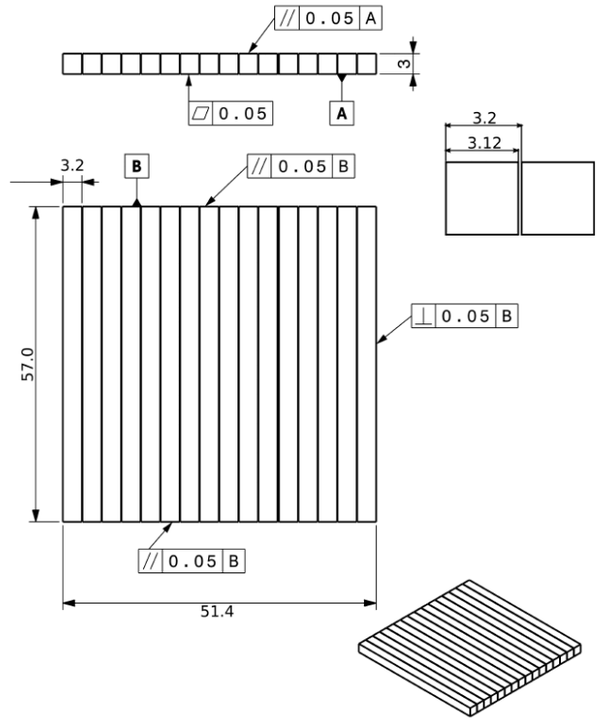

Stochastic fluctuations in the time-of-arrival of photons detected at the SiPM:

$$\sigma_t^{photostatistics} \propto \sqrt{1/N_{p.e.}} \propto \sqrt{1/(E_{dep} \times LY \times LCE \times PDE)}$$

- Dense (7.1 g/cm³): a MIP deposits **E_{dep} ~4.2 MeV** including impact angle (0.86 MeV/mm)
- Bright: light yield (LY) ~40k photons/MeV.
- Excellent radiation tolerance

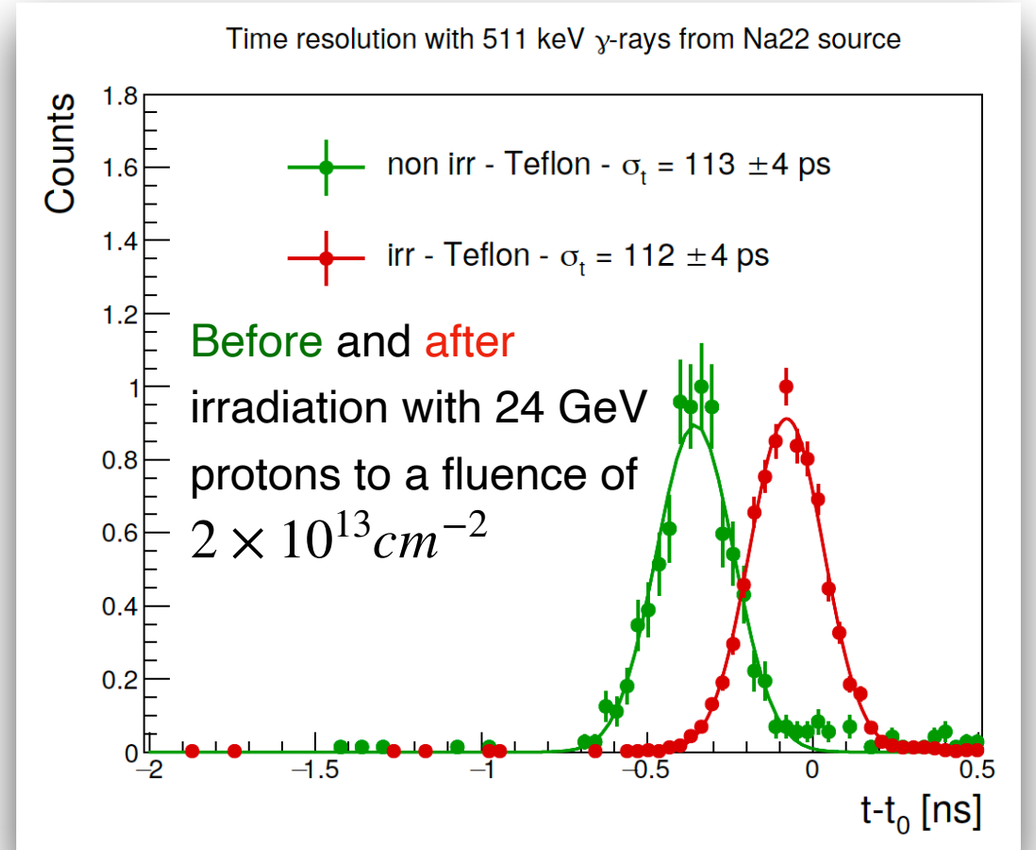

BTL sensor design - SiPM

Silicon Photomultipliers as photo sensors

- Compact, fast (single photon resolution of 100 ps), insensitive to magnetic fields, radiation hard
- SiPM active area of 9 mm^2, coupled to LYSO using glue: light collection efficiency (LCE) 15%
- Optimal SiPM cell size: 15 µm, balance between radiation tolerance and photon detection efficiency
- Gain: $1.5 - 4 \times 10^5$
- Photo detection efficiency (PDE) : 20-40%

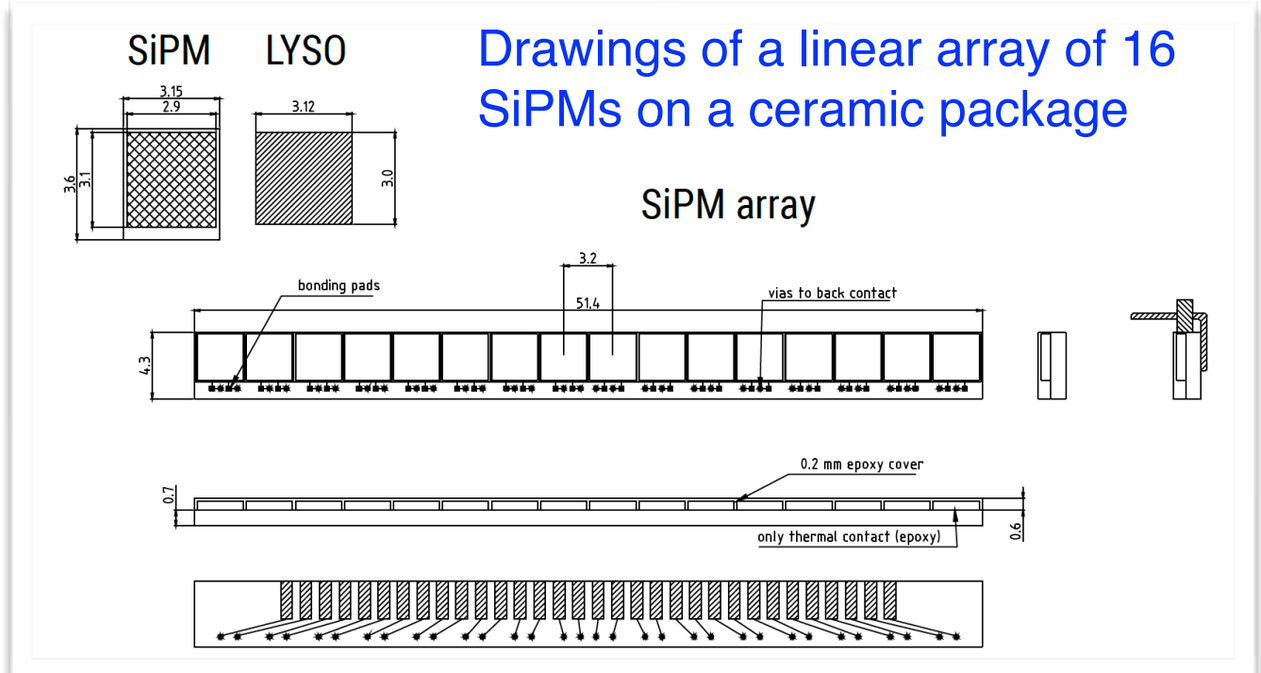

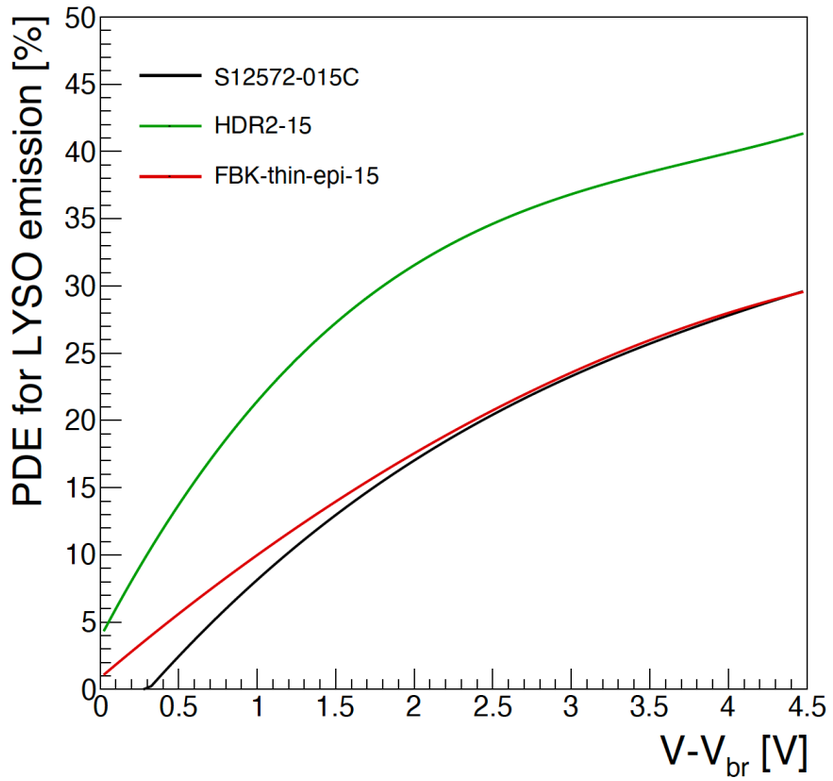

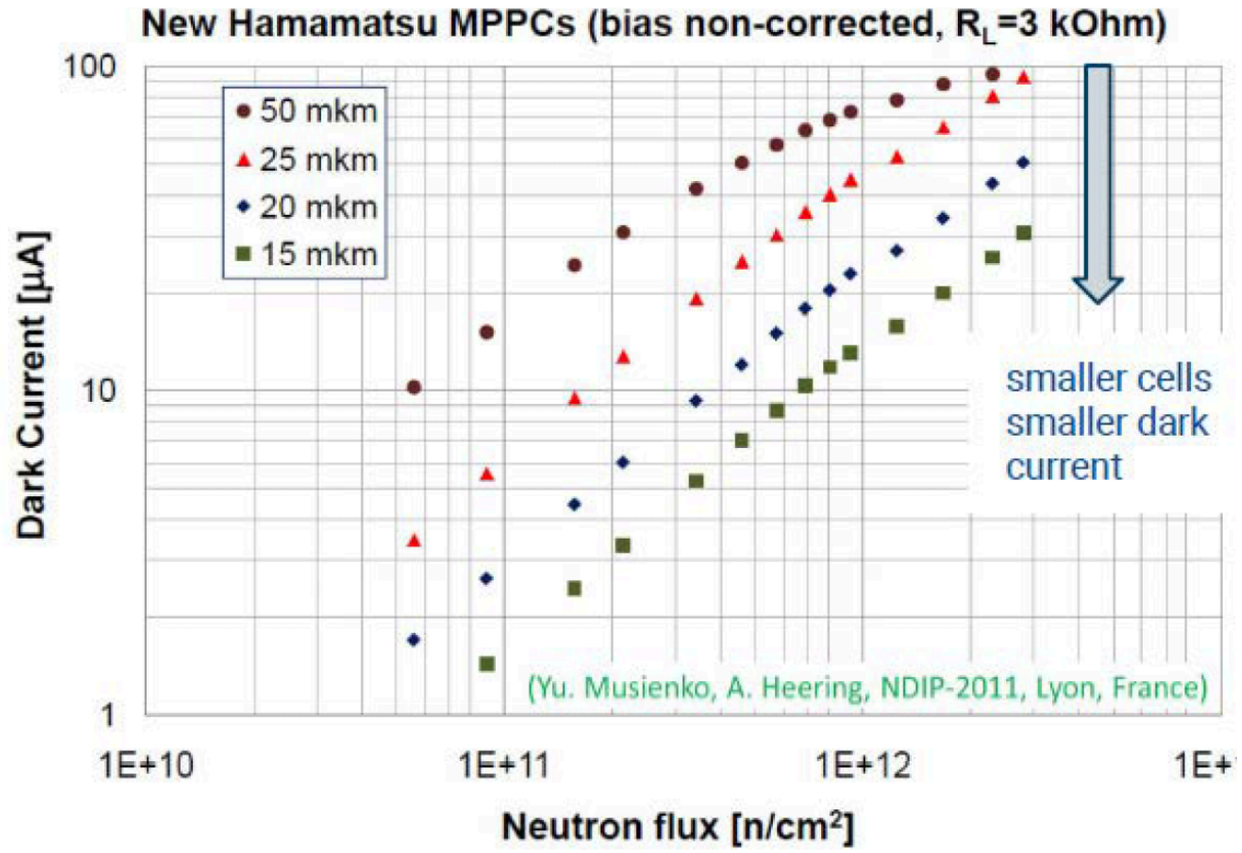

Muon efficiency with precision timing

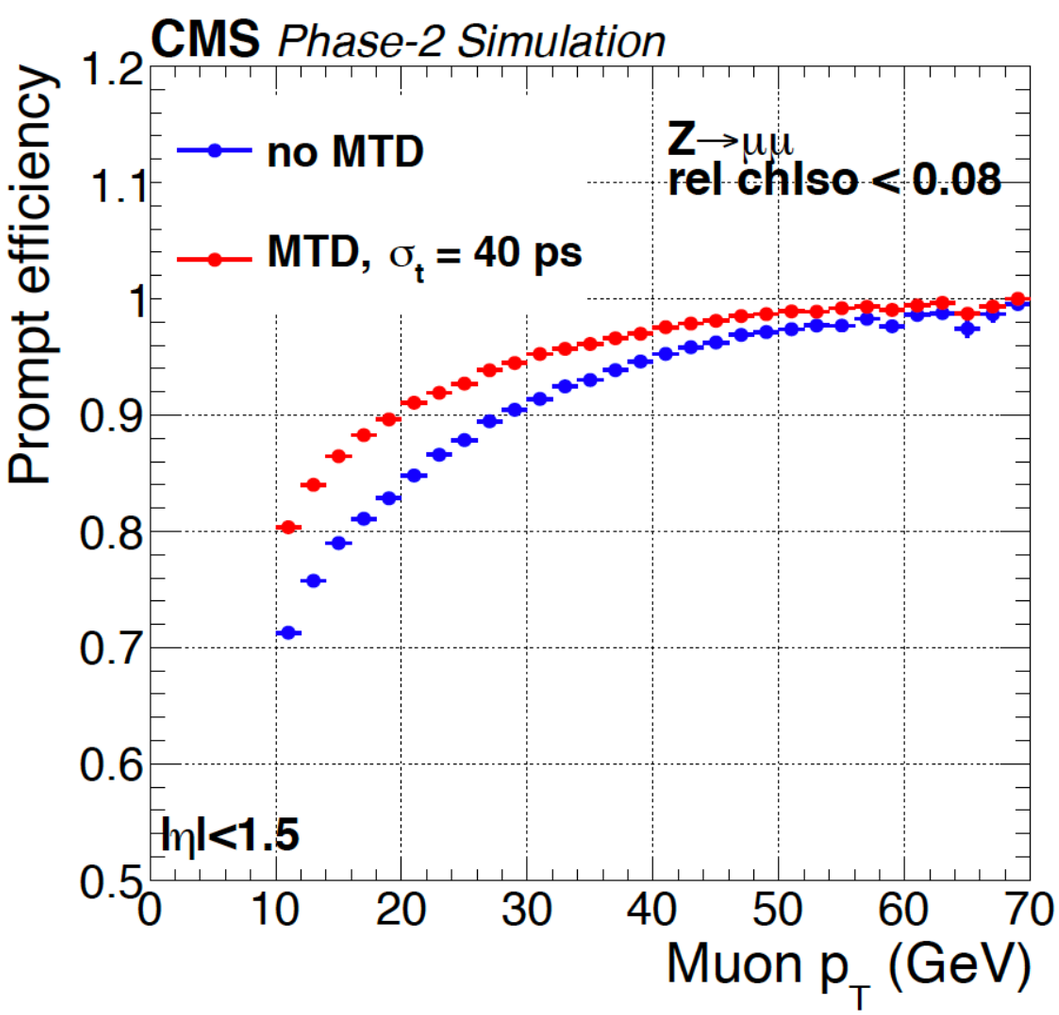

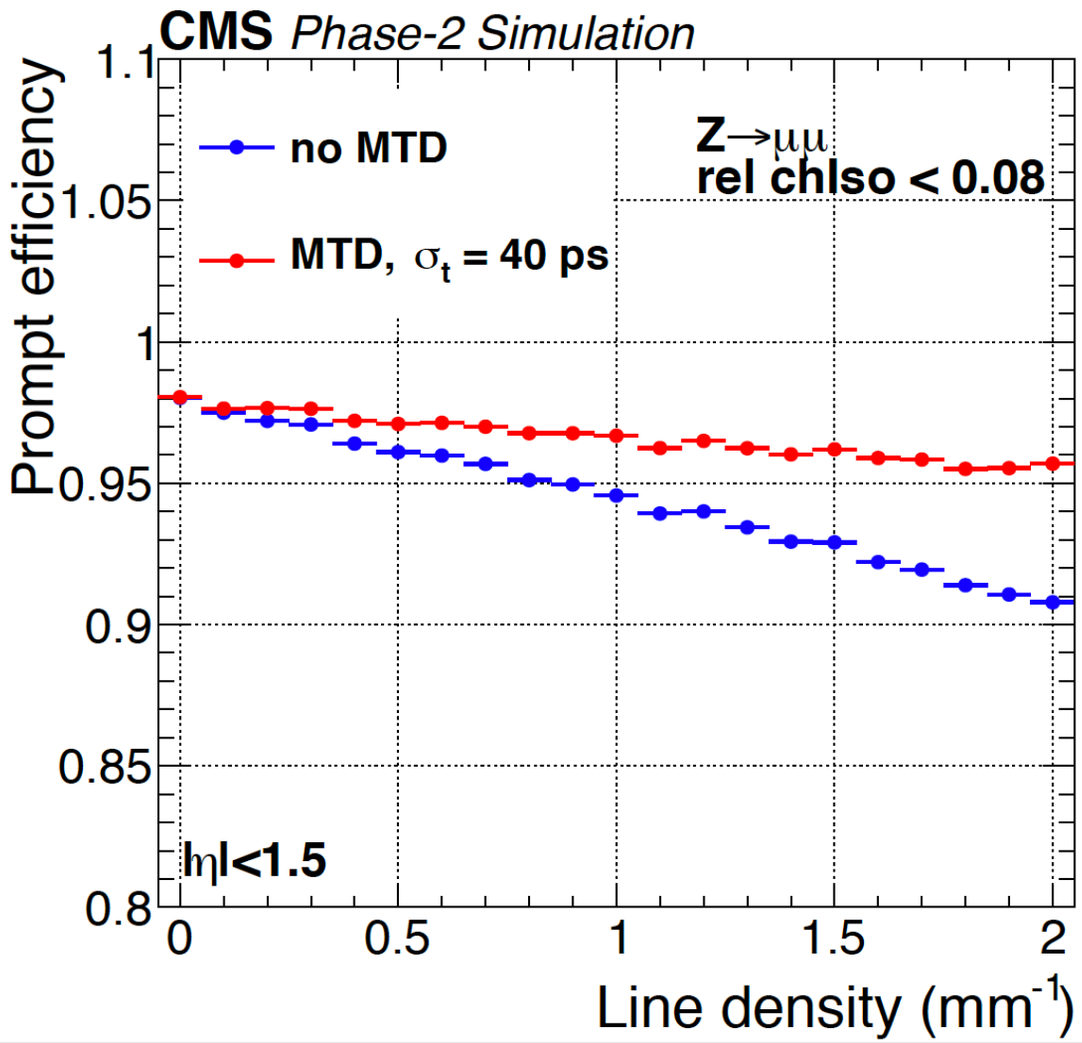

CMS-TDR-020

Phase-2 muon trigger improvement with GEM detectors